

**CO-BLENDING OF SEISMIC ATTRIBUTES FOR
INTERPRETATION OF CHANNEL GEOMETRIES AND RESERVOIR
CHARACTERIZATION IN RENCE FIELD OF NIGER DELTA,
NIGERIA**

BY

CHINWUKO, IFEANYI AUGUSTINE
(MSc. APPLIED GEOPHYSICS (NAU) & BSc. GEOLOGICAL SCIENCES (NAU))

REG. NO: 2011507001F

DEPARTMENT OF GEOLOGICAL SCIENCES

FACULTY OF PHYSICAL SCIENCES

NNAMDI AZIKIWE UNIVERSITY, AWKA

IN PARTIAL FULFILLMENT

OF THE REQUIREMENTS FOR THE AWARD OF

DOCTOR OF PHILOSOPHY (Ph.D) DEGREE

IN GEOLOGICAL SCIENCES (APPLIED GEOPHYSICS OPTION)

FEBRUARY, 2016

APPROVAL PAGE

Chinwuko Augustine Ifeanyi with Registration Number of 2011507001F has successfully completed the external defence of this Ph.D dissertation. We hereby approve the acceptance of this Ph.D dissertation to the relevant Board.

Prof. A.G. Onwuemesi
Supervisor I

Date

Dr. E. K. Anakwuba
Supervisor II

Date

Dr. N. E. Ajaegwu
Head of Department

Date

Prof. E. U. Ofoedu
Faculty PG Sub-Dean

Date

Prof. A. O. C. Nwokoye
Dean, Faculty of Physical Sciences

Date

Prof. H. I. Odumegwu
Dean, School of Post Graduate Studies

Date

Prof. E. D. Uko
External Examiner

Date

CERTIFICATION

This is to certify that Chinwuko Augustine Ifeanyi carried out this Ph.D dissertation and produced this report under our supervision in partial fulfillment of the requirement for the award of Doctor of Philosophy (Ph.D) in Applied Geophysics.

Chinwuko, Augustine Ifeanyi
Candidate

Date

Prof. A.G. Onwuemesi
Supervisor I

Date

Dr. E. K. Anakwuba
Supervisor II

Date

DEDICATION

I dedicate this dissertation to the Almighty God for granting me the grace to complete this Ph.D dissertation and to my lovely wife, Mrs. Ngozi Florence Chinwuko as well as my darling daughter, Chidera Favour.

ACKNOWLEDGEMENT

My foremost gratitude goes to my harmonious project Supervisors, Prof. A. G. Onwuemesi and Dr. E. K. Anakwuba for their efforts in providing instruction, direction, support, and knowledge during this study. I especially appreciate their accessibility and readiness to provide insight anytime I approached them throughout the execution of this work. I also acknowledge Dr. A. U. Okoro for his relentless effort and contribution towards this research work. Moreover, I wish to thank the Head of Department, Dr. N. E. Ajaegwu for his kindness and support. May I say thank you to all the lecturers in my department for their justifiable critics and encouragement towards this work.

My gratitude also goes to the Vice Chancellor of Federal University Gusau, Prof. Ben-Chuks Okeke through whom the Tertiary Education Trust Fund (TETFUND) grant was extended to me as an academic staff. To the entire Management Board, Head of Geological Department, Prof. U.A. Danbatta and my fellow staff at Federal University Gusau (FUGUS), I say thank you for all your support.

My thanks go to the Department of Petroleum Resources, Nigeria, which provided the approval and permission to use the data set for this study. I appreciate the management of SunLink Petroleum Limited, Lagos Nigeria for granting me one year graduate internship in their noble company. I am also grateful to Mr. Onyekwelu Clement Udenna of SunLink Petroleum Limited Lagos and Dr. Ebere

Benard of Southern Atlantic Petroleum Limited Lagos, Nigeria for their support throughout the period of my graduate internship in the company. I acknowledge also the support and assistance of everyone who has given me a whole new experience in my study.

I am most grateful to my lovely wife whose support, love and care for me proved overwhelming in the development of this project; baby, you are 'My Rence'. To my darling daughter, Chidera Favour may God bless you for your prayer and best wishes.

I am also grateful for the support of my family both immediate and extended. I want to specially thank my beloved brothers: Mr. Nnanwuba Chinwuko, Engr. Nnamdi Chinwuko and Mr. Azuka Chinwuko as well as my darling sisters: Mrs Chinelo Udo-Anagor, Mrs Ifeyinwa Ifeatu and Miss Obiageli Chinwuko for their prayers, financial support and encouragement. Also, I appreciate the support and advice of my cousin, Engr. Dr. Chuka Chinwuko, who is the Head of Industrial Production Engineering in this University. May I also say thank you to Mr. Chukwunenye Dike for your brotherly advice.

Finally, I give glory to the Almighty God, the giver of life and to Jesus, the Author and Finisher of our faith for giving me the wisdom, knowledge and understanding to attain this height.

ABSTRACT

Co-blending of seismic attributes was used in the interpretation of channel geometries and reservoir characterization in Rence Field of Niger Delta, Nigeria. The study aims at defining the geometries of hydrocarbon reservoirs with particular emphasis on channels in shallow marine (offshore) Niger Delta. The co-blending application enhances both the ease of detection and continuity of channels, leaving the channel environs unchanged. The methodology involved the use of three dimensional seismic reflection volume, checkshot (velocity) and well log data in order to generate all necessary interpretation and input for geological modelling from seismic and well data interpretations. Eight single seismic attributes such as average energy, root-mean-square amplitude, instantaneous frequency, reflection acoustic impedance, iso-frequency, dominant frequency, signal envelope and coherence attributes were used for interpretation in the study. Four sets of co-blending were carried out. The execution of these steps was done with the aid of Schlumberger Petrel. The result of the seismic facies analysis reveals that the Rence Field can be distinguished into two seismic facies, namely, layered complexes and chaotic complexes. The channel elements deduced from facies analysis are meander loop cut-off deposits, lateral accretionary channel deposits, and shore deposits. The result of well to seismic ties reveals high and low amplitude reflection events for sand and shale units respectively. Seismic structural interpretation of Rence Field reveals four major regional faults and twelve minor faults. Seven of the faults are antithetic and the rest are synthetic faults. One mega-channel feature that trends east - west was identified in the attribute maps generated. It is characterized by sinuosity of 1.3, with a meandering length of 22500 m, and a distance of 17500 m. The average depth of the channel is about 170 m with amplitude of 1670 m, and wavelength as high as 7640 m. A depositional model generated from the attribute maps indicates a sub-aqueous channel environment of deposition. The attribute map also shows that there was shifting in location of barrier bars within the area. The shifting could be attributed to growth faults mechanism. At the flanks of the sinusoidal channel there are prominent sand point bars sequences. The petrophysical analysis of the well data shows 90% Net-to-Gross, 28% porosity, 27% volume of shale, and 24% water saturation. These values indicate that the reservoir is of pay quality. The oil reservoir has been estimated to be 474.4 million stock tank barrels of oil initially in place. The oil/water contact was delineated at a depth of 1294m (4180ft) with the oil bearing sands having low acoustic impedance values ranging from 4600 to 5450 $\text{g/cm}^3 \cdot \text{cm/s}$ with highest porosity value of 0.36. The water sand has higher acoustic impedance values ranging from 5500 to 6150 $\text{g/cm}^3 \cdot \text{m/s}$ with the lowest porosity value of 0.12. The validity of this work is in the application of the seismic time slice at 1703ms from the attribute map generated which shows that, all the existing wells in the study area are targeting the mega-channel for oil exploitation. Based on the petrophysical analysis, results, and identification of channel deposits, the study area proves highly promising for hydrocarbon accumulation and definition of the geometries of channel in study area.

TABLE OF CONTENTS

Title Page	I
Approval Page	II
Certification	III
Dedication	IV
Acknowledgement	V
Abstract	VII
Table of Contents	VIII
List of Figures	X
List of Tables	XII
Chapter One	1
Introduction	1
1.1 Background Information	1
1.2 Statement of the Problem	3
1.3 Location of the Study Area	5
1.4 Aim and objectives of the study	8
1.5 Justification of study	9
1.6 Scope of the study	10
1.7 Significance of the study	10
Chapter Two	12
Review of Related Literature	12
2.1 Literature Review	12
2.2 Regional Geology of Niger Delta	22

2.3 Tectonic Evolution	26
2.4 Structural Styles	28
2.5 Lithostratigraphy of Niger Delta	28
2.6 Evolution of Depobelts	33
2.7 Evolution of Sequences	34
2.8 Petroleum Geology	36
2.9 Features within Channels	41
2.10 Theory of Well Correlation	44
2.11 Theory of Well Log Sequence	45
2.12 Background to Seismic Attributes	48
Chapter Three	56
Material and Methods	56
3.1 Data Availability and Description	56
3.2 Methodology	61
Chapter Four	75
Results and Discussion	75
4.0 Introduction	75
4.1 Result of Well Interpretation	75
4.2 Result of Seismic Structural Interpretation	88
4.3 Result of Seismic Attributes	100
4.4 Seismic Facies and Stratigraphic Analysis	113
4.5: Channel System and Depositional Elements Distribution	117
4.5 Discussions	120

Chapter Five	140
Summary, Conclusions and Recommendation	140
5.1 Contribution to Knowledge	140
5.1 Summary	141
5.2 Conclusions	143
5.3 Recommendations	146
References	147
Appendix	159

LIST OF FIGURES

Fig.	Page
1.1: Map of Niger Delta showing the location of the study area	6
1.2: Location map of the study area	7
2.1 Geologic map of Nigeria showing Niger Delta Basin and its relation to bounding structural feature	24
2.2: Niger Delta Basin and its stages of development	24
2.3: Physiographic sketch of the deep marine sediments in the Gulf of Guinea off the Niger Delta	35
2.4: Examples of Niger Delta Oil field structures and associated trap type	29
2.5: Stratigraphic section of the Anambra Basin and time equivalent formations in the Niger Delta	29
2.6: Lithostratigraphic section of Niger Delta	32
2.7: Regional structural elements and depobelts of the Niger Delta	32
2.8: Subsurface depth map of the Niger delta basin	40
2.9: Lithostratigraphic and chronostratigraphic interpretations of two well logs in a dip-oriented cross section	46
2.10: The direct correlation between facies and a variety of other log shapes relative to the sedimentological relationship	46
3.1: Base map showing all wells and seismic volume	58
3.2: Research Workflow	62
4.1: Distribution of GR logs in Rence Field before Normalization	76
4.2: Distribution of GR logs in Rence Field after Normalization	77
4.3: Gamma Ray Log Cut off for lithology description in Rence Field	79
4.4: Northwest –Southeast correlation panel across Rence field	81
4.5: Major Reservoir correlation panel across Rence field	83
4.6: Typical Gamma Ray log patterns of the study area	85
4. 7: Rence seismic wavelet profile extracted from Rence-1 well	87
4.8: The synthetic seismogram of the Rence field at well 1	87
4.9: The well ties posted on a seismic section within the Rence Field	88
4.10: Structural Configuration of the Rence Field	90
4.11: Seismic interpreted section on trace 13900 of Rence field	91
4.12: Time-structure map of H top reservoir horizon	93
4.13: Rence Field velocity curve	93
4.14: Depth-structural map of H top reservoir horizon	95
4.15: Multi-graph showing the oil/water contact in the study area	
4.16: Petro-Acoustic Analysis showing Oil/Water sand	99
4.17: Amplitude map generation for H-Horizon	101

Fig.	Page
4.18: Individual seismic attribute showing mega channel	102
4.19: Morphological Modelling of Geoprobe through various attributes	103
4.20: Co-blending of various seismic attribute	109
4.21: Seismic section showing seismic facies recognized in the study area	114
4.22: Line of section showing Channel morphology and architecture	118
4.23: Visible Channel resulting from Co-blending of Reflection Acoustic Impedance, Coherency and Instantaneous Frequency	119
4.24: 3D Reservoir modelling within the study area	122
4.25: Line of section showing strata termination, fault pattern and facies assemblage within the study area	124
4.26: Distinct Strata Patterns within the study area	126
4.27: Multi-well stratigraphic cross-section (Datum: H Reservoir top) showing the mega channel	127
4.28: Characterization of the depositional features within the study area	128
4.29: Idealized diagram of depositional model within the study area	130
4.30: Co-blended Seismic Time Slice showing mega-channel and fault	133
4.31: Channel reservoir elements within the study area	133
4.32: Amplitude thickness map of H-Reservoir	136

LIST OF TABLES

Table	Page
3.1: List of Available Well Logs and Core Data	60
4.1: Summary of Petrophysical Properties in the study area for H-Reservoir	96
4.2: Characteristics of different facies within the Rence field	115
4.3: Estimated channel geometries within the Rence field	119

CHAPTER ONE

INTRODUCTION

1.1 BACKGROUND TO THE STUDY

Nigeria is the largest crude oil producing country in Africa, the sixth petroleum giant in the Organization of Petroleum Exporting Countries (OPEC) and the eleventh in the world (Okodudu, 2007). It gained world class fame only in the year 2000 through oil production in its Niger Delta region. The Niger Delta is situated in the Gulf of Guinea and extends throughout the Niger Delta Province (Klett *et al*, 1997). From the Eocene till Recent, the delta has prograded southwestwardly, forming depobelts that represent the most active portion of the delta at each stage of its development (Doust *et al*, 1990). The present day national petroleum reserves asset of about 32 billion barrels of oil and 170 trillion standard ft³ of gas (Obaje *et al*, 2004) are derived solely from the onshore and offshore of Niger Delta Basin.

Consequently, Seismic data are routinely and effectively used to estimate the structure of reservoir bodies as well as estimating the spatial distribution of rock properties. Taner *et al*. (1994) have investigated the possible relations between individual seismic attributes and rock properties. The simultaneous use of seismic attributes with well log data leads to better prediction of reservoir or rock properties, compared to estimations using only well data (Schultz *et al.*, 1994). Furthermore, Chopra and Marfurt (2011) studied blended data and observed that the seismic attributes need to be visualized in such a way that they add maximum value to a seismic interpretation. They also observed that three dimensional (3D) visualization capabilities can be a powerful tool

to integrate different types of data. Barnes *et al.*, (2011) revealed that the combination of structural and stratigraphic attributes through volume blending with illumination enhanced structural elements in the data such as canyon walls, faults, anticlines, diapirs, channels, and other features.

Knowing fully that seismic signal features are directly caused by rock physics phenomena, the links between these two are complex and difficult to derive theoretically. Seismic response depends on many variables, such as temperature, volume of clay, overburden, pressure, nature and geometry of the layering, and other factors which affect elastic and absorption responses. These complex relations can vary from one layer to another, and even within a single layer or reservoir compartment, Schultz *et al.* (1994). Also, Schultz *et al.* (1994) showed that simultaneous use of seismic attributes with well log data leads to better prediction of reservoir or rock properties, compared to estimations using only well data.

Furthermore, hydrocarbon exploration has moved away from traditional prospecting for structural traps alone. Presently, prospects are more often defined by stratigraphic subtle traps such as channels, pinch-out, bars, reefs, onlap, valley fills and permeability barriers. The particular innovation introduced by this project is the additional value obtained by attributes co-blending. The application of co-blending attributes shall display superior images of the channels because co-blending improves imaging of geological structures and strongly defines the depositional environment.

The enhanced image of co-blended attributes shall compensate poor visualization by single attributes only.

Hence, our study aims at identifying seismic geobodies on 3-D with particular emphasis on channel geometries in shallow marine sands (offshore) Niger Delta. It is worthy to note that, sinuous channels host significant hydrocarbon reserves on a variety of continental margins according to Mayall *et al.*, (2006), which appear in our study area and they can serve as major conduits for transfer of sediments from continental shelf to deep ocean (Khripounoff *et al.*, 2003). The findings of this work will be applicable to nearby active areas in the region as well as other areas that exhibit similar challenges such as the Gulf of Mexico Basin.

1.2 STATEMENT OF THE PROBLEM

The aim of seismic amplitude analysis is to make accurate lithologic prediction from the wide spread seismic data (or observed data), based on the available well data (or known data), utilising all prior knowledge, throughout a seismic volume. To minimize reservoir lithology and structural uncertainty, we need to have high resolution seismic data. However, due to the inherent limitation of the seismic data (particularly low bandwidth) having low seismic resolution at deeper section, it is not possible to map the lithology and other structural features with confidence in far depth within the Rence field. Some information about the study area that is considered confidential to the Company is removed due to the nature of oil and gas business.

At first sight, the connection between the geology and seismic sections might seem obvious and relatively uncomplicated. Many modern seismic sections (and some of the older ones also) bear a striking resemblance to geological cross sections. But how far can we really go with such a comparison? Is it possible to translate all that we see in a seismic section into geology? The seismic system sees with a biased eye. It can only detect lithological boundaries if there is acoustic impedance contrast across the boundary and this contrast must be above the threshold unit of the seismic system. So, at best, the seismic system detects only a limited proportion of boundaries, and when these boundaries are closely spaced, interference affects the seismic response, complicating or making impossible our perception of the geology.

That the subsurface is viewed not in depth but in terms of two-way time (TWT) is a further handicap. The distortion introduced by this last factor alone makes a simple and direct link between geology and seismic sections more problematic since there is both vertical and lateral change in velocity. Also, the information gap between what was observed in the seismic section and what the geology most probably is has to be filled by the interpreter. The interpreter must be able to identify and eliminate all noise and also the interpreter must employ considerable geological skill, including knowledge of sedimentology, stratigraphy and structural geological reality.

In addition, the detection of channels and their infill lithology have always posed a challenge for exploration geologists and geophysicists, and the study area which is Rence Field in the Niger Delta Basin does not fall outside of this challenge. Hence,

channels can be difficult to detect, due to structural complexity, poor resolution and lack of skills by the interpreter.

There was no biostratigraphic information provided; this would have created good support to the field's sequence stratigraphy. However, the information provided was basic for this work.

1.3 LOCATION OF THE STUDY AREA

The Niger Delta is situated in Southern Nigeria between latitudes 4⁰N and 6⁰N and longitudes 3⁰E and 9⁰E (Nwachukwu and Chukwura, 1986, Anakwuba *et al.*, 2008). Rence field is situated within the conventional water offshore of the South East Niger Delta (Figs. 1.1 and 1.2), about 55 km from the Bonny Oil Terminal, in a water depth ranging from 60 to 100 m. The acreage has been operated from 1970 to date by the Nigerian National Petroleum Cooperation (NNPC), which drilled 4 exploratory wells, resulting in two oil/gas discoveries in deltaic to off-shelf sandstone of Pliocene age.

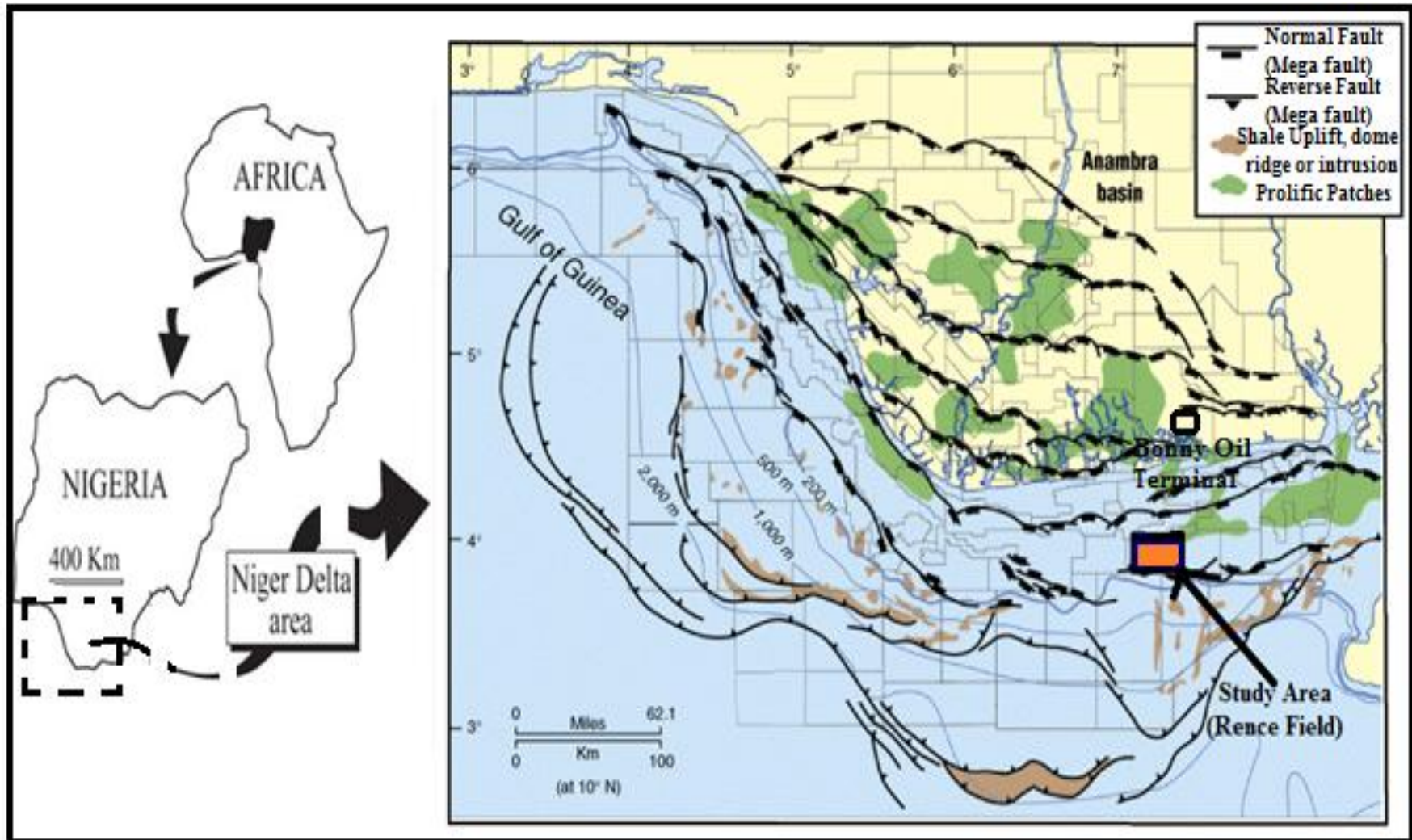


Fig.1.1: Map of Nigeria showing Niger Delta (Modified after Haack, 1997)

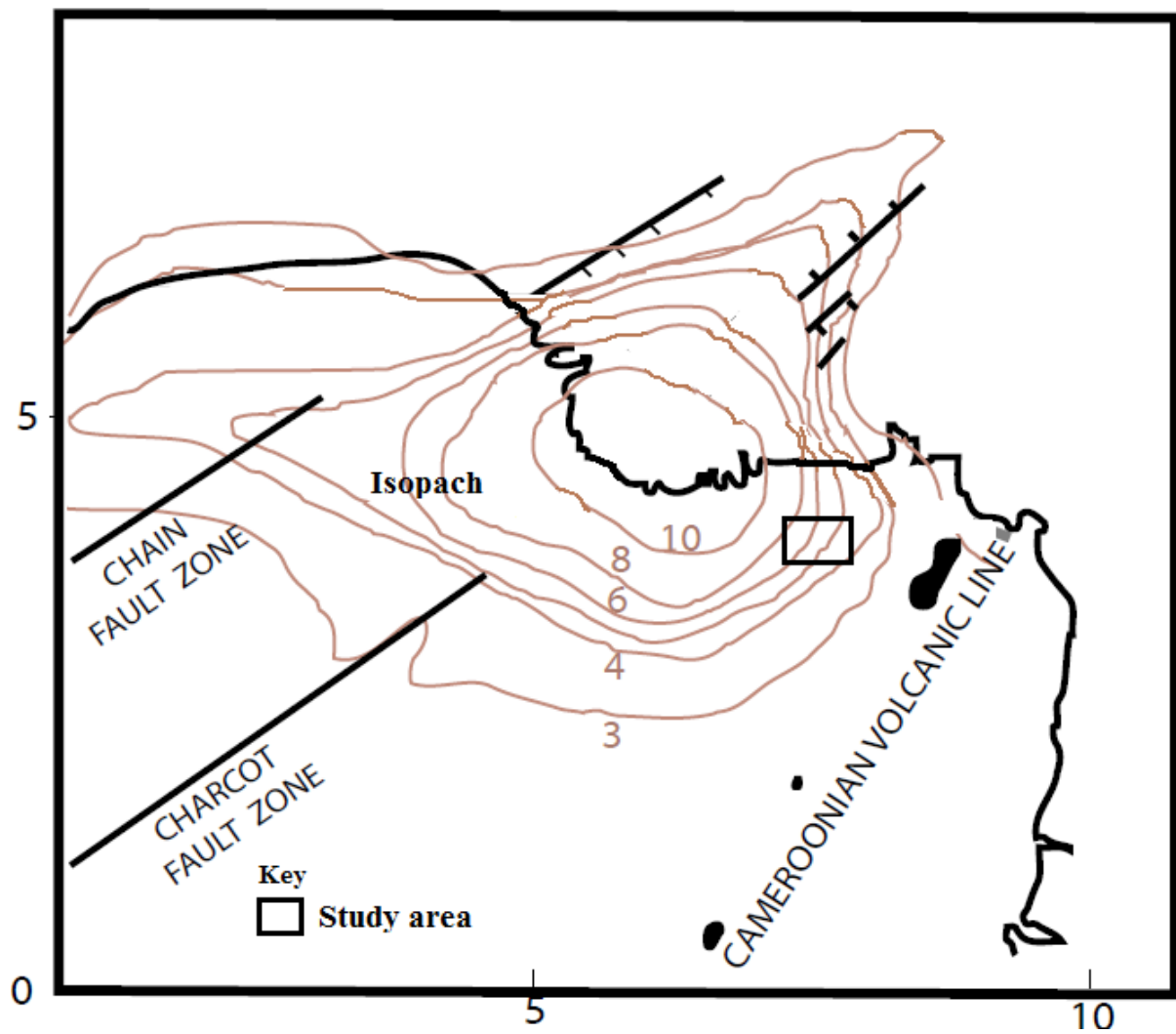


Fig.1.2: Location map of the study area (Modified after Tuttle *et al.*, 1999)

1.4 AIM AND OBJECTIVES OF THE STUDY

1.4.1 AIM OF THE STUDY

This project is aimed at co-blending of seismic attributes for interpretation of channel geometries and reservoir characteristics Rence field in the Niger Delta basin.

1.4.2 OBJECTIVES OF THE STUDY

The objectives of the study is:

1. To carry out a detailed well interpretation which includes log normalization, well correlation and well log responses.
2. To construct and generate the well-to-seismic ties within the study area.
3. To construct structural time and depth contour maps of the identified reservoir in the study area.
4. To estimate the petrophysical parameters within the study area.
5. To carryout volumetric estimation of potential reservoir in the study area.
6. To map the hydrocarbon bearing zones and hydrocarbon-water contacts.
7. To carry out 3D seismic stratigraphic interpretation, in which the structural pattern of the area is interpreted.
8. To carry out a detailed seismic facies analysis within the study.
9. To generate various seismic attributes sections and geologic models from the interpreted seismic data of the study area.

10. To generate attribute maps that will reveal stratigraphic structures and depositional environment.
11. To build reservoir model from the obtained petrophysical values within the study area.
12. To compute geometrical characteristics of the shallow marine channels identify in the study area.
13. To analyze shallow marine channel architectural elements in a Niger delta shelf environment, using architectural characteristics of the deposits filling the channels to evaluate the possible differences in the associated deposits based on the channel types.
14. To produce a depositional model for the shallow marine water of Niger delta shelf.

1.5 JUSTIFICATION OF STUDY

This study is to take a new look at seismic attributes given the considerable well control that has been acquired during the past decade. By using this well understood reservoir as a natural laboratory, we calibrate the response of various attributes to generate attribute maps that will yield visible stratigraphic traps such as channels and incised valley fills as well as aid delineation of depositional model for the study area. Furthermore, the drilling bit has encountered many seismically ‘invisible channels’ that are of economic value and the present study will definitely unveil these channels. This research will also help to bring geology and geophysics together within a

workflow that is designed to directly translate geophysical data into geological understanding.

1.6 SCOPE OF THE STUDY

The scope of this study is limited to continental shelf in shallow marine (offshore) environment of the Niger Delta, Nigeria. In this study, the co-blending attributes technique would compensate for poor visualization of the channel by single attributes only, in order to aid envisage the stratigraphic traps like channel that can accommodate huge hydrocarbon. Therefore, the focus is shifting to big single stratigraphic traps such channels and incised valley fills that would yield better value investment ratio.

1.7 SIGNIFICANCE OF THE STUDY

At the end of this research, a lot of people especially those in the petroleum sector will find the solution to the lack of identification of stratigraphic traps such as channels and incised valley fills in seismic data of any given hydrocarbon basin. Those to benefit in the study includes, the government, oil workers, future researchers and students.

The knowledge gained from the study will help the government through their agencies in the oil sector to know the oil reserves and production rate of the hydrocarbon basin within their territory for a huge economic growth. This is because oil is used for a wide range of applications, such as powering internal combustion engines, power

generation, space heating, bitumen generation, agriculture product, plastics and synthetics component.

More so, oil workers will find this new interpretational technique useful because the technique will help them in seismically defining the geometries of hydrocarbon reservoirs with particular emphasis on channels. The technique will also revealed to the oil workers how effective it is in enhancing both the ease of detection and continuity of channels as well as delineation of the depositional features.

Finally, future researchers and students who intend to undertake related study on the co-blending of seismic attributes for interpretation of channel geometries and reservoir characterization will hopefully find the study useful. Literature reviewed as well as findings from the study will present them with vital information that will adequately guide their research. More so, the findings of this work will be applicable to nearby active areas in the region as well as other areas that exhibit similar challenges such as the Gulf of Mexico Basin.

CHAPTER TWO REVIEW OF RELATED LITERATURES

2.1 LITERATURE REVIEW

The Niger Delta Basin occupies the Gulf of Guinea continental margin in equatorial West Africa between Latitudes 4⁰N and 6⁰N and longitudes 3⁰E and 9⁰E. It ranks among the world's most prolific petroleum producing Tertiary Deltas (Selley, 1997). The stratigraphy, sedimentology, structural configuration and paleo environment in which the reservoir rocks accumulated have been studied by various workers. These include Short and Stauble, 1967; Weber, 1971; Burke, 1972; Weber and Daukoru, 1975; Evamy *et al.*, 1978; Rider, 1996; Selley, 1997; Anakwuba *et al.*, 2010; Anakwuba *et al.*, 2013, Anakwuba *et al.*, 2015.

More so, the Niger Delta is a large, arcuate delta of the destructive, wave-dominated type (Weber and Daukoru, 1975). A sequence of under-compacted marine clays, overlain by paralic deposits, in turn covered by continental sands, is present throughout, built-up by the imbricated super-position of numerous offlap cycles. Basement faulting affected delta development and thus affects sediment thickness distribution. In the paralic interval, growth fault with associated rollover structures trapped hydrocarbons. Faults in general play an important role in the hydrocarbon distribution. Growth faults may even function as hydrocarbon migration paths from the overpressured marine clays.

Meanwhile, 3D Seismic data are most commonly used in the exploration world to delineate geological structures evident by continuous lateral reflection events. Brown

(2013) defined seismic interpretation as the extraction of subsurface geologic information from seismic data. He further wrote that reflection seismic data comprises of continuity of reflections indicating geologic structure; variability of reflections indicating stratigraphy, fluids and reservoir fabric; the seismic wavelet and noise of various kinds and data defects. Seismic interpretation is the thoughtful procedure of separating these effects. The interpreter is not directly interested in the wavelet itself but rather in the geological information that it carries. Thus, understanding the wavelet and distinguishing its characteristics from details of the geology is one of the critical tasks of today's interpreter. The primary task facing a seismic interpreter is to recognize and attribute a geologic significance to observable pattern in the seismic response. The most apparent patterns are found in seismic reflections. In recent years, the oil industry is using subtle patterns and connecting them to such attributes as porosity, lithology and fluid content as well as underground structure (Smith and Starcey, 2011).

More so, Oyanyan *et al.* (2012) carried out geological analysis of core samples and qualitative interpretation of wireline log shapes which aid the identification of seven depositional environments of various sand units in Sam-Bis oil field of Niger Delta Basin. These include distributary channels, mouth bar, point bar, tidal channel, tidal flat, middle shoreface and lower shoreface.

The observations reported by Bubb and Hatledid (1977) remain basically unchanged for 3D seismic data and 3D seismic attributes. Carbonate build-ups buried in shale will give rise to structural highs and positive curvature along the shallower, more

easily picked horizons. Carbonate build-ups buried in salt will appear as structural lows, giving rise to a negative curvature anomaly. Sheriff (1992) carried out a research work on amplitude variations of 3D seismic data with specific physical properties. He stated that amplitude variation of the same reflection is interpreted in terms of lateral and vertical changes in petrophysical properties and lithologies.

Omoboriowo *et al.* (2012) wrote that once an accumulation of petroleum has been discovered, it is better to characterize the reservoir as accurately as possible in order to calculate the reserves and to determine the most effective way of recovering as much of the petroleum as possible. Hence, Tinker (1996) defined reservoir characterization as the quantification, integration, reduction and analysis of geological, petrochemical, seismic and engineering data.

Adeogba *et al.*, (2005) have interpreted a near surface, 3D seismic data set from the Niger Delta continental slope, offshore Nigeria and revealed important stratigraphy and architectural features. Architectural features and sediment deposits interpreted from seismic character and seismic stratigraphy in the absence of borehole data include mass transport complexes, distributary channels, submarine fans and hemipelagic drape complex. Also, Siddiqui *et al.*, (2013) revealed that depositional environment of shallow-marine sandstones have been regarded as tide dominated, wave dominated and storm dominated which reveals the reservoir heterogeneities and variation in sand body geometry.

Pokhriyal (2011) wrote that seismic resolution (or bandwidth) plays an important role for better visualization or quantification of interesting geological features in interpretation, which helps in reducing the exploration risk. It is difficult to extract the embedded geological information in the seismic data having a low seismic bandwidth. Thus application of seismic attribute generation and analysis will provide a better result in such type of seismic data (low bandwidth). He further wrote that a new seismic attribute volume has been generated using a mathematical relation, which provides an improved mapping of morphological features (for example, pinch outs, faults, channels etc.) and reflectivity (for example, lithology, reservoir thickness etc.) components of seismic data with geological objects and also explain the observed results at a set of wells.

Furthermore, the seismic data is treated as an analytic trace which contains real components (original input trace) and the complex (imaginary) component, usually generated from the Hilbert transforms from which various amplitudes, phase and frequency attributes can be deduced (Ayolabi and Adigun, 2013). This complex trace allows the amplitude, phase, frequency and reflector polarity attributes of a seismic data to be calculated in a rigorous mathematical sense. Subrahmanyam (2008) also wrote that Seismic attributes are the components of the seismic data which are obtained by measurement, computation, and other methods from the seismic data. Seismic Attributes were introduced as a part of the seismic interpretation in early 1970's. Since then many new attributes were derived and computed. Most of these

attributes are of commercial interest and the use of many of the attributes, are yet to be understood by many interpreters and users.

Mehdi and De-Hua (2011) stated that a method for 3D modeling and interpretation of log properties from complex seismic attributes (obtained from 3D post stack seismic data) is developed by integrating Principal Component Analysis and Local Linear Modeling. Complex seismic attributes have non-linear relationships with petrophysical properties of rocks. These complicated relationships can be approximated using statistical methods. This method has been tested successfully on real data sets.

Aizebeokhai and Olayinka (2011) used structural and stratigraphic mapping of Emi field, offshore Niger Delta to assert that oil and gas are predominantly trapped in sandstones and unconsolidated sands in the Agbada formation of Niger Delta, ranked among the world's major hydrocarbon provinces. In their study, seismic data were integrated with well logs to define the subsurface geometry, stratigraphy and hydrocarbon trapping potential of Emi-field, off shore Niger Delta.

Furthermore, Bahorich and Farmer (1995) stated that their coherence methodology was the first published method of revealing fault surfaces within a 3D volume for which no fault reflections had been recorded. Their volume of coherence coefficients computed from the seismic amplitudes on adjacent traces using a crosscorrelation technique, clearly portrayed faults and other stratigraphic anomalies on time and

horizontal slices. The coherence images distinctly revealed buried deltas, river channels, reefs, and dewatering features.

According to Dan and Robert (1996), attribute analysis of 3-D seismic data in time slices presents a great opportunity for reservoir characterization. The interpretable information of the 3-D seismic data can be enhanced with complex seismic trace attributes. The correlation between various P-wave seismic attributes and lithology has been used for some time; however, the multi component seismic techniques promise augmented development.

Marfurt *et al.* (1998) wrote that seismic coherency is a measure of lateral changes in the seismic response caused by variation in structure, stratigraphy, lithology, porosity, and the presence of hydrocarbons. Unlike shaded relief maps that allow 3-D visualization of faults and channels from horizon picks, seismic coherency operates on the seismic data itself and is therefore creative by interpreter or automatic picker biases. They wrote further by saying that the calculation of reflector dip/azimuth throughout the data volume allows them to generalize the calculation of conventional complex trace attributes (including envelope, phase, frequency, and bandwidth) to the calculation of complex reflector attributes generated by slant stacking the input data along the reflector dip within the coherency analysis window.

Liu and Marfurt (2007) reported that the use of instantaneous spectral attributes which were derived from using the short-window discrete Fourier transform (SWDFT) are

excellent method or tool for mapping channels along interpreted horizons. They wrote that channels filled with porous rock and encased in a nonporous matrix constitute one of the more important stratigraphic exploration plays. Although attributes such as coherence can be used to map channel width, they are relatively insensitive to channel thickness. In contrast, spectral decomposition can be used to map subtle changes in channel thickness. Because they are interested in mapping high-reflectivity channels encased in a lower-reflectivity matrix, they found that a composite plot of the peak frequency and the average peak amplitude accentuates highly tuned channels. Finally, by generating a composite volume using peak frequency, peak amplitude, and coherence, they were able to establish not only the channel thickness, but also its width.

According to Chopra and Marfurt (2007) coherence is a measure of similarity between waveforms or traces. Peyton et al. (1998) showed the use of edge detection attribute to identify channel boundaries in the Red Fork level by comparing the horizon slice with a modern coherence algorithm. Their result also show additional features and enhances the channel levee.

In addition, Sigismondi and Soldo (2003) revealed that curvature attribute maps are powerful tool for visualization and interpretation of structural features. They also carried out a comparison between common dip attribute and various curvature attributes has been made in order to highlight the main differences between them. In

both cases, a higher contrast in the curvature attribute helps to better identify the fault system.

Klein *et al.* (2008) wrote on 3D curvature attributes, a new approach for seismic interpretation and they disclosed that the proposed new technique was to compute volumetric curvature attributes in a single step, without requiring any pre-computation of intermediate volumes such as dip and azimuth. Curvature attributes allow quantifying and qualifying lateral continuity of the fault and its vertical displacement. They supported the analysis of structural traps occurring against faults. Hence, the qualitative and quantitative information extracted from the curvature attributes yielded a huge result in mapping of fracture density and orientation. As a future perspective, a post processing of the curvature attributes may be implemented in order to sort out singular geological lineament orientations. This approach could also be used to remove non-geological lineaments such as acquisition footprints. The curvature attributes can augment the coherency attribute in the analysis of the geological scheme.

Chopra (2008) reveals that seismic attributes extract information from seismic reflection data which can be used for quantitative and qualitative interpretation. He said that attributes are used by geologists, geophysicists, and petrophysicists to map features from basin to reservoir scale. Some attributes, such as seismic amplitude, root mean square (RMS) amplitude, spectral magnitude, acoustic impedance, elastic impedance, and average energy are directly sensitive to changes in seismic

impedance. Other attributes such as peak-to-trough thickness, peak frequency, and bandwidth are sensitive to layer thicknesses. Also, he wrote that seismic attributes such as coherence, Sobel filter-based edge detectors, amplitude gradients, dip-azimuth, curvature, and gray level co-occurrence matrix measures are directly sensitive to seismic textures and morphology.

Chopra and Marfurt (2011) studied on blended data and observed that the seismic attributes need to be visualized in such a way that they add maximum value to a seismic interpretation. They also observed that 3-D visualization capability can be a powerful tool to integrate different types of data. Considering the well log curves, vertical sounding profile (VSP) data or micro seismic data also can be brought together in 3-D views to provide visual corroboration of data information and to build higher levels of confidence in interpretations.

Yenugu *et al.* (2011) wrote on seismic attribute mapping for identification of Cypress Sands, Illinois Basin, Indiana, USA. They used modern 3D visualization tools of opacity and Hue-Lightness-Saturation (HLS) color modulation to co-render complementary seismic attributes along stratal slices at 2ms intervals. Such co-rendering allows them to interactively cluster mathematically independent attributes that are coupled through the same geologic features (e.g. low impedance with lower peak frequency). They present their findings through a suite of multi-attribute displays and animations loops through the data volume to highlight the subtle lenticular sand bodies associated with structural faults/ridges characteristic of braided channels.

Chopra and Marfurt (2012) reported that Channel features are often identified by their meandering and dendritic morphology on maps. They said that positive curvature anomalies over channel features indicate that these channels are filled with a lithology that is less compactable than the surrounding matrix, indicating the presence of sand. Negative curvature anomalies over channel features are more problematic. If the channels are in near-shore environment and have been filled by rising sea level, there is a very high probability that they are filled with shale, indicating that sand should be found in the surrounding, less-compacted point bars and levees that often express a positive curvature anomaly.

Urazimanova *et al.* (2013) carried out a research work on iterative depositional model interpretations using seismic attributes. They revealed that channel morphology was best delineated by the variance attribute which helped better understand and construct more precise depositional models of the formations in the area. On the other hand, RMS amplitude and negative energy attributes helped clustering and delineating the same lithologies within the meandering channels, which in turn separated sands from mud and shale.

Li *et al.*, 2013 carried out research in order to examine the oil resource potentials, reservoir characteristics, and oil chemistry/physical properties of Eocene-Oligocene Shahejie Formation in the Jiyang Super-depression, Bohai Bay Basin of in eastern China. They revealed several significant differences between the lacustrine and

marine shale systems. These include (1) the greater heterogeneities in lacustrine sediments and more limited connectivity between source and conventional reservoirs in the distal portions of lacustrine systems; (2) the close proximity to terrestrial source that creates opportunity for higher plant contribution and more waxy oils from lacustrine source rocks in oil window; (3) the relatively narrow but generally higher activation energy range in the kinetics of hydrocarbon generation from type I kerogens in carbonate-rich lacustrine kinetics that have clear implications for kerogen-oil interaction behavior, oil flow characteristics, and gas to oil ratio within the lacustrine system; (4) high temperature thermochemical sulphate reduction that tend to form significant amounts of hydrogen sulphide, with various undesirable effects.

2.2 REGIONAL GEOLOGY OF THE NIGER DELTA

The Niger Delta region of Nigeria is among the world's largest petroleum provinces and its importance lies on its hydrocarbon resources (Amadi *et al.*, 2012). The Niger Delta region of Nigeria is the most prolific and advantageous sedimentary basin in Nigeria due to its world class petroleum accumulations.

The Niger delta is one of the world's largest deltaic systems. The delta covers an approximate area of about 300,000 km² (Kulke, 1995), with sediment volume of 500,000 km³ (Hospers, 1965) and sediment thickness ranging between 9,000 and 12,000 m. The delta extends more than 300 km from apex to mouth (Doust and Omatsola, 1990). Galloway (1975) classified the Niger delta as a wave- dominated tidal-influenced delta. The Niger delta is bounded to the north by the Anambra Basin,

to the west by the Okitipupa High and the Benin Flank, and to the east by the volcanic rocks of the Cameroon volcanic zone (Fig. 2.1). There was an original paleo-high that separated the eastern from the western delta, but that has been covered with sediments over a very long period of time.

The Niger delta is an overall regressive sequence (Fig. 2.2) formed by an interplay between the rate of deposition or sediment supply and the rate of subsidence or accommodation space creation. For this delta, the rate of deposition far exceeded the rate of subsidence, which resulted in an overall progradational delta (Knox and Omatsola, 1989). Major submarine canyons delivered sediments from the shelf edge into the deep-water environment. Some of the canyons are: Lagos, Avon and Mahin in the west, Niger canyon at the center, and Kwa Ibo and Calabar in the east (Fig. 2.3).

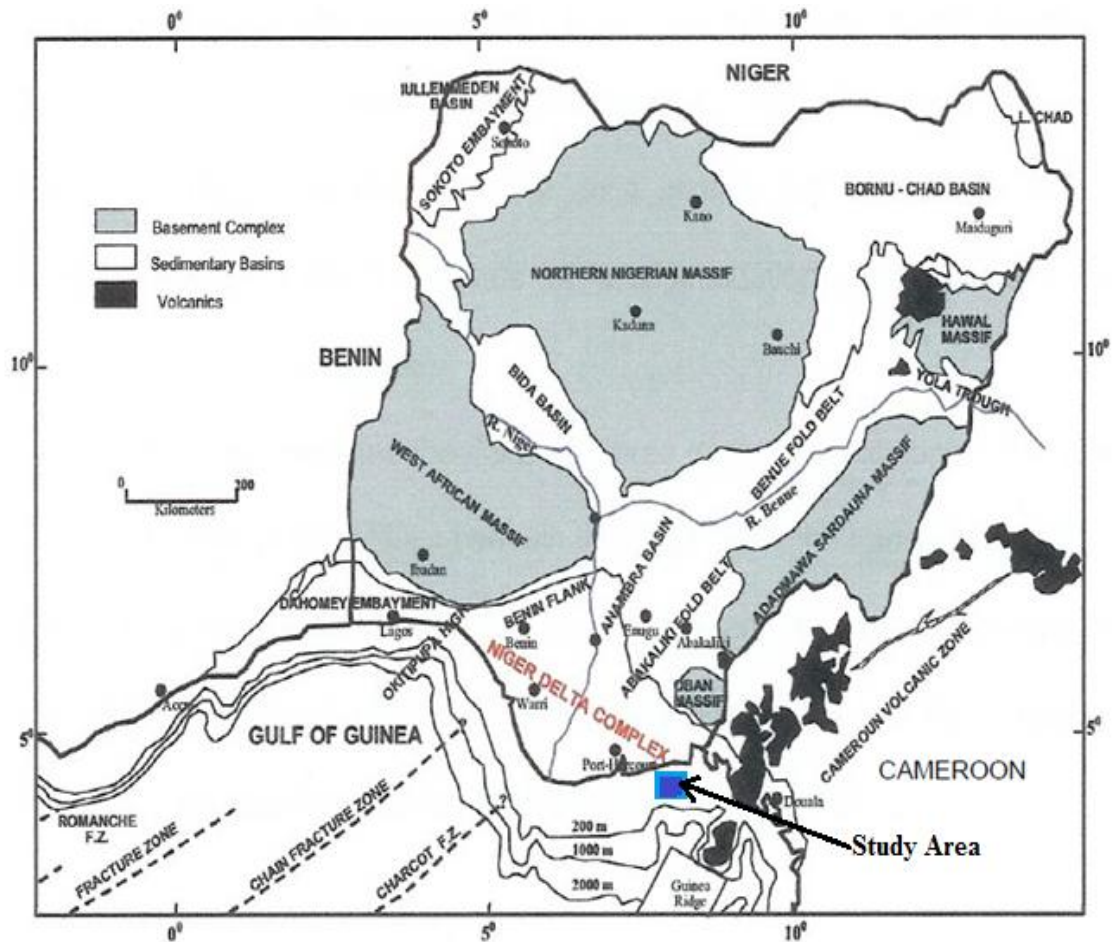


Fig. 2.1: Geologic map of Nigeria showing Niger Delta basin and its relation to bounding structural feature (Whiteman, 1982).

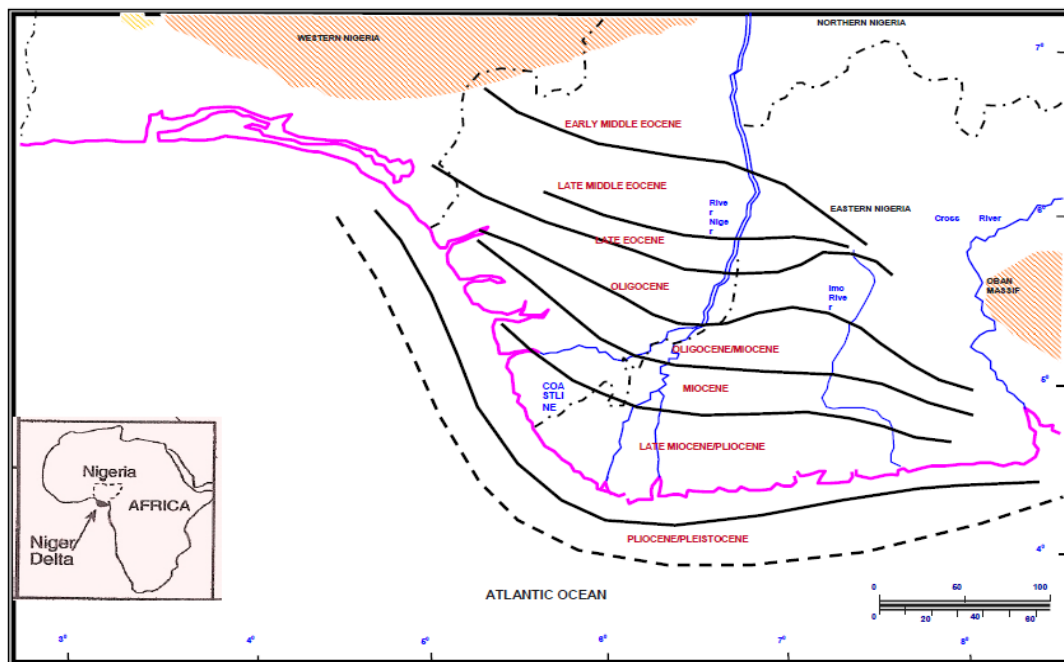


Fig. 2.2: Niger delta basin and its stages of development (After Short and Stauble, 1967).

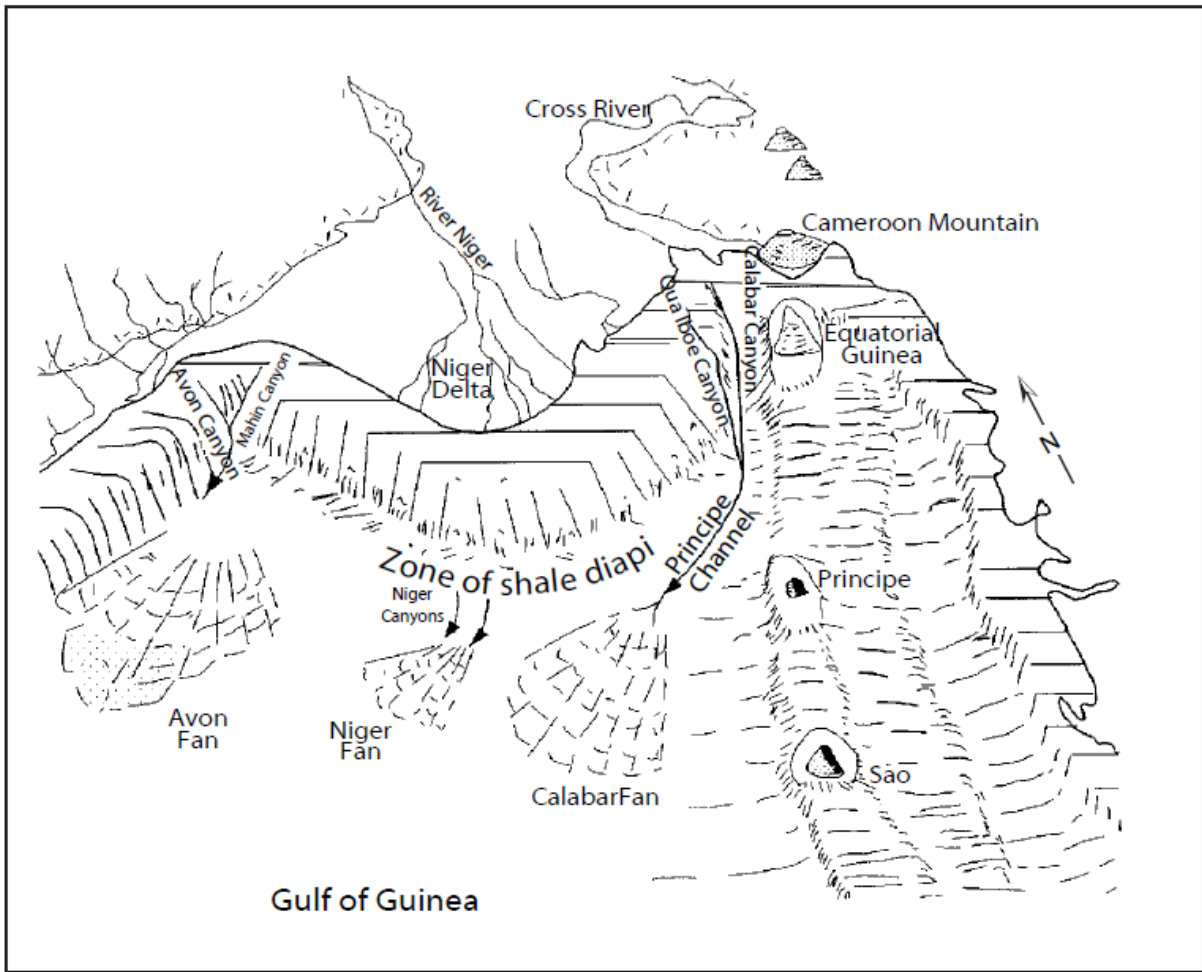


Fig. 2.3: Physiographic sketch of the deep marine sediments in the Gulf of Guinea off the Niger Delta (After, Burke, 1972 and Reijers et al., 1997)

2.3 TECTONIC EVOLUTION

The Niger Delta Basin is situated on the coastal and oceanward part of a much larger and older tectonic feature, the Benue Trough, which is a NE-SW folded rift basin that runs diagonally across Nigeria. The tectonic framework of the continental margin along the west coast of equatorial Africa is controlled by Cretaceous fracture zones expressed as trenches and ridges in the deep Atlantic (Fig. 2.1). The fracture zone ridges subdivide the margin into individual basins, and in Nigeria, from the boundary faults of the Cretaceous Benue – Abakiliki trough that cuts far into the West African shield. The trough represents a failed arm of a triple junction associated with the opening of the South Atlantic. In this region, rifting started in the Late Jurassic and persisted into the Middle Cretaceous (Lehner and De Ruiter, 1977). The subsidence that occurred along fundamental transform faults is the landward continuation of the Chain and Charcot ocean fracture zones (Doust and Omatsola, 1990). In the Niger Delta, rifting diminished altogether in the Late Cretaceous.

After rifting ceased, gravity tectonics became the primary deformational process. Shale mobility induced internal deformation and occurred in response to two processes (Kulke, 1995). First, shale diapirs formed from loading of poorly compacted, over-pressured, prodelta and delta-slope clays (Akata Formation.) by the higher density delta-front sands (Agbada Formation.). Second, slope instability occurred due to a lack of lateral, basinward, support for the under-compacted delta-slope clays (Akata Formation).

For any given depobelt, gravity tectonics were completed before the deposition of the Benin Formation and are expressed in complex structures, including Shale diapirs, rollover anticlines, collapsed growth faults crests, back to back features and steeply dipping, closely spaced flank faults (Evamy *et al.*, 1978; Xiao and Suppe, 1992). These faults mostly offset different parts of the Agbada Formation and flatten into detachment planes near the top of the Akata Formation.

2.4 STRUCTURAL STYLES

The influence of basement tectonics on the structural evolution of the Niger Delta was largely limited to movements along the Equatorial Atlantic Ocean fracture zones, which extend beneath the delta and determines the initial locus of the proto Niger Delta in the Benue Trough (Short and Stauble, 1967; Doust and Omatsola, 1990; Reijers *et al.*, 1997). As the Delta advanced onto thinned continental crust and possibly later onto actual oceanic crust, continuous subsidence and thinning of the basement created more space for the thick sedimentary pile of the prograding Cenozoic Niger Delta (Doust and Omatsola, 1990). On the eastern flank of the Niger Delta Basin, uplift of the Cameroon volcanic ranges provided the dominant sedimentary source into the Cross River Delta (Rio Del Rey Basin).

Growth faults, triggered by a pene-contemporaneous deformation of deltaic sediments, are the dominant structural features in the Niger Delta (Doust and Omatsola, 1990). They are generated by rapid sedimentation load and the gravitational instability of the Agbada sediment pile accumulating on the mobile, under-compacted Akata Shales. There is little

or no growth faulting extending into the Benin Formation due to its occurrence and sedimentation. Toe thrusting at the delta front, lateral flow and extrusion of the Akata prodelta Shales during growth faulting and related extension also account for the diapiric structures on the continental slope of the Niger Delta in front of the prograding depocentre with paralic sediments (Doust and Omatsola, 1990).

Growth faults comprise synthetic faults and the major structure building faults (some of which bound the depobelts) steep, parallel crestal faults which cut the rollover structures associated with the structure building faults are the rollover anticlinal structures (Doust and Omatsola, 1990).

The complexity of these structures is dependent on the overall sediment burden; in the initial phases of growth faulting displacement only occurs along the major bounding faults. With increased overburden and increased horizontal displacement accommodation becomes more complex and finally occurs along numerous small faults, which form the typical collapsed crest structures (Fig 2.4).

2.5 LITHOSTRATIGRAPHY

The Cretaceous section has not been penetrated beneath the Niger Delta, the youngest and the southernmost sub-basin in the Benue - Abakiliki trough (Reijers *et al.*, 1997). Lithologies of Cretaceous rocks deposited in what is now the Niger Delta Basin can only be extrapolated from the exposed Cretaceous section in the next basin to the northeast – the Anambra Basin (Fig. 2.5).

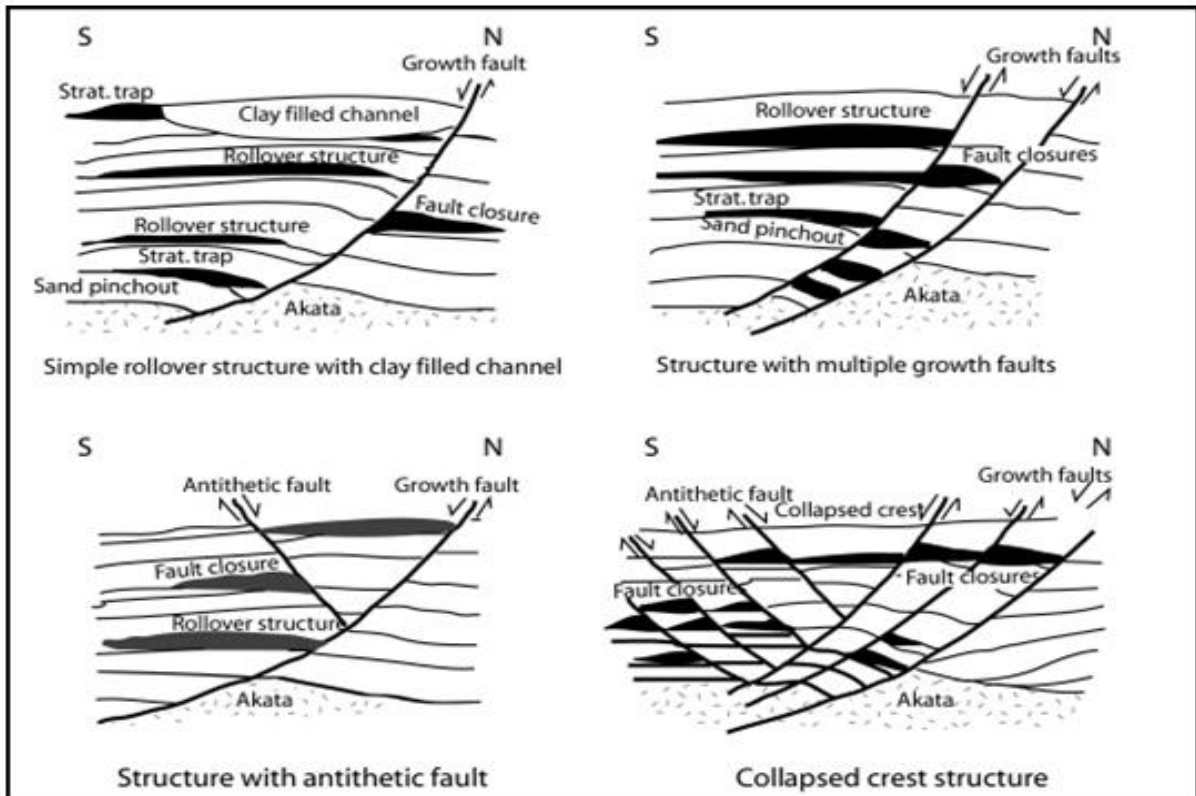


Fig 2.4 Examples of Niger Delta Oil field structures and associated trap types (After Doust and Omatsola, 1990 and Statcher, 1995).

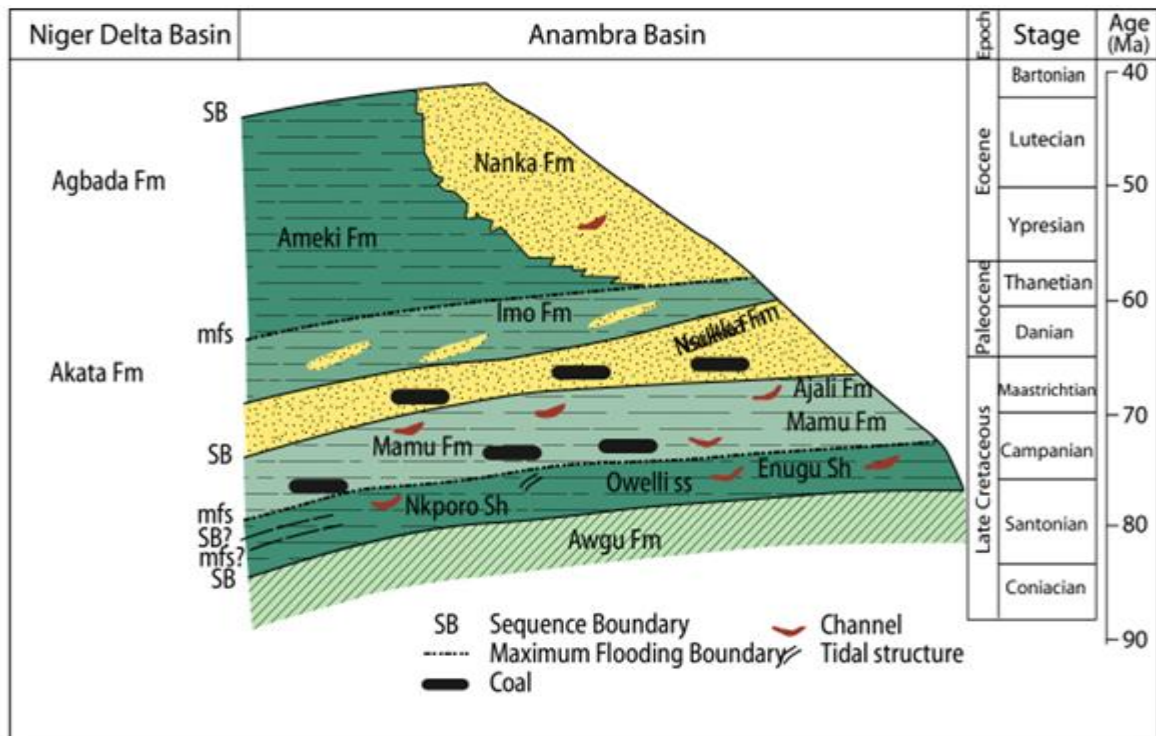


Fig 2.5: Stratigraphic section of the Anambra Basin and time equivalent formations in the Niger Delta (Adapted from Reigers *et al.*, 1997)

From the Campanian through the Paleocene (Fig 2.5), the shoreline was concave into the Anambra Basin, resulting in convergent long shore drift cells that produce tide-dominated deltaic sedimentation during transgressions and river-dominated sedimentation during regressions. Shallow marine classics were deposited farther offshore and in the Anambra Basin, are represented by the Albian – Cenomanian ASU River Group, Cenomanian-Santonian Eze-Aku and Awgu Shales and Campanian - Maastrichtian Nkporo Shales, among others (Reijers *et al.*, 1997). In the Paleocene, a major transgression began with the Imo Shale being deposited in the Anambra Basin to the northeast and the Akata Shale in the Niger Delta area to the southwest. In the Eocene, the coastline shape became convexly curvilinear, the long shore drift cells switched to divergent and sedimentation changed to being wave dominated. At this time, deposition of paralic sediments began in the Niger Delta area proper and as the sediments prograded south, the coastline became progressively more convex seaward.

Hence, the lithologies of the area experience changes due to several factors. One factor would be the types of sediment coming through the delta, which could be influenced by sea level, or maybe volcanic activity in the area. The type of environment of deposition will also change the sediment type. The early Cretaceous sediments were thought to be from a tide dominated system that were deposited on a concave shoreline, and throughout time the shoreline has become convexed and it is currently a wave dominated system.

The Tertiary section of the Niger Delta is divided into three formations (Fig. 2.6), representing prograding depositional facies that are distinguished mostly on the basis

of sand/shale ratios. The type sections of these formations are described in Short and Stauble (1967) and summarized in a variety of papers (e.g. Avbobvo, 1978; Doust and Omatsola, 1990; Kulke, 1995).

2.5.1 Akata Formation

The Akata Formation at the base of the delta is of marine origin and is composed of thick shale sequences (potential source rock), turbidite sand (potential reservoirs in deep water) and minor amounts of clay and silt. Beginning in the Paleocene and through the recent, the Akata Formation formed during lowstands when the terrestrial organic matter and clays were transported to deep water areas characterized by low energy conditions and oxygen deficiency (Stacher, 1995).

Though little of the formation has been drilled, it is estimated to be up to 7000 meters thick (Doust and Omatsola, 1990). The formation underlies the entire delta and is typically overpressured.

2.5.2 Agbada Formation

The deposition of the overlying Agbada Formation, the major petroleum-bearing unit began in the Eocene and continues into the Recent. The formation consists of paralic siliciclastics over 3700m thick (Tuttle *et al.*, 1999) and represents the actual deltaic portion of the sequence. The classics accumulated in delta front, delta top set and fluvio-deltaic environment. In the lower Agbada Formation, shale and sandstone beds were deposited in equal proportions; however, the upper portion is mostly sand with only minor shale interbeds.

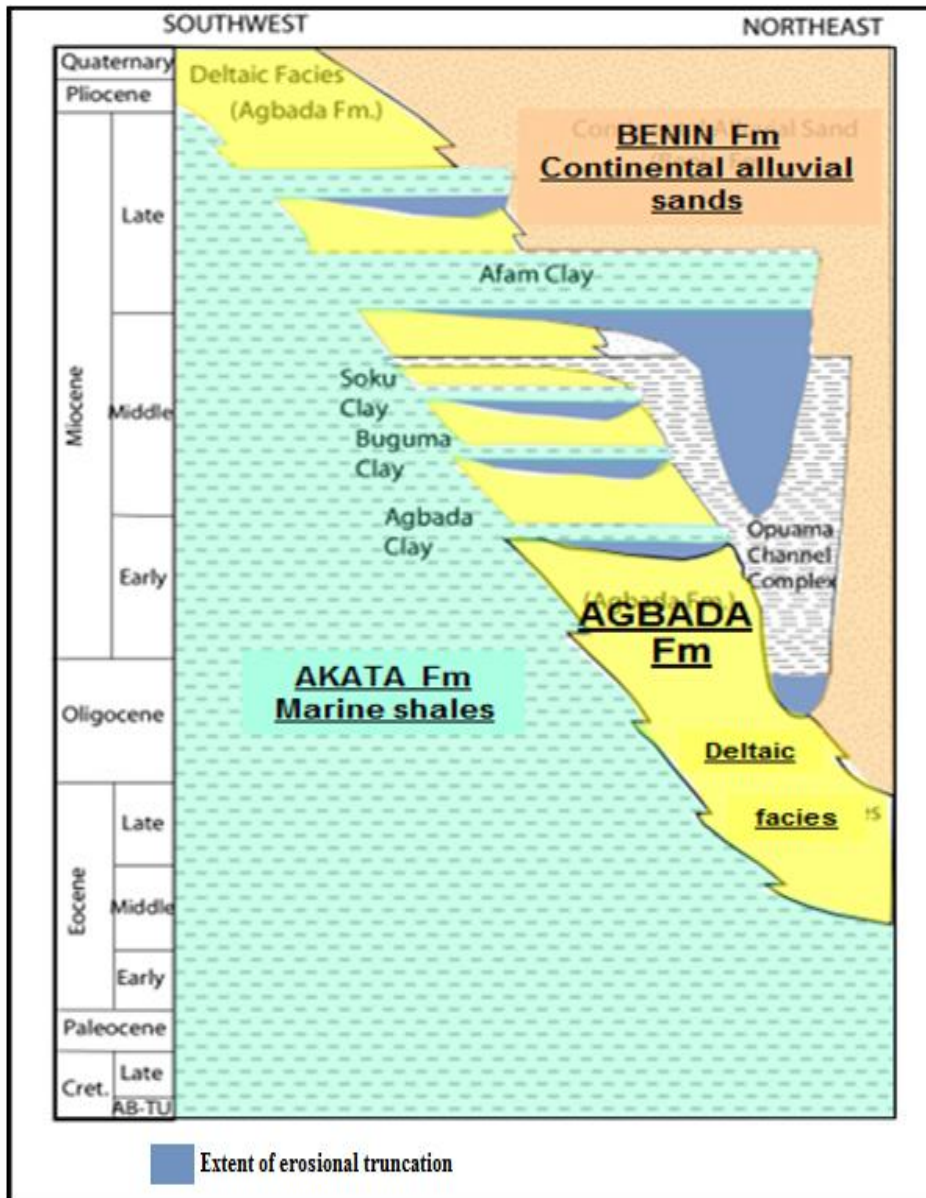


Fig 2.6: Lithostratigraphic section of Niger Delta (Adapted from Tuttle *et al.*, 1999)

2.5.3 Benin Formation

The Benin Formation, an upper delta – top lithologies, overlies the Agbada Formation. It consists of predominantly massive, highly porous, fresh water-bearing sandstones with local thin shale interbeds that are considered to be of braided stream origin. The formation is up to 2000 m thick and ranges from Late Eocene to Recent in age (Avbobvo, 1978). Most companies exploring for oil in the Niger Delta arbitrarily define the base of the formation by the deepest fresh water bearing sandstones that exhibit high resistivity. However, Short and Stauble (1967) defined the base of Benin Formation by the appearance of first marine foraminifera within shales, as the formation is non-marine in origin.

2.6 EVOLUTION OF DEPOBELTS

The deposition of the three formations of the Tertiary Niger Delta occurred in each of the five off-lapping siliciclastic sedimentation cycles that comprise the Niger Delta. These cycles (depobelts) are 30-60 km wide, prograde southwestward 250 km over the oceanic crust into the Gulf of Guinea (Stacher, 1995) and are defined by synsedimentary faulting that occurred in response to variable rates of subsidence and sediment supply (Doust and Omatsola, 1990). The interplay of subsidence and supply rates resulted in deposition of discrete depobelts when further crustal subsidence of the basin could no longer be accommodated, the focus of sediment deposition shifted seaward, forming a new depobelt. Each depobelt is a separate unit that corresponds to a break in regional dip of the Delta and is bounded landward by growth faults and seaward by large counter-regional faults or the growth faults of the next seaward belt

(Evamy *et al.*, 1978; Doust and Omatsola, 1990). Generally six major depobelts are recognized in the Niger Delta (Fig. 2.7). They include Northern Delta, Greater Ugheli, Central Swamp I and II, Coastal Swamp and Offshore depobelts. Each of these has its own sedimentation, deformation and petroleum history.

Doust and Omatsola (1990) described three depobelt provinces based on structure. The Northern Delta province that overlies relatively shallow basement has the oldest growth faults that are generally rotational, evenly spaced and increased steepness seaward. The Central Delta province has depobelts with well-defined structures such as successively deeper rollover crests that shift seaward for any given growth faults. Lastly, the Distal Delta province is the most structurally complex due to the internal gravity tectonics on the modern continental slope.

2.7 EVOLUTION OF SEQUENCES

From the Eocene onwards, the long-term eustatic sea level curve reflects global regression, which caused the Niger Delta to prograde (Fig. 2.7). Periodic eustatic rises interrupted this trend resulting in transgression with temporary landward shift of the palaeo-coastline and formation of delta-wide depositional wedges of marine clay that grade up dip into fluvial clays. Compaction, clay movement and/or growth faulting locally triggered autocyclic sedimentation.

As a result, the Cenozoic Niger Delta is a composite of fills with localized depocentres bounded by macro and mega structures and its evolution driven by autocyclic processes. The results are characteristic progradational, aggradational and retrogradational stacking patterns of deltaic parasequences.

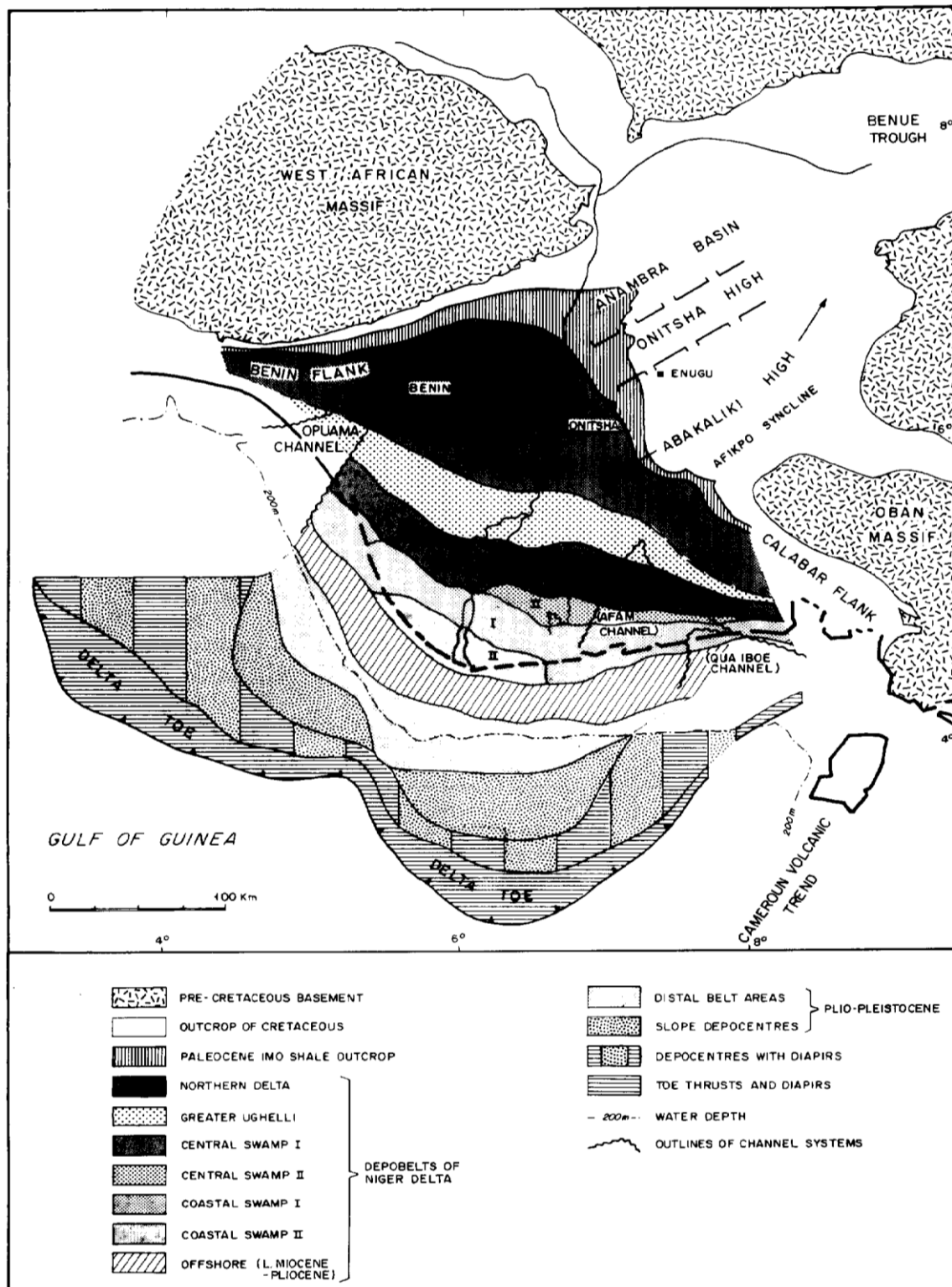


Fig. 2.7 Regional structural elements and depobelts of the Niger Delta

(After, Doust and Omatsola, 1990)

The Niger Delta sediments span a period of 54.6 Ma during which third-order eustatic sea level rises have been recognized. Correlation with Harland *et al* (1992) confirms the presence of nineteen of such named marine flooding surfaces in the Niger Delta. Eight of these are only locally developed. Eleven define lithological mega-units with regionally mappable transgressive shale markers traceable across depobelt boundary faults. These units are the genetic sequences which can be used as a basis for lithostratigraphy in the Niger Delta (Reijers *et al.*, 1997). Next to the genetic sequences are other sequences that are bounded and defined by seismically detectable erosional features (Vail, 1987). The Niger Delta incised valleys or ‘channels’ with depths up to several hundreds feet and widths of several kilometers are example of these features. Erosive cutting of the channel took place during a sea level lowstand and infilling during the initial slow, later rapid rise in sea level. Variable sediment supply and sea level fluctuations filled these channels with a range of sands, heteroliths and mudstones. Both Vail (1987) and Galloway (1975) sequences are recognized elsewhere but the Niger Delta sequence stratigraphic and lithostratigraphic framework is based on the genetic sequence.

2.8 PETROLEUM GEOLOGY

The Niger Delta holds enormous petroleum reserves, estimated recently at about 34.5 billion barrels of oil and 93.8 trillion cubic feet of gas (Petroconsultants, 1996). The source rock of hydrocarbon in the basin is certainly shales of the Akata Formation. The hydrocarbons generated in the Akata Formation definitely migrated up dip

through growth faults to accumulate in shallow reservoirs of the Agbada Formation.

The petroleum geology of the Delta is discussed below:

2.8.1 Source Rock

The hydrocarbon source rock in the Niger Delta has been discussed extensively. Possibilities include variable contributions from marine interbedded shales in the Agbada Formation, the marine Akata Shales, and Cretaceous Shales (Ekweozor and Okoye, 1980; Stacher, 1995; Haack *et al.*, 1997). The Cretaceous section has never been drilled beneath the delta due to its great depth; therefore, no data exist on its source-rock potential. Also migration of oil from the Cretaceous section into the reservoirs in the Agbada would have required an intricate faults/fracture network, as the Akata Shale is very thick. No data exist to support such a network of fracture. Although, the Agbada Formation has intervals that contain organic carbon contents sufficient to be considered good source rocks, the intervals, however, rarely reach thickness sufficient to produce a world class oil province and is immature in various parts of the Delta (Stacher, 1995). The Akata Shale is present in large volumes beneath the Agbada Formation and is at least volumetrically sufficient to generate enough oil for a world-class oil province such as the Niger Delta.

2.8.2 Reservoir Rock

Petroleum in the Niger Delta is produced from sandstones and unconsolidated sands predominantly in the Agbada Formation. Known reservoir rocks are Eocene to Pliocene in age, ranging from 15 to 45meters in thickness (Tuttle *et al.*, 1999). The

grain size of the reservoir sandstone is highly variable with fluvial sandstones tending to be coarser than their delta front counterparts, point bars fine upward and barrier bars do have the best grain sorting. Porosity only slowly decreases with depth because of the young age of the sediment. In the outer portion of the delta complex, deep-sea channel sands, low-stand sand bodies and proximal turbidites create potential reservoirs (Beka and Oti, 1995). Burke (1972), Damuth and many others described three deep-water fans (namely, Avon fan, Niger fan and Calabar fan) that are likely to be active through much of the Delta's history (Fig. 2.3).

2.8.3 Traps and Seal

Most known traps in the Niger Delta are structural, although stratigraphic traps are not uncommon (Fig. 2.3). The structural traps developed during synsedimentary deformation of the Agbada paralic sequence (Stacher, 1995). Doust and Omatsola (1990) described a variety of structural trapping elements including those associated with simple rollover structures, clay filled channels, structure with multiple growth faults, antithetic faults and collapsed crest structures. Also stratigraphic traps related to palaeo-channel fills, regional sand pinchouts and truncation occur. The primary seal rock in the Niger Delta is the interbedded shale within the Agbada Formation. The shale provides three types of seals; clay smears along faults, interbedded sealing units against which reservoir sands juxtaposed due to faulting and vertical seal (Doust and Omatsola, 1990).

2.8.4 Petroleum Maturation and Migration

Evamy *et al.* (1978) set the top of the present-day oil window in the Niger delta at the 240⁰F (115⁰C) isotherm. In the northwestern portion of the delta, the oil window (active source-rock interval) lies in the upper Akata Formation and the lower Agbada Formation as shown in Fig. 2.8. To the southeast, the top of the oil window is stratigraphically lower (Evamy *et al.*, 1978).

Migration from the lower Agbada Formation into the reservoir rocks is through conduits of deep-seated regional and counter-regional extensional faults. However, migration from mature, overpressured shales is similar to that described from overpressured shales in the Gulf of Mexico. Migration in these basins really occurs from a structurally low area to a higher area in the subsurface because of the relative buoyancy of hydrocarbons in comparison to the surrounding rock.

Hunt (1990) related episodic expulsion of petroleum from abnormally pressured, mature source rocks to fracturing and resealing of the top seal of the overpressured interval. This type of cyclic expulsion is plausible for the Niger delta basin where the Akata Formation is overpressured.

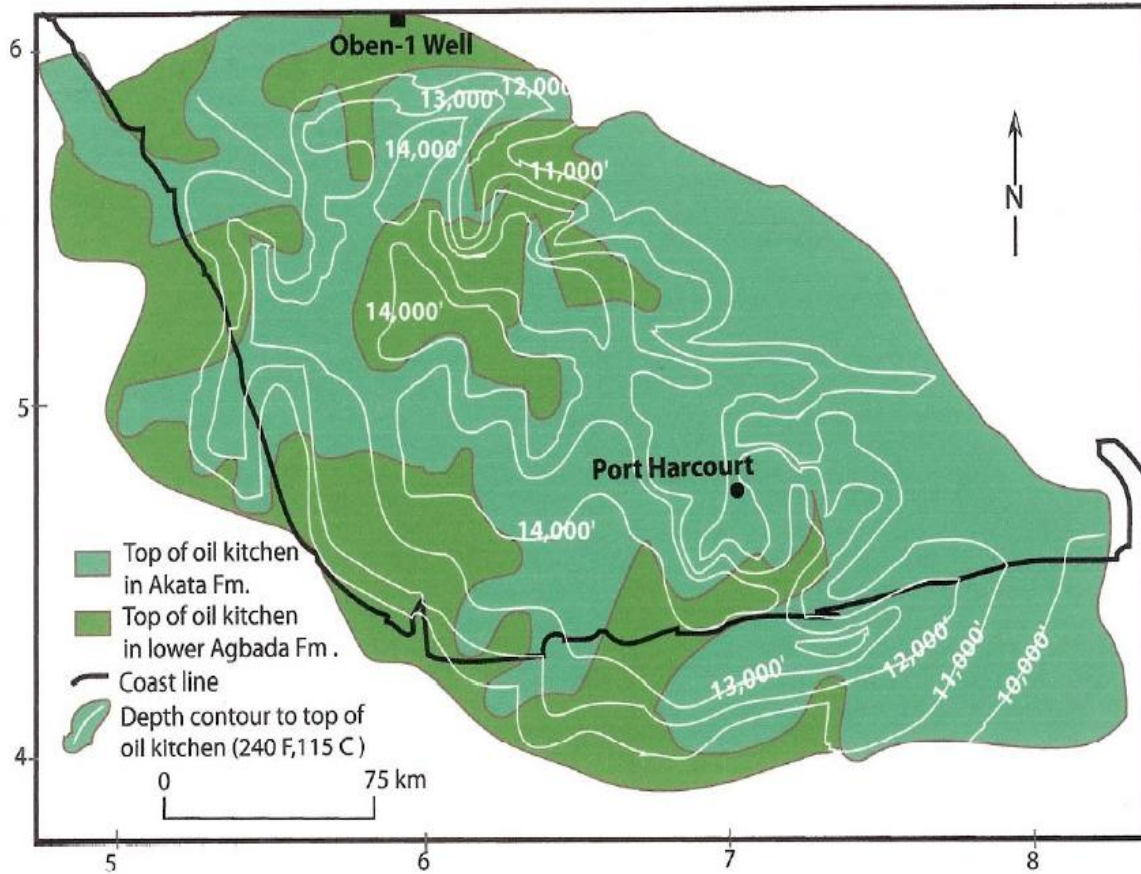


Fig. 2.8: Subsurface depth map of the Niger Delta Basin (contours are in feet) (Evamy *et al.*, 1978; Tuttle *et al.*, 1999).

2.9 CHANNEL FEATURES

Channel floors are often incised by a relatively narrow ‘inner’ channel called the thalweg, while coarse-grained channel-fill deposits often generate high-amplitude reflectors (HARs) on seismic profiles. In hydrological and fluvial landforms, the thalweg is a line drawn to join the lowest points along the entire length of a stream bed or valley in its downward slope, defining its deepest channel. Hence, high-amplitude reflector packages (HARPs) commonly occur at the bases of channel–levee systems, and represent relatively coarse grained, unconfined deposits that accumulate in lows between channel–levee systems (Flood *et al.*, 1991); they typically result from channel wall breaching and switching (avulsion) events. The points where channels separate (bifurcate) are sometimes called avulsion nodes.

Channel floors are host to a complex interplay of erosional and depositional processes; consequently, a range of features can be observed, depending on the level of data resolution available. Large-scale (10 to 100 metres) erosional scours and depositional bed forms, e.g. coarse grained sediment waves (Wynn *et al.*, 2002) are often widespread, together with smaller-scale (centimetres to metres) features such as current ripples, dunes and flute marks. A characteristic feature of sinuous channels is depositional point bars on the inside of sinuous loops, which can amalgamate during channel lateral migration to form lateral accretion packages/deposits (Abreu *et al.*, 2003). It is worthy to note that, sinuous channels host significant hydrocarbon reserves on a variety of continental margins (Mayall *et al.*, 2006); they are major

conduits for transfer of sediments from continental shelf to deep ocean (Khripounoff *et al.*, 2003).

Furthermore, channels have always been essential geologic features in the exploration for oil and gas. With enhanced 3D seismic data they can be mapped easily on time or depth slices. In other situations they can be difficult to detect, due to structural complexity. There are a number of image-processing algorithms that can be used to enhance linear features such as channels in 3D seismic volumes.

Mathewson and Hale (2004) revealed that sands associated with channels often make good reservoirs for hydrocarbons. For this reason, the identification of channels is an important part of seismic interpretation for oil and gas exploration. From 3D seismic data it is possible, for horizontal layering, to perform detailed mapping of channel systems directly on time slices. However, in the majority of cases layers are not horizontal, and horizon flattening needs to be done first.

According to Mathewson and Hale (2004), it is possible to automatically detect channels whether or not they are horizontal because they have unique characteristics that differentiate them from other types of features that we encounter in 3D seismic data. Channels are long, sinuous objects with arbitrary orientation. They are locally linear in that their extent is much greater in one direction than in any other direction, at a given point. Other features in a 3D seismic volume are either locally planar (such as bedding planes, faults) or locally isotropic (like pinnacle reefs, salt bodies). This

difference in dimensionality between different features in the input image can be used to detect and enhance (or attenuate) particular types of features.

Analysis of dimensionality can be done using the co-blending seismic attribute techniques and knowledgeable skills in interpretation of seismic sections. The co-blending seismic attribute technique is essentially a multi-scale process which, given the diversity of shapes and sizes of channels.

An understanding of fan structure and growth is important because many oil and gas deposits occur in sandy layers in older fan sediments. Some workers like Posamentier and Allen (1993) have suggested that sandy sediments are not common in muddy fans, or that they are present only in channels or when the fan first becomes active. However, Flood et al., 1991 suggested that sandy layers are more common because they also form as channel patterns evolve.

Flood *et al.*, (1991) and Posamentier and Allen (1993) revealed that Channels, levees and other facies can be interpreted on seismic records that have high resolution. They showed that a sequence of channels and levees were active on the fan whenever sea level was low, and inactive when sea level was high. Sedimentation patterns related to channel evolution (especially the formation of new channels by branching off of older channels) created coarse, flat-lying sand deposits that extend into still deeper water. These sandy deposits are newly described units that may significantly change our understanding of how and when sandy sediment deposits form on continental margins.

Furthermore, Naseer, T.M., *et al.* (2014) carried out a research on application of seismic attributes for delineation of channel geometries and analysis of various aspects in terms of lithological and structural perspectives of Lower Goru Formation, Pakistan. In their study, they aimed at delineating the channels reservoirs and other stratigraphic features in such a terrain where there is always a challenge for the geoscientist to search and exploit the channelled reservoirs. To resolve this issue, they have utilized attribute analysis on high resolution 3D-seismic data for the detailed comparative studies for the channels. Also according to Naseer, T.M., *et al.* (2014), seismic attributes such as coherency and frequency are sensitive to the channel edges that are applied for the channel delineation and their geometrical analysis. They also said that spectral decomposition techniques can be applied for the delineation of channels and to appropriately select the best band for channels identification. Three types of channel geometries are recognized in their study: 1) highly sinuous channel; 2) narrow-broad meandering belts; 3) moderate to high sinuous channel. NW-SE, N-W trending faults can be helpful to compartmentalize the reservoir. Finally, they wrote that instantaneous and dominant frequency are more beneficial for further field development based on Gamma Ray logs from nearby drilled wells and dimensional perspectives analysis of the channel reservoir.

2.10 THEORY OF WELL CORRELATION

The development of geologic pattern displayed by structural and stratigraphic units that are equivalent in time, age, or stratigraphic position through the use of geophysical well logs is generally referred to as log correlation (Reed, 1999). Two

main types of geological correlation strategies exist; lithostratigraphic and chronostratigraphic (Van Wagoner *et al.*, 1990). The method applied in this study is lithostatratigraphic correlation.

A lithostratigraphic correlation would suggest that as a typical delta builds across a continental shelf, the sandy near shore and shallow-marine sediments build outward across muddy prodelta deposits (Fig. 2.9). In contrast, the chronostratigraphic model recognizes that a deltaic depositional system progrades through time and that at any given time, facies grade laterally from one to another. As a result, minor lateral changes in depositional environments through time can create abrupt vertical facies changes, as well as lateral changes in lithology. Chronostratigraphic correlation lines highlight changes in depositional geometry. Finally, lithostratigraphic correlation (upper diagram- Fig. 2.9) assumes no dip in sand bodies towards basin, whereas chronostratigraphic correlation (lower diagram- Fig. 2.9) assumes basinward-dipping clinoforms.

2.11 THEORY OF WELL LOG SEQUENCE

This involves the recognition of well log responses based on sediment characteristics (Fig. 2.10). The analysis of the stacking patterns of the gamma-ray log is used in interpreting the various systems tracts (Mitchum *et al*, 1991), sedimentary facies and their depositional environments.

More so, the grain size of terrigenous sediment depends primarily on the energy of the depositing current. Generally, higher-energy currents produce coarser-grained

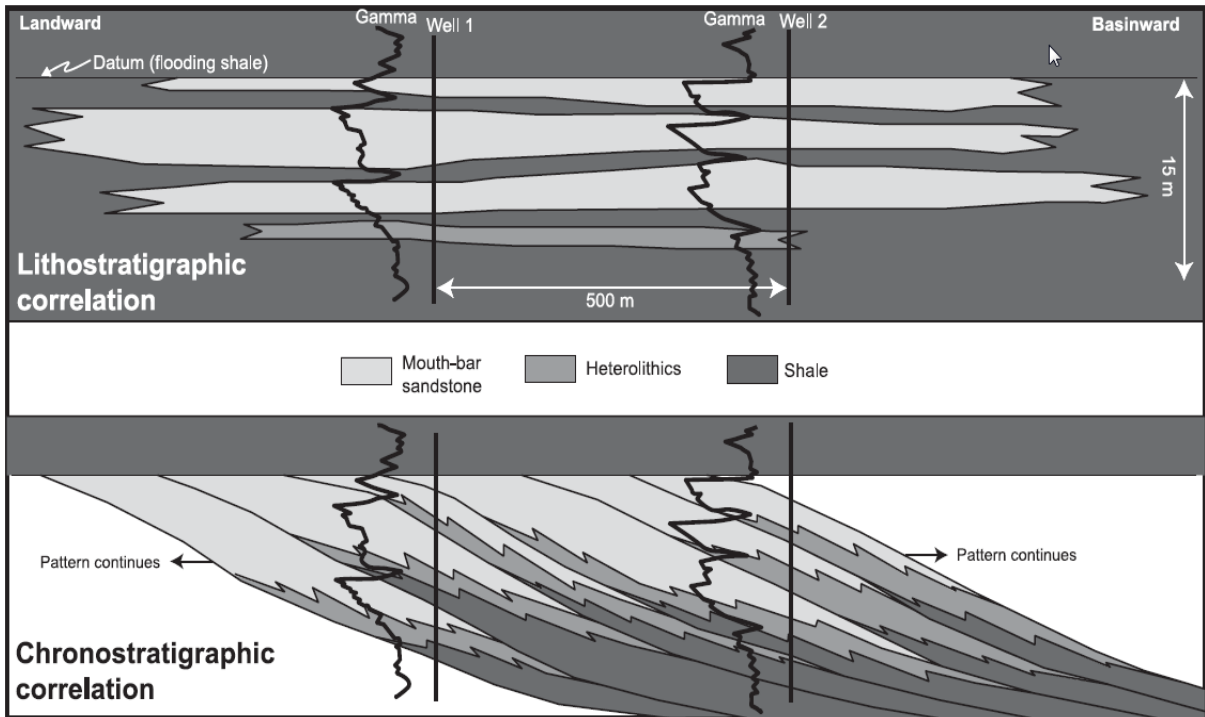
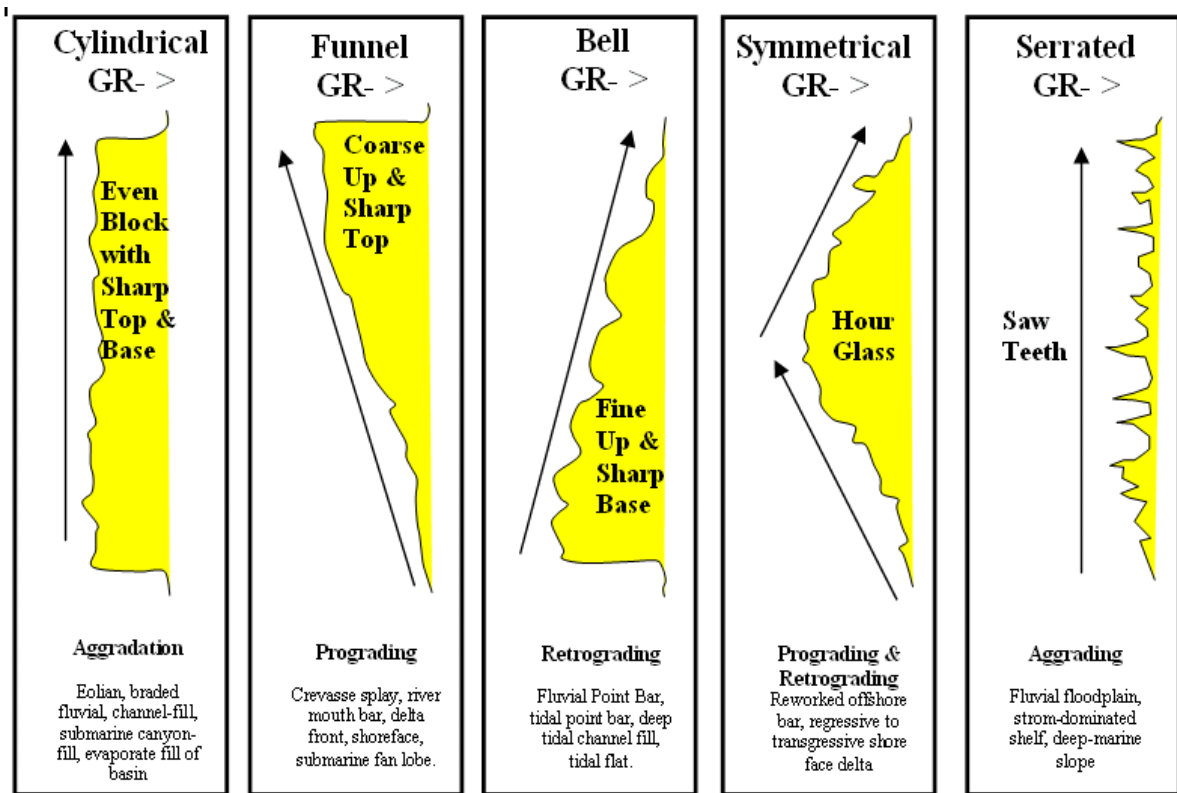


Fig. 2.9: Lithostratigraphic and chronostratigraphic interpretations of two well along depositional dip (modified after Ainsworth et al., 1999).



(a) (b) (c) (d) (e)

Fig. 2.10: The direct correlation between facies and gamma ray log responses relative to the sedimentary environments (Cant, 1992 and Siddiqui et al., 2013.)

sediments and lower-energy environments produce finer-grained sediments. Grain size tends to decrease in the direction of transportation, with the gravel size fraction displaying this feature more so than sand. Sorting increases along with current energy and the length of time the current is active.

Sedimentary facies commonly display characteristic vertical profiles in which grain size fines upward, coarsens upward, or remains constant. The determination of such vertical variations in grain size can be extremely valuable in the diagnosis of depositional environment. Fig. 2.10 shows Vertical grain -size profiles of some common sandstone facies which illustrates characteristic vertical grain-size profiles of some important clastic sedimentary facies.

Channel sequences usually form by lateral accretion and many channel sands display, to some degree, profiles that fine upward, generally from a scoured base (Fig. 2.10a). On the other hand, "bar"-type sands almost always display coarsening-upward profiles, often capped by an abrupt facies change to fine-grained material (Fig. 2.10b).

Examples include regressive barrier-island sands, shallow marine bars, delta-front bars, and even aeolian dunes. Some facies - for example, braided-stream sands, tidal sand ridges, and submarine channels - often display "blocky" profiles whereby grain size remains relatively constant (Fig. 2.10c). It is important to remember, however, that vertical variations in grain size can be due to more than one process or depositional setting; i.e., not all fining-upward sequences are channels, or coarsening-upward sequences, marine bars. For example, deposition from turbidity currents

produces fining-upward sequences in submarine fans. Also, crevasse subdeltas form coarsening-upward grain-size profiles similar in appearance to marine bars.

Sands originating in different sub-environments commonly coalesce to form a single vertical grain-size profile. An example is deltaic point-bar channel sand that, as it builds outward, incises down into underlying delta-front bar sand, forming a deltaic couplet (Fig. 2.10b). The surface that divides the two facies is sometimes difficult to determine from well logs, requiring detailed study of well cuttings and cores.

2.12. BACKGROUND TO SEISMIC ATTRIBUTES

Seismic attributes are the fundamental pieces of information contained within a recorded seismic trace: time, amplitude, frequency, and attenuation (Brown, 2001). They are also defined as quantitative derivatives of a basic seismic measurement that may be extracted along a seismic trace, a horizons surface, or summed over a time window (Brown, 1996). More so, Seismic attributes can be conveniently defined as “the quantities that are measured, computed or implied from the seismic data” (Subrahmanyam, 2008).

From the time of their introduction in early 1970’s, seismic attributes have gone a long way and they have become an aid for geoscientists for reservoir characterization and also as a tool for quality control. The analysis of seismic attributes allows the identification of petrophysical and structural aspects of a buried volume of rock that would typically be beneath the resolution of traditional seismic amplitude data. In the

petroleum industry, seismic attributes are used to identify areas of high porosity or permeability, lateral changes in the aspect or dip direction of a horizon, continuity of reflectors, stratigraphic pinch-outs, and a multitude of other properties of use in petroleum exploration and field development (Siguaw *et al.*, 2001). Actually, development of a wide variety of seismic attributes warrants a systematic classification. A systematic approach is needed to understand the use of each of these attributes and also their limitations under different circumstances.

2.12.1 Classification of Seismic Attributes

The Seismic Attributes are classified basically into 2 categories namely; Physical attributes and Geometric attributes (Brown, 1996; Brown, 2001; Taner, 2001 and Subrahmanyam, 2008).

❖ Physical Attributes

Physical attributes are defined as those attributes which are directly related to the wave propagation, lithology, bright spots, gas accumulation, sequence boundaries, major changes or depositional environments, thin-bed tuning effects, and unconformities. These physical attributes can be further classified as instantaneous and wavelet attributes. Instantaneous attributes are computed sample by sample and indicate continuous change of attributes along the time and space axis. The Wavelet attributes, on the other hand represent characteristics of wavelet and their amplitude spectrum.

The attribute is a result of the properties derived from the complex seismic signal. The concept of complex traces was first described by Taner *et al.* (1979). The complex trace is defined as:

$$C_T(t) = T(t) + iH(t) \quad 2.1$$

Where:

CT(t) = complex trace; T(t) = seismic trace; H(t) = Hilbert's transform of T(t);

H(t) is a 90⁰ phase shift of T(t).

Below are the physical attributes used in the study area:

a) Signal Envelope (E) or Reflection Strength

The Signal Envelope (E) is calculated from the complex trace by the formula according to Taner *et al.* (1979):

$$E(t) = SQRT[T^2(t) + H^2(t)]$$

2.2

The envelope is the envelope of the seismic signal. It has a low frequency appearance and only positive amplitudes. This attribute is good for looking at packages of amplitudes. This attribute represents mainly the acoustic impedance contrast, hence reflectivity. It is mainly useful in identifying: bright spots, gas accumulation, sequence boundaries, major changes or depositional environments, thin-bed tuning effects, unconformities, major changes of lithology, local changes indicating faulting, spatial correlation to porosity and other lithologic variations as well as indicates the group, rather than phase component of seismic wave propagation.

b) Instantaneous Phase

Instantaneous phase is the angle of lag or lead of the harmonic components of a seismic pulse with respect to a reference. For example, a zero-phase wave would be symmetric whereas a 90° phase wave would be perfectly asymmetric (Sheriff, 1973). Instantaneous phase is measured in radians ($-\pi, \pi$). Phase along horizon would not change in principle; changes can arise if there is a picking problem, or if the layer changes laterally due to “sink-holes” or other phenomena. This attribute is useful as: best indicator of lateral continuity, relates to the phase component of the wave propagation, can be used to compute the phase velocity, has no amplitude information, shows continuous sequence boundaries, detailed visualization of bedding configurations and used in computation of instantaneous frequency and acceleration.

c) Instantaneous Frequency

Instantaneous frequency describes the duration of a seismic pulse and it is commonly sub-equal to the centroid of the power spectrum of the seismic wavelet (Taner, 2001). The instantaneous frequency is the time derivative of instantaneous phase, that is, the rate of change of the phase (Taner *et al.*, 1979, Barnes, 1992; Sheriff and Geldart, 1995; Cohen, 1995):

$$F(t) = d(\phi(t))/dt \quad 2.3$$

Instantaneous frequency attribute is useful in the following aspect: represents the mean amplitude of the wavelet, indicate bed thickness and also lithology

parameters, corresponds to the average frequency (centroid) of the amplitude spectrum of the seismic wavelet, seismic character correlator, indicates the edges of low impedance thin beds, hydrocarbon indicator by low frequency anomaly, unconsolidated sands due to the oil content of the pores, fracture zone indicator, appear as lower frequency zones, chaotic reflection zone indicator, bed thickness indicator (higher frequencies indicate sharp interfaces or thin shale bedding, lower frequencies indicate sand rich bedding) and sand/shale ratio indicator.

d) Dominant Frequency (F_c)

The reciprocal of any dominant period (T_c) is a measure of the dominant frequency (F_c) of the signal or wavelet spectrum. Dominant period of any response corresponds to the time one peak to the next or from one trough to the next.

$$F_c = 1/T_c \tag{2.4}$$

e) Relative Acoustic Impedance

Acoustic impedance is the product of seismic velocity and density which yields a basic physical rock property. It can yield important information concerning the nature of the rock and changes in lithology. The seismic traces are first transformed into pseudoreflexion-coefficient time series, then converted into acoustic impedances according to Becquey *et al.* (1979):

$$Z_{i+1} = Z_i \frac{1+K_i}{1-K_i} \tag{2.5}$$

Where Z_i = the acoustic impedance in the *i*th layer

K_i = the pressure amplitude reflection coefficient at the i th interface

This attribute calculates the running sum of the trace to which a low cut filter is applied. It is an indicator of impedance changes, in a relative sense. The low cut filter is applied to remove direct current (DC) shift which is typical in impedance data. (If the value of the low cut filter is zero, then it is not applied.). The calculated trace is the result of simple integration of the complex trace. It represents the approximation of the high frequency component of the relative acoustic impedance.

f) **Average Energy**

The average energy of a seismic signal is proportional to the sum of the amplitudes of the signal squared. The average amplitude of the stacked trace over time window t to $t+m\Delta t$ is (Sheriff and Geldart, 1995):

$$C_A = \frac{\sum_t^{t+m\Delta t} \left| \sum_{i=1}^N g_{ti} \right|}{t + m\Delta t} \quad 2.6$$

The average energy of a seismic signal is proportional to the sum of the amplitudes of the signal squared. Referring to equation 3.6, this can be illustrated for a single trace i as

$$\langle E \rangle = C_A^2 \quad 2.7$$

Where,

g_{ti} is the amplitude of channel i at time t and $\langle E \rangle$ is average energy.

(g) RMS Amplitude

This attribute is a measure of the reflectivity within a time window (Sheriff and Geldart, 1995). To be more specific, it is the square root of the sum of the squares of the amplitudes within the window interval (Sheriff and Geldart, 1995):

$$A = \sqrt{C_A^2} \quad 2.8$$

Where,

A =RMS amplitude,

C_A^2 = the sum of the squares of the amplitudes within the window interval

It is conventionally used as a direct hydrocarbon indicator in a zone. The first use of amplitude information as hydrocarbon indicators was in the early 1970s when it was found that bright-spot amplitude anomalies could be associated with hydrocarbon traps.

❖ Geometrical Attributes

Geometric attributes relate to the physical properties of the reflected data. These attributes describe the spatial and temporal relationship of all other attributes (Taner, 2001). This category includes attributes such as variance/semblance, dip, azimuth, curvature, discontinuity as well as coherency and spectral decomposition. Dip, azimuth, and curvature may all relate to depositional patterns and are commonly used for stratigraphic interpretation.

These attributes measure the lateral relations in the data. They are described as follows:

- (a) **Variance**, or its cousin attribute semblance, measures the continuity of the data and is good indicator of bedding similarity and potential faults.
- (b) The **Dip attribute** or amplitude of the data corresponds to the dip of the seismic events. Dip is useful in that it makes faults more discernible.
- (c) The amplitude of the data on the **Azimuth attribute** corresponds to the azimuth of the maximum dip direction of the seismic feature. Note that azimuth is a true value in degrees. Azimuth can be calculated with respect to the North or inline direction. Note also that dip is true for depth volumes only. If input data is time or time migrated, the dip represents relative values (time dip). The derivation of the directional attribute is done by considering several traces together to reveal the geometry (dip and azimuth) of the beds.
- (d) **Discontinuity** is a geometrical attribute, and measures the lateral relations in the data. It is designed to emphasize the discontinuous events such as faults. High amplitude values on these attribute corresponds to discontinuities in the data, while low amplitude values correspond to continuous features. Discontinuity varies between zero and one, where zero is continuous and one is discontinuous. This attribute can be used in understanding coherency at maximum coherency direction, minimum coherency direction, event terminations, picked horizons, fault detection, zones of parallel bedding, zones of chaotic bedding, non-reflecting zones, converging and diverging bedding patterns, unconformities etc.

(e) Coherence

Analysis of horizon attributes began with the examination of coherence values of interpreted horizons. Coherence is the measure of the similarity in appearance and shape of waveforms from trace to trace. The ratio of stacked energies of traces over a selected spatial area compared to the sum of the energies of the individual components is (Sheriff and Geldart, 1995):

$$E_T = \frac{\left(\sum_{i=1}^N g_{ti} \right)^2}{N \sum_{i=1}^N (g_{ti})^2} \quad 2.9$$

In conclusion, the suitability of blending seismic attributes and seismic interpretation techniques has been discussed by many authors (Taner, 2001; Adeogba *et al.*, 2005; Pilcher and Blumstein, 2007; Chopra 2008; Subrahmanyam, 2008; Klein *et al.* 2008; Ferguson *et al.*, 2010; Pokhriyal 2011; Chopra and Marfurt 2011; Barnes *et al.* 2011; Chopra and Marfurt 2012, Anakwuba *et al.*, 2013, Anakwuba *et al.*, 2015). There are some seismic attributes that are sensitive to the edges of the stratigraphic events (Such as channels). They are coherence, frequency, spectral decomposition, acoustic impedance, average energy, and signal envelop which are the most distinguished means of mapping the channel boundaries within the study area which is supported by Bahorich and Farmer (1995), Chopra and Marfurt (2006), Liu and Marfurt (2006), Partyka *et al.*, (1999); Peyton *et al.* (1998). Although these attributes when co-blended will easily detect channel edges, geometries and depositional environment.

CHAPTER THREE

MATERIALS AND METHODS

3.1 DATA AVAILABILITY AND DESCRIPTION

The data sets available for this research project include geophysical well logs from nine wells, 3-D seismic volume and velocity data (precisely check shots). A brief description of the available data set is presented below:

3.1.1 3-D Seismic Volume

A regional seismic survey around the study area was provided by Department of Petroleum Resources (DPR), a subsidiary of Nigerian National Petroleum Cooperation (NNPC). The survey was previously processed in 1987 by Eni Exploration and Production Division using post stack time migration. This was later reprocessed in 1999 using pre-stack imaging (PSI). The zero phased PSI migrated data manifests moderate data quality down to 2.5 seconds. Below 2.5 seconds, data quality deteriorates. In 2002, a subset of the seismic volume (covering the study area) was reprocessed as a pre-stack depth migration (PSDM). The reprocessed 3-D PSDM seismic was used in this study. The seismic volume is characterized by a series of parallel reflections offsets and deformed by major listric normal faults. Also, the seismic volume contains 8 in-lines and 11 cross-lines within the study area (Fig. 3.1). The character of the seismic record changes with depth. This study focuses on reflections between 2.7 and 1.5seconds (two way travelttime (TWT)), inferred to be from Agbada Formation based on regional studies (Short and Stauble, 1967; Doust and Omatsola, 1990; Morgan, 2004; Anakwuba, 2009). Reflections within this interval have moderate to good continuity and high amplitude variations (Fig. 3.2).

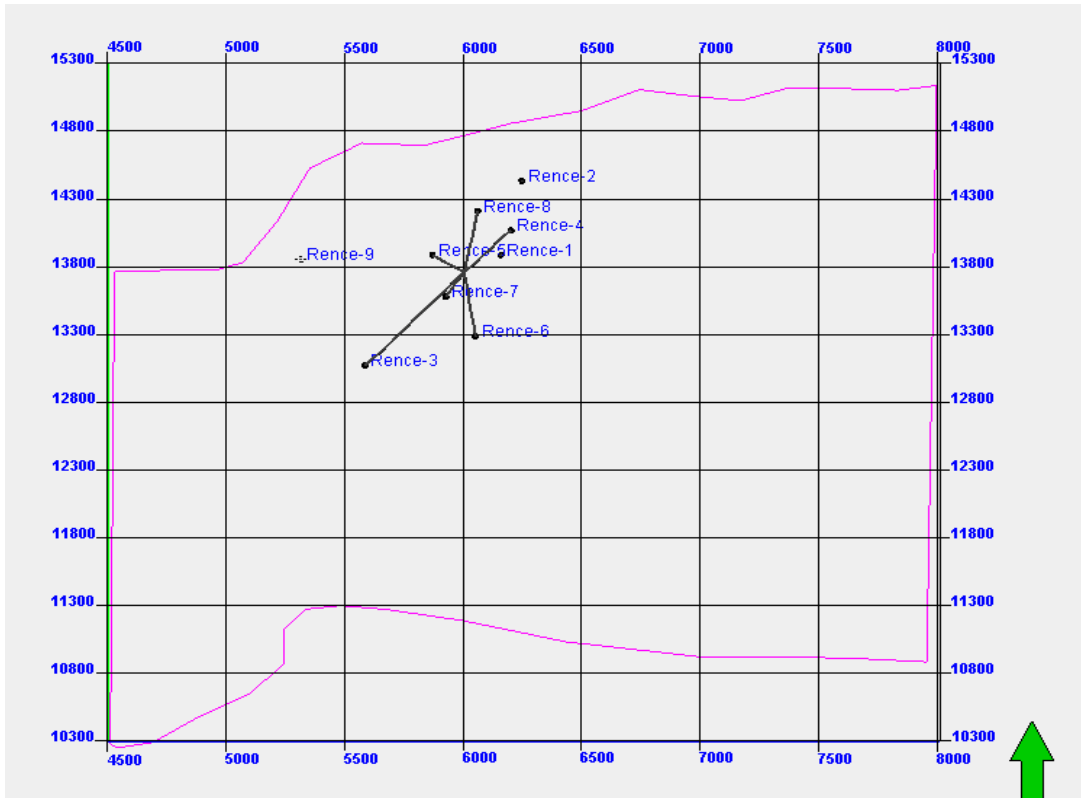


Fig. 3.1: Base map showing all wells and seismic lines

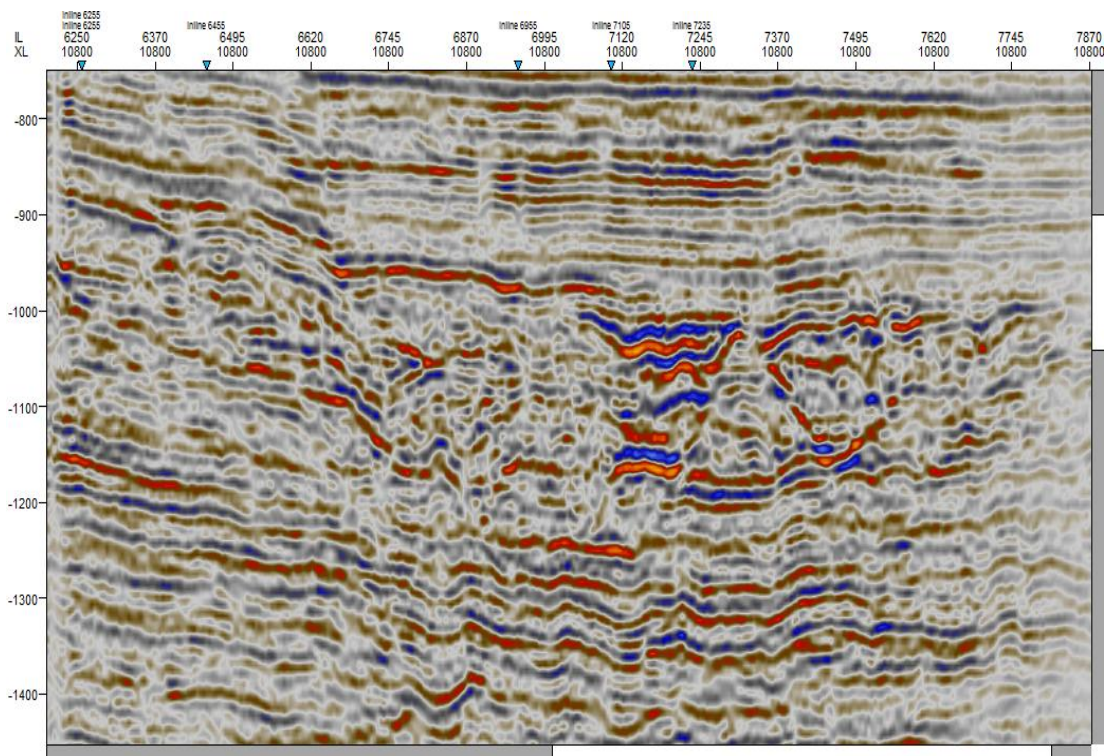


Fig. 3.2: Seismic reflections within the study area

3.1.2 Well Log Data

All the wells within the study area were drilled between 1978 and 1982, hence are old vintage logs. The suite of logs available for the study includes gamma ray, resistivity, density, sonic and neutron logs (Table 3.1). Basically all the wells have gamma ray and resistivity. Wells 6 and 8 do not have sonic logs whereas other wells do have sonic logs. Density logs are present in all the wells except well 9, while neutron logs are present in all the wells, except wells 1 and 2. The quality of the available logs was judged fair to good; however, there is no availability of core data. The log setting is given as shown below: gamma ray log (GR) = 0 – 150; sonic log (DT) = 40 – 240; density log (DEN) = 1.95 – 2.95; neutron log (NEU) = -0.15 – 45; porosity log (PHIE) = 0 – 0.50 and water saturation (S_w) = 0 – 1.00.

Table 3.1: List of available well logs and core data (A=available and NA=Not-available)

Name	GR	DT	Density	Phie	Neutron	Hdra	RT	MD	Sw	VSH	TVDSS	OWT	Perm_Welltest	Core_GR	Core_Phie	Core_DT	GR_Sw	GR_Res
RENCE 1	A	A	A	A	NA	NA	NA	A	A	A	A	A	NA	NA	NA	NA	NA	NA
RENCE 2	A	A A	A	A	A	NA	NA	A	A	A	A	A	NA	NA	NA	NA	A	NA
RENCE3	A	A A	A	A	A	A	A	A	A	A	A	A	A	A	A	A	A	NA
RENCE 4	A		A	A	A	A	NA	A	A	A	A	A	A	NA	NA	NA	NA	A
RENCE 5	A	A N	A	A	A	A	NA	A	A	A	A	A	A	NA	NA	NA	NA	NA
RENCE 6	A	A	A	A	A	A	NA	A	A	A	A	A	A	NA	NA	NA	NA	NA
RENCE 7	A	A N	A	A	A	NA	NA	A	A	A	A	A	A	NA	NA	NA	Yes	NA
RENCE 8	A	A	A	A	A	A	NA	A	A	A	A	A	NA	NA	NA	NA	NA	NA
RENCE 9	A	A	NA	A	NA	NA	NA	A	A	A	NA	A	NA	NA	NA	NA	NA	NA

LENGEND

GR- Gamma ray log; **DT-** Sonic log; **Phie-** Porosity log;

Hdra- Hydration data; **RT-** Real travelttime; **MD-** Measured depth;

S_w – Water saturation; **VSH-** Volume of shale; Res-Resistivity log

TVDSS- True vertical depth sub-sea; **OWT-** Oil water contact;

Perm_welltest- Permeability from well test;

3.2 METHODOLOGY

This section is a system of broad principles or rules from which specific methods or procedures may be derived to interpret or solve different problems within the scope of this particular study. Unlike an algorithm, a methodology is not a formula but a set of practices.

3.2.1 Summary of Workflow

The workflow approach used in this present study is illustrated in Fig. 3.3. The study involved the use of 3-dimensional seismic reflection data, check shot velocity data, core data and well log data. The execution of these steps was done with the aid of Schlumberger Petrel[®].

The overview target of the workflow is to generate all necessary interpretation and input for application of co-blending of seismic attributes as well as produce geological modelling. All the inputted data set of interest is aimed at using the seismic attributes to enhance the visualization of channel morphology and environment of deposition within the study area. Details of the materials available and the description of methods used to carry out the workflow are given below.

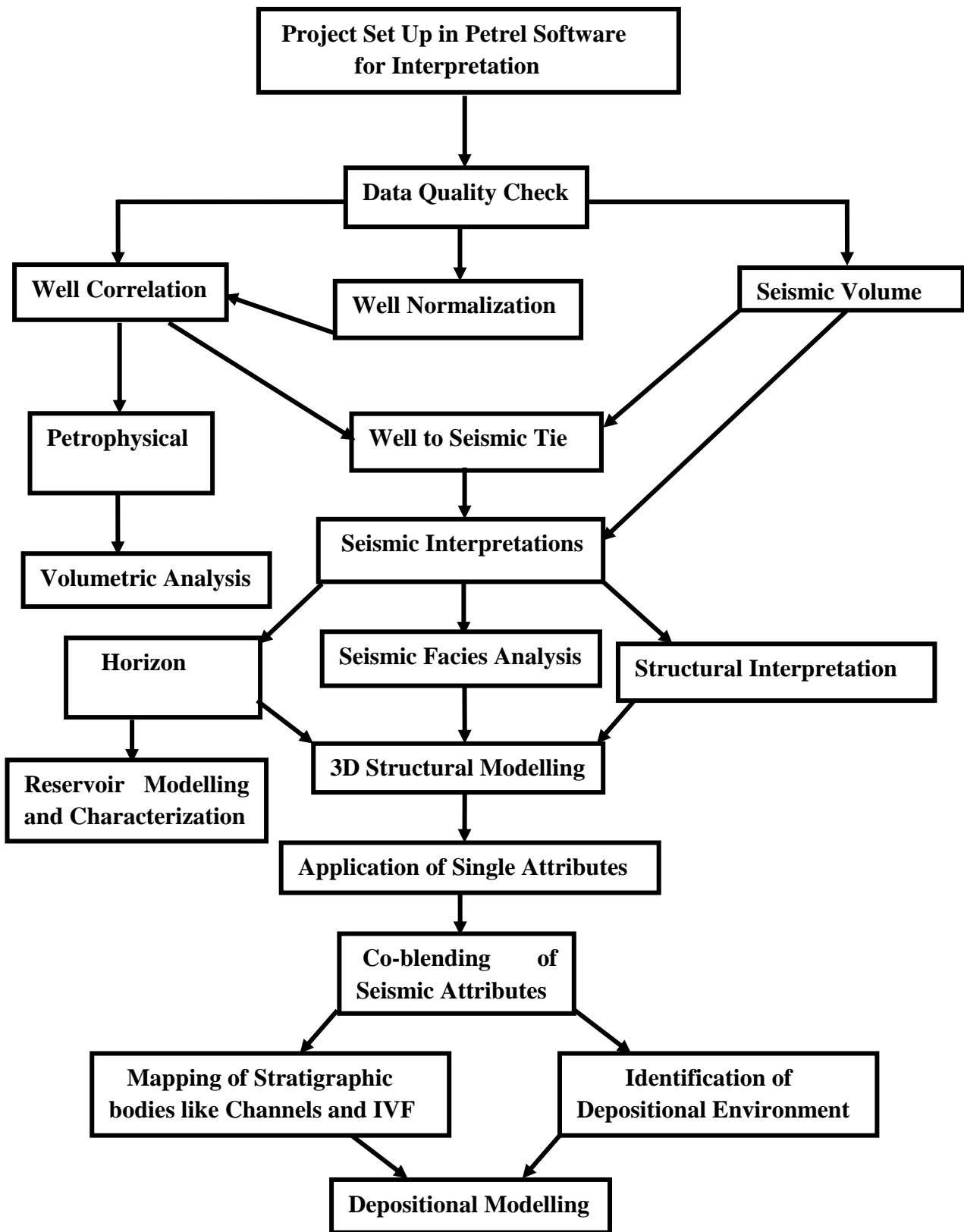


Fig. 3.3: Research Workflow

2.10.2 Application Software (Schlumberger Petrel)

Petrel is a window-based software application which covers a wide range of workflows from seismic interpretation to reservoir simulation. The basic principle of Petrel integrated solution is that geophysicists, geologists and reservoir engineers can move just across domains within one software application, rather than moving between different software applications. One of the key benefits of integrated solutions such as Petrel is the elimination of import and export problems and encouragement of parallel working procedure against a serial workflow approach. Moreover this type of solutions promotes and encourages collaboration between different domains.

3.2.3 Well correlation

Well correlation was carried out in the dip direction in order to reveal the structural features of the Rence field during interpretation. Mapping of various well tops well data was first taken to subdivide the section of interest into packages made up of sequences or parasequences. Then, identification of the mega reservoirs and structural features were done. Also, the mapping of channels within the well logs, precisely at the mega reservoir was also done. Finally, the biofacies or lithologic units of the area will be obtained.

3.2.4 Well log responses

Mapping of well log responses on the gamma ray log data across the study area was carried in order to reveal the depositional features prominent as well as to give a guide

during detailed seismic facies analysis. Channel features will be traced and deduced from the well log responses. At this point, It should be noted that no single environment has a unique grain-size profile, and similar profiles may be produced by different environments. Therefore, profiles should be interpreted with as much supplementary data as possible.

3.2.5 Well to Seismic Tie

The usual way of tying log and seismic data is through the generation of synthetic seismograms. These "synthetics" are created by using sonic and density logs to generate acoustic impedance logs, then converting to reflection coefficients. The reflection coefficients are then convolved with a wavelet that matches the frequency and phase characteristics of the seismic data. The resultant zero-offset synthetic is considered to be what the seismic data should look like for a stacked seismic trace that corresponds to the borehole location.

The tying of log and seismic data was carried out within the study area through the generation of synthetic seismograms. These "synthetics" are generated by using sonic and density logs to generate acoustic impedance logs, then converting to reflection coefficients. The reflection coefficients are then convolved with a wavelet that matches the frequency and phase characteristics of the seismic data. The resultant synthetic is considered to be what the seismic data should look like for a seismic trace that corresponds to the borehole location. The quality of the log data obviously plays a key role in determining what the synthetic looks like. One of the key needs when tying

logs to seismic data is having a means of converting from time to depth units. In this study, checkshots data were used to generate a velocity model.

3.2.6 Reservoir Petrophysics

The petrophysical analysis was carried out using the well log data. Volume of Shale was estimated using gamma ray log and corrected to compensate for the unconsolidated sand of the Tertiary Niger Delta. Porosity was calculated using both density and sonic logs and then the log porosity values were calibrated using the core data from wells.

Shale Volume (V_{sh})

The Gamma Ray Index option was employed to determine the percentage of shale and implicitly, the dominant lithology. This was achieved by determining the shale base line from Gamma Ray logs. Correction was made on the gamma ray index to compensate for the unconsolidated sand of the Niger Delta (Tertiary). The volume of shale was calculated using equations 3.1 (Schlumberger, 1974):

$$I_{gr} = \frac{GR_{log} - GR_{min}}{GR_{max} - GR_{min}}$$

3.1

Where,

GR_{log} = GR of formation measured from log; GR_{min} = Least GR in zone of interest.

GR_{max} = Maximum GR reading in formation of interest, I_{gr} = Gamma Ray Index.

For the purpose of this project work, Larionov's (1969) volume of shale formula for Tertiary rocks was used below:

$$V_{sh} = 0.083 \times 2^{(3.7 \times Igr)} - 1.0 \quad 3.2$$

Where,

Igr = Gamma Ray Index; V_{sh} = Volume of Shale.

Porosity

The porosity was estimated from both the density and sonic logs. The effective porosity was deduced by introducing the shale volume percentage into the equation. The equations below were used for porosity estimation according to (Schlumberger, 1974):

$$\phi_D = \frac{\rho_{ma} - \rho_b}{\rho_{ma} - \rho_{fluid}} \quad 3.3$$

$$\phi_S = C \frac{\Delta t_{log} - \Delta t_{ma}}{\Delta t_{log}} \quad 3.4$$

Where,

ϕ_D = Density log porosity; ρ_{ma} = Matrix density; ρ_b = Bulk density log reading
 ρ_f = Fluid density; Δt_{log} = sonic log reading; Δt_{ma} = interval transit time of the matrix material; C = Empirical correlation factor and matrix density = 2.65(g/cm³)
fluid density = 1.0(g/cm³).

Net-to-gross ratio (NTG)

This refers to the proportion of clean sand to shale within a reservoir unit. The gross sand is the whole thickness of the reservoir; the non-net sand is the shaly sequences within the whole reservoir thickness; the net sand is thus obtained by subtracting the non-net sand from the gross sand. The Net-to-gross ratio reflects the quality of the sands as potential reservoirs. The higher the NTG value, the better the quality of the sand.

$$\text{NTG} = \text{Net sand} / \text{Gross sand} \quad 3.5$$

$$\text{Net sand} = \text{gross sand} - \text{shaly intervals} \quad 3.6$$

Water and hydrocarbon saturation

The water and hydrocarbon saturations are much related. In this research work, water saturation was derived using Archie's equation (Archie, 1942) for water saturation in consolidated zone:

$$S_w = [(a * R_w) / (R_t * \phi^m)]^{1/n}$$

3.7

$$S_h = 1 - S_w \quad 3.8$$

Where,

S_w = water saturation; R_w = resistivity in the water leg (that is resistivity of formation water); R_t = true formation resistivity derived from the deep induction resistivity log; ϕ = porosity; n = saturation exponent usually taken as 2.0; m = cementation factor (2.0); a = consolidation factor/tortuosity (0.62).

Bulk volume of water (BVW)

This is the product of water saturation and porosity corrected for shale (Adepelumi *et al.*, 201; Asquith and Krygowski, 2004):

$$BVW = S_w * \Phi_e \quad 3.9$$

Where BVW = bulk volume of water; S_w = water saturation; Φ_e = effective porosity.

If values for BVW calculated at several depths within a formation are coherent, then the zone is considered to be homogeneous and at irreducible water saturation. It follows therefore that hydrocarbon production from such zone should be water free (Peter and Peter, 2013).

Permeability

This is a measure of the ease with which a fluid (gas, oil or water) flows through connecting pore spaces of reservoir rock. It is very important in predicting the rate of production from a reservoir. Permeability was calculated using Timur's equation (Timur, 1968) as follows;

$$k = 0.136(4.4/S_{wirr}^2) \quad 3.10$$

Where, k = permeability (millidarcy); S_{wirr} = irreducible water saturation

3.2.5 Oil-Water Contact (OWC)

Oil-water contact is a bounding surface in a reservoir above which predominantly oil occurs and below which predominantly water occurs. Although oil and water are immiscible, the contact between oil and water is commonly a transition zone and there

is usually irreducible water adsorbed by the grains in the rock and immovable oil that cannot be produced. The oil-water contact is not always a flat horizontal surface, but instead might be tilted or irregular. Measurements of both the areal closure and the distance from the apex to the lowest closing contour are typically incorporated in calculations of the estimated hydrocarbon content of a trap. The area of oil closure is calculated according to Schlumberger (1968) which used grids line with respect to the scale of the map. However, the oil-water contact was measured in the study area using the following calibrations:

- Areas with low acoustic impedance, low volume of shale, low water saturation and high porosity will depict oil sand, while
- Areas with high acoustic impedance, high volume of shale, high water saturation and low porosity will depict water sand.

3.2.6 Volumetric Estimation of Oil

The volumetric method entails determining the physical size of the reservoir, the pore volume within the rock matrix, and the fluid content within the void space. This provides an estimate of the hydrocarbons-in-place, from which ultimate recovery can be estimated by using an appropriate recovery factor. The reserve for the H-horizons mapped within the study area was estimated using oil volumetric calculations initiated by various petroleum geologists (Dean, 2007; Etris and Stewart, 2003; Obah *et al.*, 2012 and many more) and they are shown as follows:

$$\text{Rock Volume (V}_R\text{) (acre feet) = A * h} \quad 3.11$$

$$\text{OOIP} = (7758 * V_R * S_h * \emptyset * \text{NTG}) \quad 3.12$$

$$\text{STOOIP} = (\text{OOIP} * B_{oil}) \quad 3.13$$

Where:

OOIP = oil originally in place; STOOIP = stock tank oil originally in place

A = Drainage area, acres; h = Net pay thickness, feet;

7,758 = API Bbl per acre-foot (converts acre-feet to stock tank barrels)

\emptyset = Porosity, fraction of rock volume available to store fluids

S_w = Volume fraction of porosity filled with interstitial water

S_h = Hydrocarbon saturation

B_{oil} = Formation volume factor for oil = $(0.81 / \emptyset^2)$; 1 acre = 43,560 sq. ft.

3.2.7 Normalization of Gamma Ray Log

GR Log normalization was carried out because each well drilled has different characteristics that causes well deviation of one well from another. Such characteristics include variation in sizes of hole due to various sizes of drilling bits, viscosity of the drilling mud varies as a result of different geologic formations encountered, drilling gauge are not the same at every well and well log drilled have different fluid content. Hence, three wells went out of range in the study area namely, well-2, well-3 and well-4.

Certainly, a normalized GR Log should coincide with the reference shale base line of the GR Log. The reference shale baseline for GR log within the study area is approximately 75API (American Petroleum Industry).

$$\boxed{GR_N = GR_{SBL}} \quad (3.14)$$

Where, GR_N = normalized Gamma Ray Log and GR_{SBL} = Shale base line for Gamma Ray Log.

Also,

$$\boxed{GR_N = GR_W * X} \quad (3.15)$$

Where, GR_W = Gamma Ray Log of well to be normalized; X = normalizing factor

Combining equations (3.14) and (3.15) as well as solving for X , we have:

$$\boxed{X = \frac{GR_{SBL}}{GR_W}} \quad (3.16)$$

3.2.8 Seismic Data Interpretation

The seismic sections through the field were interpreted structurally and stratigraphically for hydrocarbon exploration uses. Seismic data interpretation involves horizon and fault interpretation as well as generation of time-structure maps. Key continuous horizons and faults were interpreted on 3D seismic data in both in-line (Line) and cross-line (Trace) directions.

The Seismic data interpretation carried out in the study area entails the identification of the structural geometry of the reservoir and the geologic boundaries of the field,

extracting the structural framework of the reservoirs and creation of velocity model of the field for the purpose of depth conversion. All these will help in generating all structural and rock physics input for the static modeling of the reservoir.

3.2.9 Reservoir Characterization

Reservoir characterization was carried out in order to delineate the key horizons and faults within the study area as well as to identify the major reservoir for an effective hydrocarbon generation and exploration. Reservoir characterization essentially refers to all the pertinent information that is required to describe a reservoir in terms of its ability to store and produce hydrocarbons. This entails knowing the complete reservoir architecture including the internal and external geometry, its static model with distribution of reservoir properties (such as porosity, permeability, heterogeneity, net pay thickness, etc.), and understanding the fluid flow within the reservoir (dynamic model). This information help improve production rates, rejuvenate oil fields, predict future reservoir performance, minimize costly expenditure, and help the managements of oil companies to draw up accurate financial models.

It is worth knowing that reservoir characterization integrates the technical disciplines of geology, geophysics, reservoir engineering, petrophysics, economics and data management. The success of the reservoir characterization effort depends on how well the integration of the above disciplines is carried out, an elusive goal in some cases, and the success of each project could vary.

3.2.10 Generation of Seismic Attributes

Eight single seismic attributes such as average energy, root-mean-square (RMS) amplitude, instantaneous frequency, reflective acoustic impedance, iso-frequency, dominant frequency, signal envelope (reflection strength) and coherence attributes were used for interpretation in the study. Application of these single attributes on the geoprobe from interpreted 3D seismic data have very low impact in the visualization of channel and depositional features.

3.2.11 Co-blending of Seismic Attributes

Co-blending of seismic attributes was done for clearer images; in order to aid envisage the channel outline and structural geometry. The channel morphology is related to an amalgamation of depositional processes and environment. The enhanced channel image of co-blended attributes compensates for poor visualization by single attributes only. Meanwhile, Co-blending of seismic attributes means to blend two or more seismic attributes into a single and unified data display.

Actually, four sets of co-blending were carried out: (a) co-blending of Signal Envelope and Dominant Frequency Attributes (b) co-blending of Reflection Acoustic Impedance and RMS Amplitude Attributes (c) co-blending of Reflection Acoustic Impedance, Instantaneous Frequency and Average Energy Attributes (d) co-blending of Reflection Acoustic Impedance, Iso-frequency and Coherency Attributes.

3.2.12 Seismic Facies and Stratigraphic Analysis

The seismic sections of the field were interpreted for seismic facies analysis. The seismic facies units were defined from reflection configuration patterns, continuity, amplitude and other attributes as well as their boundary conditions. The analysis of seismic facies along with stratigraphic development from seismic character was also carried out. These facies were related to the associated well log character. The interpreted seismic facies sequence concurs with that recognized by previous workers in other basin.

3.2.13 Depositional Model

A depositional model was created by integrating all the necessary interpretations. It is good to note that sediments are transported and deposited in a variety of depositional environments. On land, sedimentary environments include stream flood plains, swamps, dunes and desert basins. Along the coastal regions sediments accumulate in river deltas, lagoons, beaches, and barrier islands. Most sediment ultimately come to rest in the ocean, accumulating in massive deposits that form the continental shelves, or continuing to the deep basins beyond the continental shelf margin.

CHAPTER FOUR RESULTS AND DISCUSSION

4.0 INTRODUCTION

This chapter presents the results obtained from the log interpretations, seismic interpretations, co-blending of seismic attributes and the geologic interpretations within the Rence field. Rence field was characterized using 3D Seismic Volume; well logs from 9 wells and checkshots. Core permeability data from five wells were also utilized in the study.

4.1 RESULT OF WELL INTERPRETATION

4.1.1 Result of Log Normalization

Before well interpretation, the wells within the field must be normalized due to human error during or after data collection and to normalize those shift wells that went out of range to their natural point. Gamma ray log normalisation was carried out on three (3) wells within the Rence field namely: Rence 2, 3 and 4 using Rence 7 Gamma ray log as the calibration log. Fig. 4.1 shows clearly the shifted wells that went out of range.

Using equation (3.15), the three (3) that went out of range were normalized:

At well 3 and 4, putting $GR_W = 110API$ and $GR_{SBL} = 75API$ into equation (3.16), the normalizing factor (X) obtained is 0.6818.

Also, for well 2, putting $GR_W = 61API$ and $GR_{SBL} = 75API$ into equation (3.16), the normalizing factor (X) obtained is 1.2295.

The normalizing factors obtained are used to multiply the respective wells that went out of range. The results of the above equations are shown clearly in Fig. 4.2.

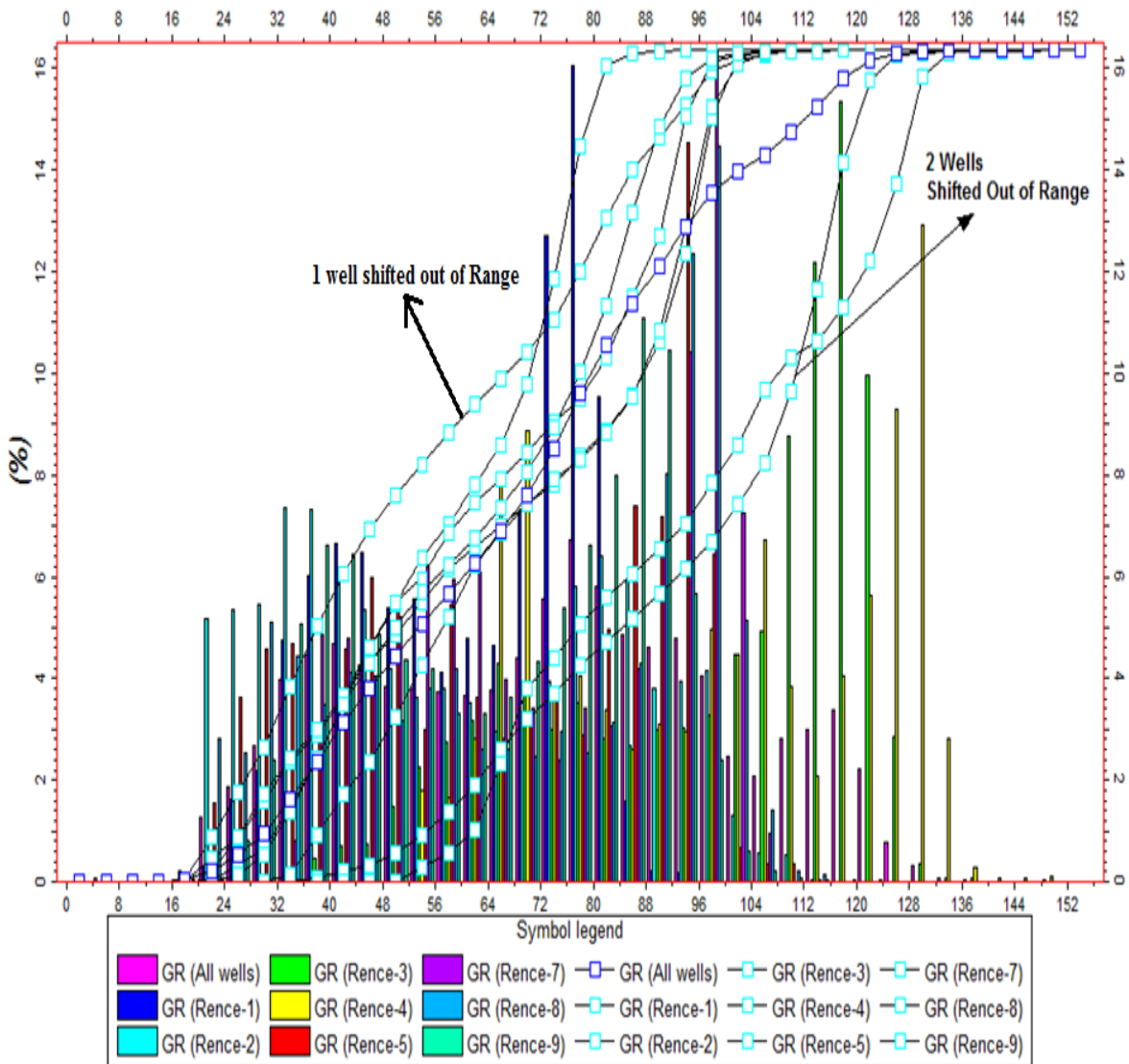


Fig. 4.1: Distribution of GR logs in Rence Field before Normalization

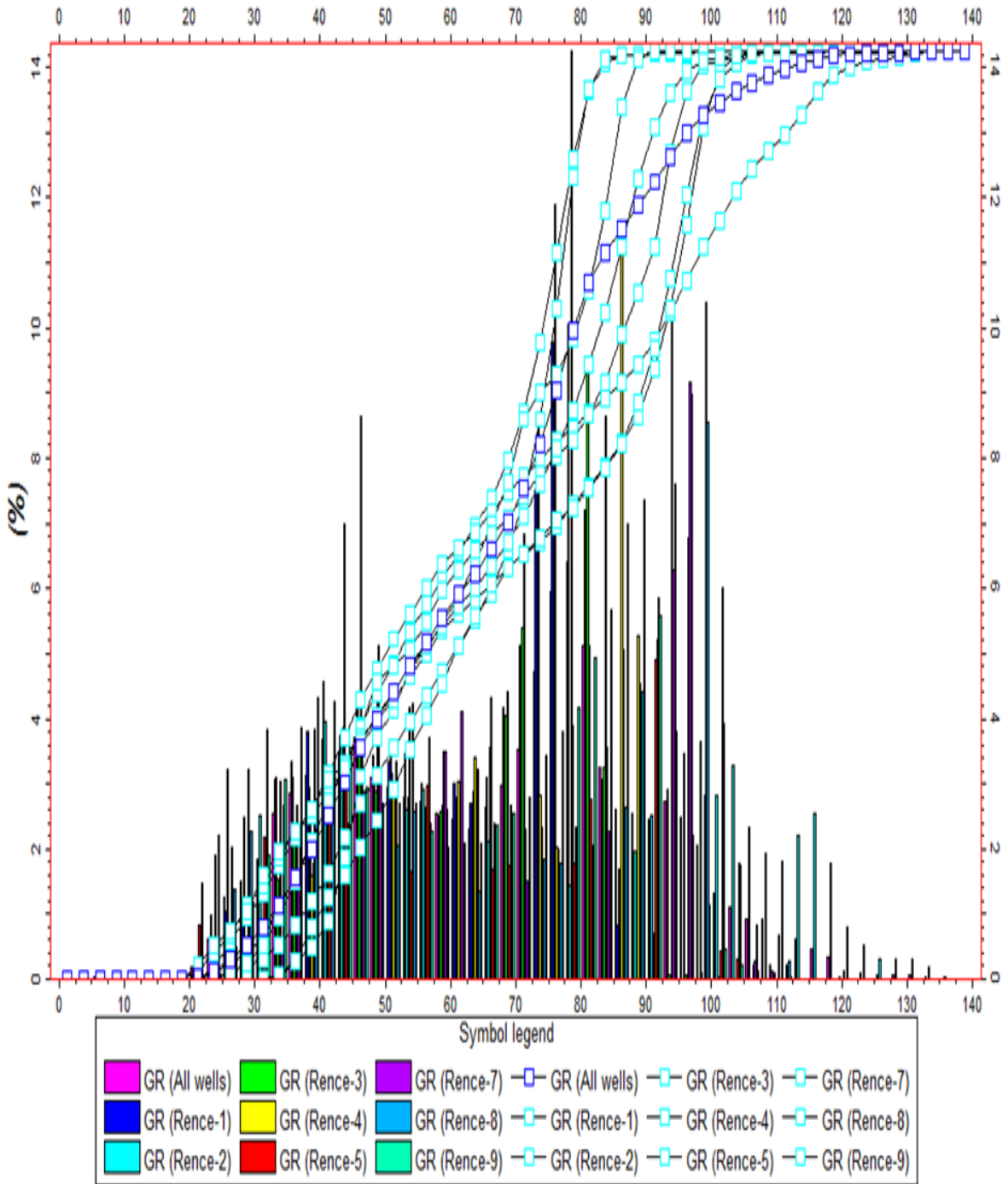


Fig. 4.2 Distribution of GR logs in Rence Field after Normalization

Fig. 4.3 is the GR Ray Log cut for lithology description within the Rence field. The result was achieved from normalization of the log which yields a bimodal distribution and estimation of the lithology using the equation below:

$$\text{Lithology} = \text{if}(\text{GR} < \text{T}, 0, 1) \quad 4.1$$

Where,

GR = Gamma Ray Log value; T = Statistical value; 0 = Shale; 1 = Sand

- Estimation of the median (from the nine wells) = (Total Range of the data)/2
= 150/2 = 75 API

Where, API means American Petroleum Institute

Using the equation 4.3 gives:

$$\text{Lithology} = \text{if}(\text{GR} < 75, 0, 1)$$

- Estimation of the mean (from the nine wells) = 69.22 API

Using the equation 4.3 gives

$$\text{Lithology} = \text{if}(\text{GR} < 69.22, 0, 1)$$

- Application of bimodal classification = 66 API

Using the equation 4.3 gives

$$\text{Lithology} = \text{if}(\text{GR} < 66, 0, 1)$$

The results of all these calculations are shown in Fig. 4.3 and the most acceptable in this research work is the mean estimation as shown in Fig.4.3. It shows two facies variation namely shale and sand.

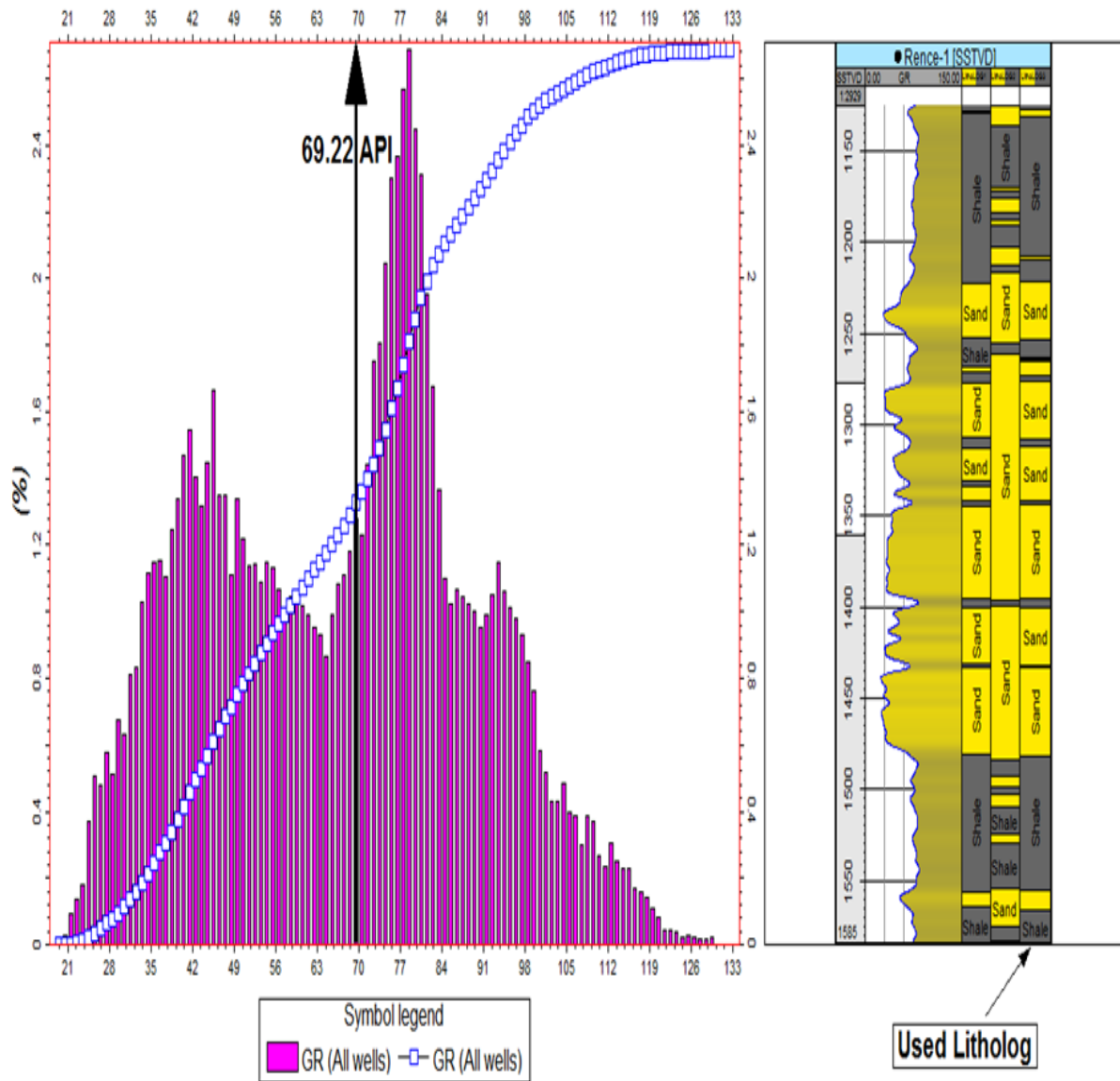


Fig. 4.3: Gamma ray log cut off for lithology description in Rence Field

4.1.2 Result of Well Correlation

In the study area, only well 1, 2 and 9 are vertical wells whereas other wells appear to be drilled from the same platform, hence it is spider plot. The result of correlation across the entire field is shown in Fig. 4.4. Gamma ray log of the wells were used in the correlation. Hence, Fig. 4.5 shows the major reservoir along northwest –southeast correlation panel across Rence field. The major reservoir is labelled H-reservoir.

This hydrocarbon interval is delineated by too distinctive sand sequence with shale intercalation (high gamma ray API value) in-between. They are of typical paralic Agbada Formation. There is substantive variation in average thickness observed across all the wells. Also observed are the variations in net sand distribution representing the well locations in different parts of fluvial-marine depositional environment. The sand thickness in the H-reservoir is highest at Rence 1 because of the rapid rate of deposition in response to the continental shelf which creates more accommodation space than at Rence 3, which has the lowest sand thickness across the field.

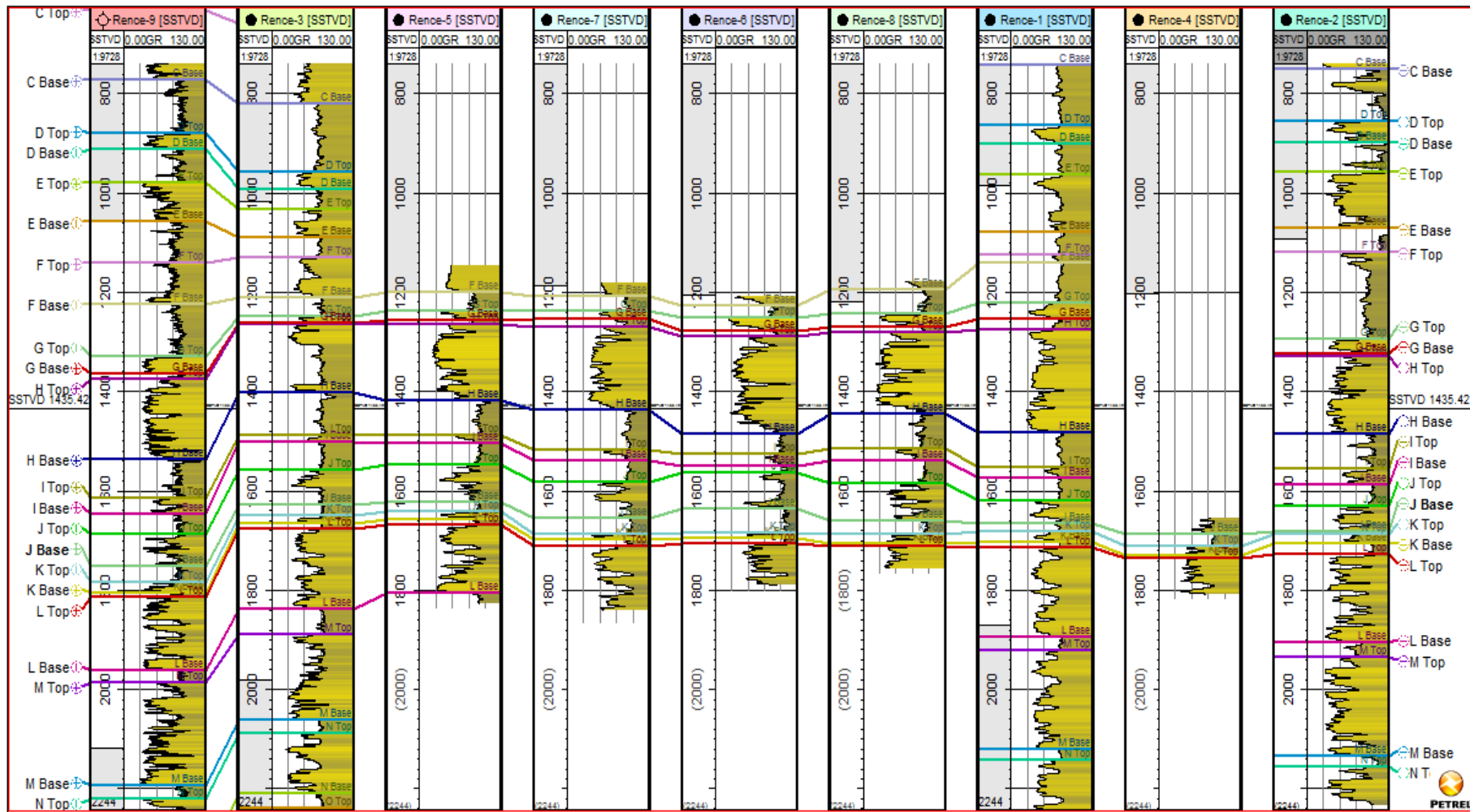


Fig. 4.4a: A northwest –southeast correlation panel across Rence field for all the wells

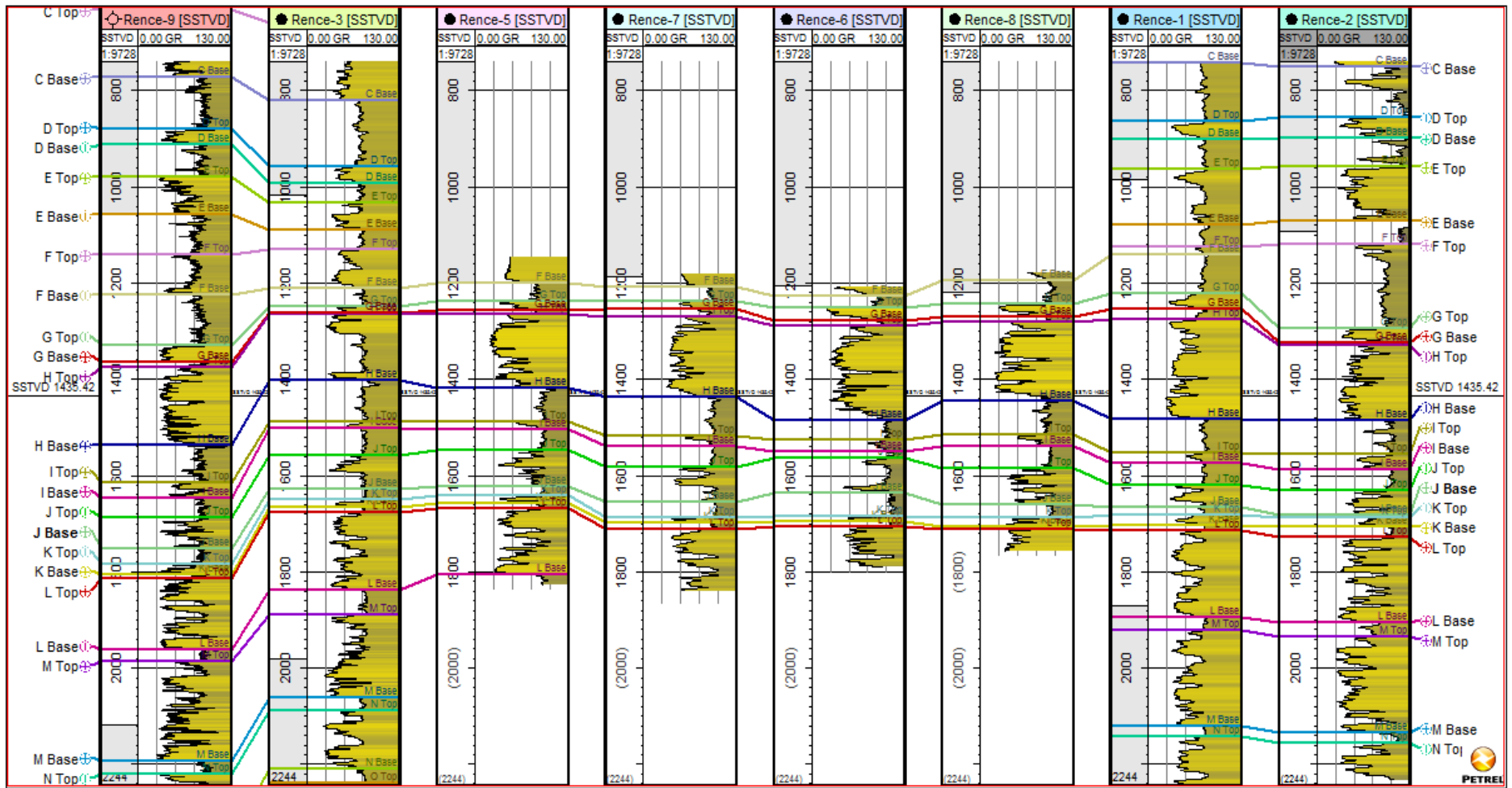


Fig. 4.4b: A northwest –southeast correlation panel across Rence field for 8 wells

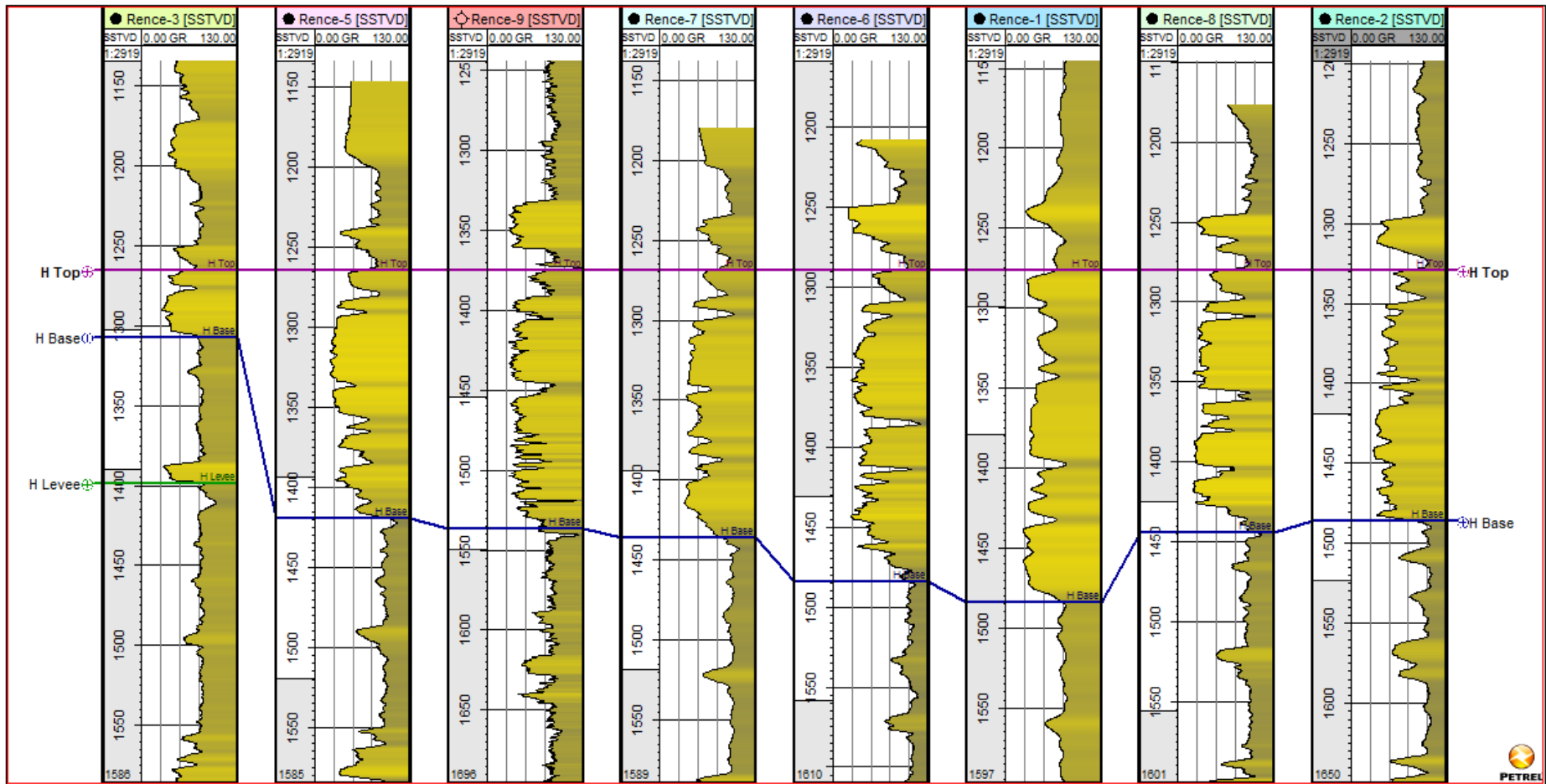


Fig. 4.5: Major reservoir correlation panel across Rence field

4.1.3 Result of Well Log Responses

Within the field, five general log signatures (Fig. 4.6) are defined over the stratigraphic intervals ranging from several tens to hundreds of feet thick as follows:

- (a) **Bell shape:** A gradual upward increase in gamma-ray response. This trend may reflect upward fining (for example a lithology change from sand to shale) or upward fining of sand beds in a thinly bedded sand-shale unit. This trend usually implies a decrease in depositional energy. In a shallow marine setting, this trend usually reflects an upward deepening and a decrease in depositional energy (shoreline retreat).
- (b) **Funnel Shape:** A gradual upward decrease in gamma-ray response. In shallow marine settings, this trend reflects a change from shale-rich into sand-rich lithology and upward increase in depositional energy with shallowing-upward and coarsening.
- (c) **Symmetric patterns** defined by initial gradual decrease and then increase in gamma-ray values interpreted to record a gradual coarsening and then gradual fining of deposits.
- (d) **Blocky intervals** defined by abrupt decrease in gamma-ray value overlain by an interval with uniformly low values. This trend has low gamma values and sharp boundaries with no internal change.
- (e) **Serrated patterns** defined by intervals with high gamma ray values.

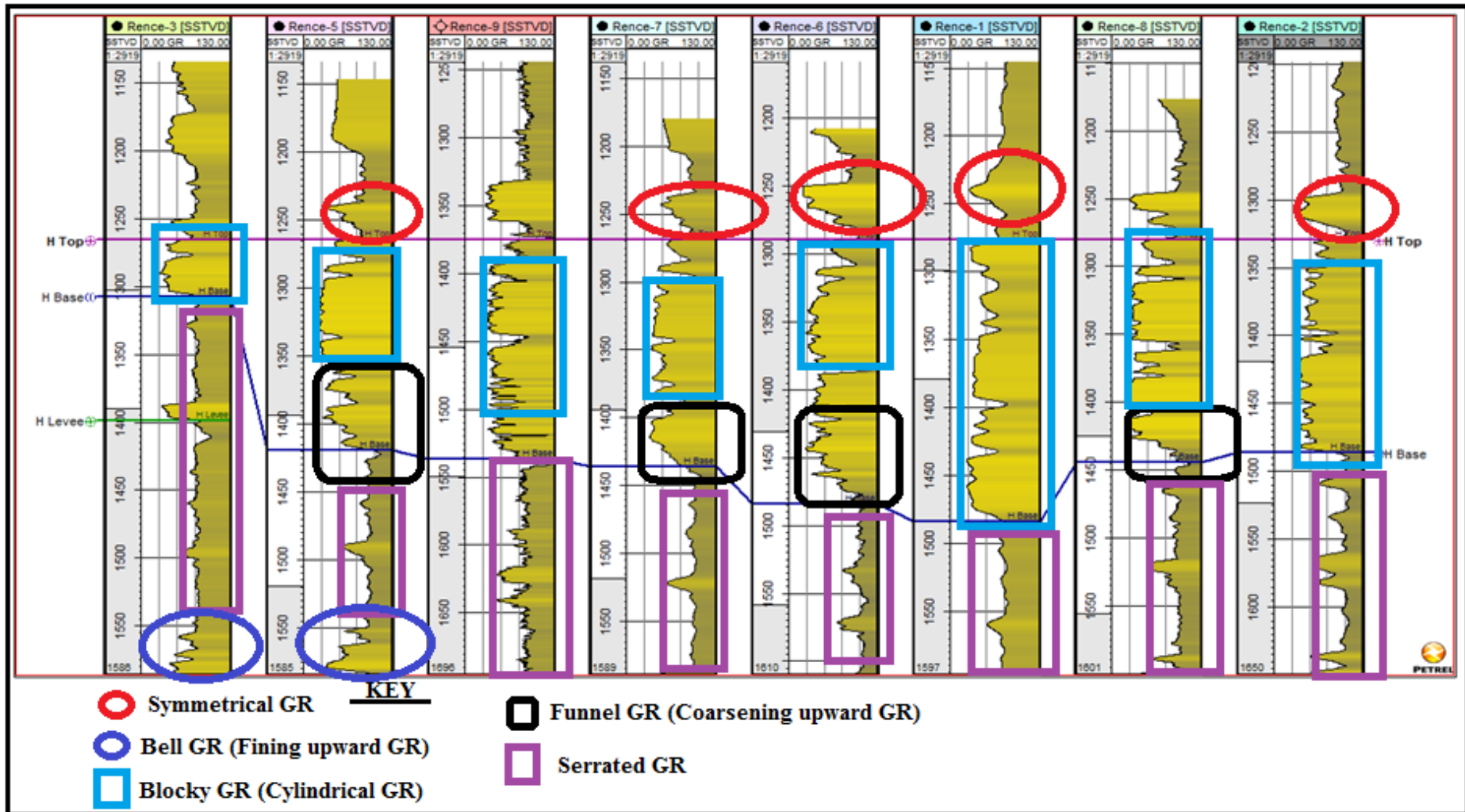


Fig. 4.6: Typical Gamma Ray log patterns of the study area

4.1.4 Result of Well to Seismic Tie

The well to seismic profile indicates zero phase shift and SEG normal polarity wavelet (Fig. 4.7). The wavelet enveloped spectrum shows a dominant frequency of about 25 Hz. Radial wells seismic were extracted around each well and they were used to match the synthetic to the seismic data.

Finally, a complete synthetics package for each well was generated as a result of the seismic modeling process (Figs. 4.8 and 4.9). Fig. 4.8 shows the synthetic seismogram generated at wells 1 and 2 in the Rence field, with all the inputs to this process while Fig. 4.9 shows the well to seismic matching (shifting) at some of the wells. Synthetics seismograms are normally not exact match to the seismic. In order to match the generated synthetic Seismograms to the seismic trace, minor stretching and squeezing are required until an acceptable level of match is reached. This was achieved by manual adjustments to match the conspicuous event in the well (picks and troughs) with their corresponding seismic events. In Petrel[®], adjustments of the synthetics need to be done with the help of the formation tops generated from well correlation (Appendix I).

More so, well to seismic ties in Fig. 4.9 revealed that high amplitude reflection events (bluish colour) correspond to sand units, whereas, low amplitude reflection events (yellowish colour) correspond to shale units.

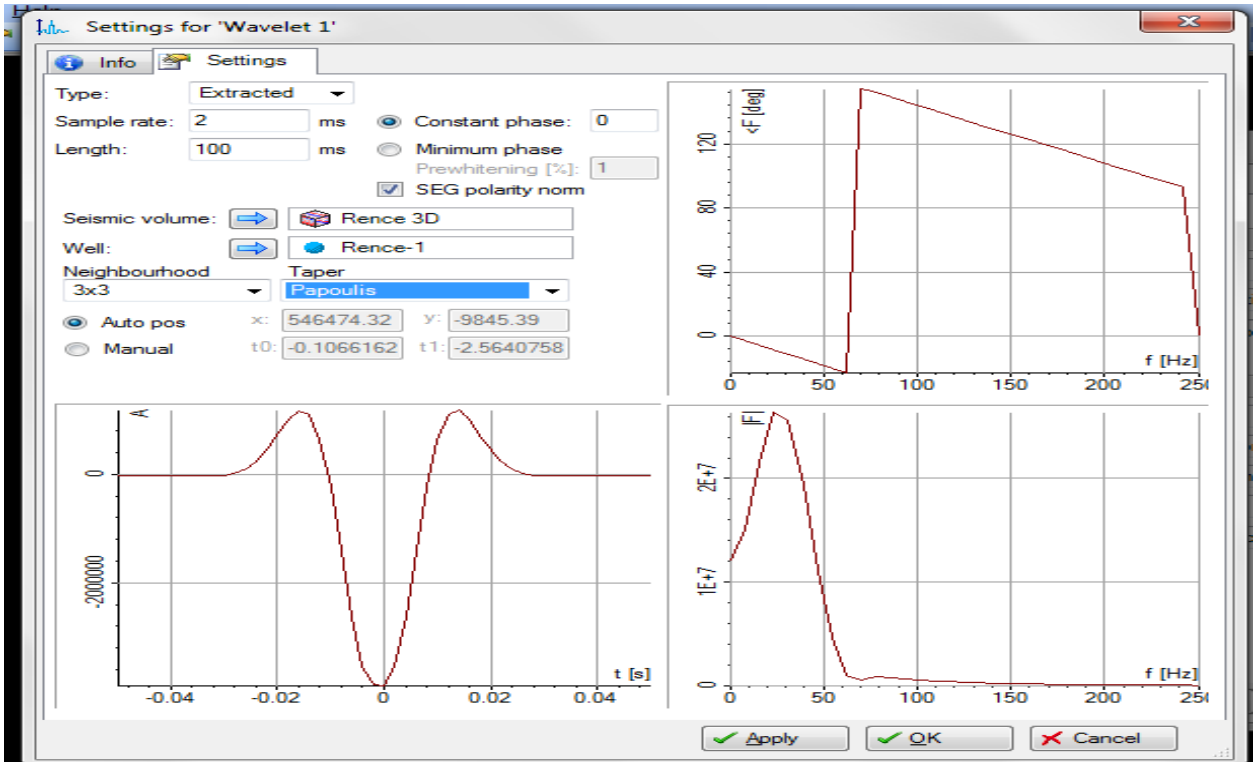


Fig. 4.7: Rence seismic wavelet profile extracted from Rence-1 well

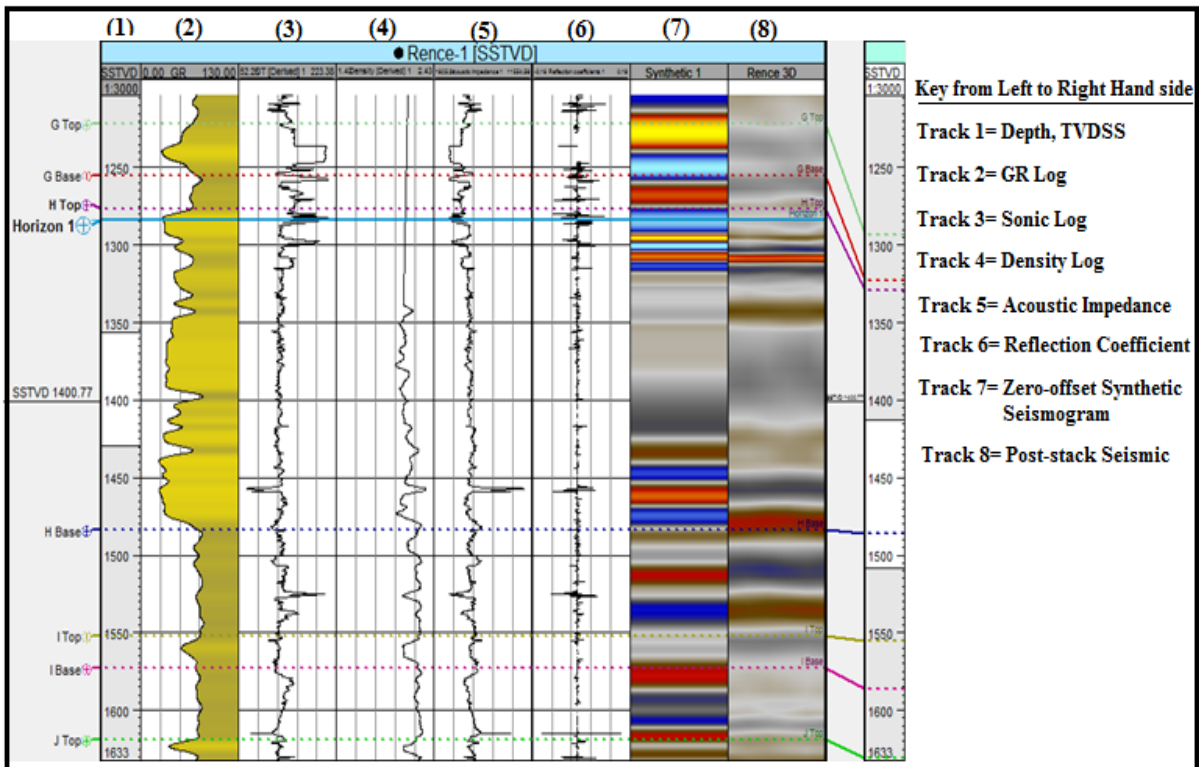


Fig.4.8a: The synthetic seismogram of the Rence field at well 1

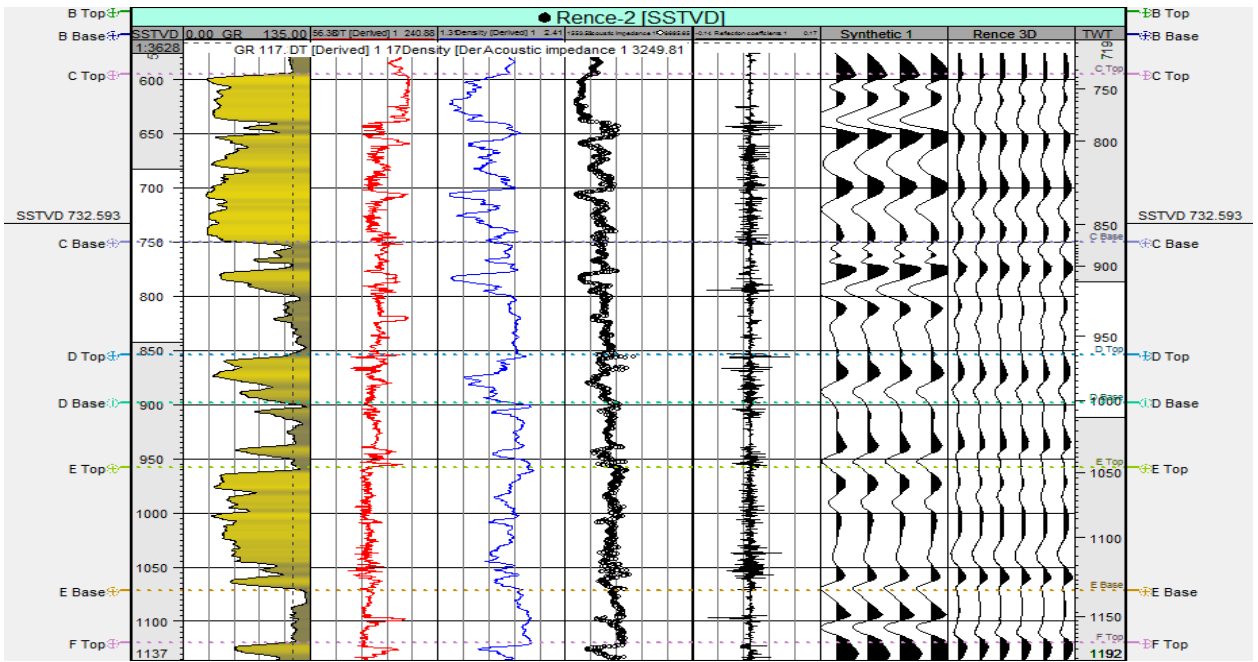


Fig.4.8b: The synthetic seismogram of the Rence field at well 2

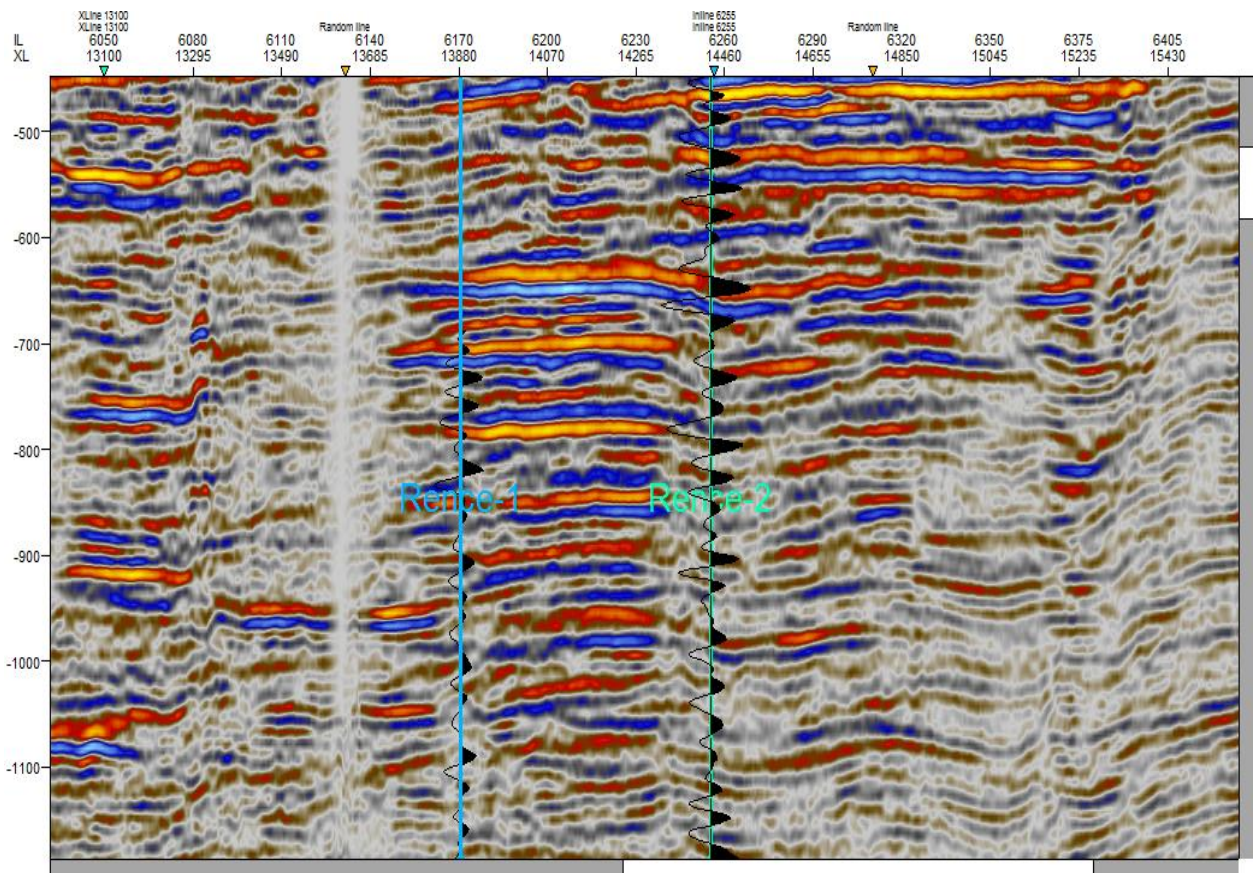


Fig. 4.9: The well ties posted on a seismic section within the Rence Field

4.2 RESULT OF SEISMIC STRUCTURAL INTERPRETATION

A detailed study of seismic structural interpretation in this project (Fig. 4.10) includes: the definition of reservoir geometry and the geologic boundaries of the field, extracting the structural framework of the reservoirs and creation of velocity model of the field for the purpose of depth conversion. These will help in generating all structural and rock physics input for the static modeling of the reservoir.

4.2.1 Fault interpretation

Fig. 4.11 shows the result of the structural interpretation of the 3-D seismic data of the study area. The interpreted seismic sections show the mapped horizons and faults. Sixteen faults were mapped all through the 8-inlines and 11-crosslines within the study area. The faults have curved concave-upward fault planes in down dip direction. Their slope progressively decreases until they became horizontal or flat, which is synonymous with growth faults.

Four major regional faults and twelve minor faults were interpreted. Seven of the faults are antithetic and dips landwards to the continent while the rest are synthetic faults dipping basin ward. Some of the faults were interpreted as back-to-back counter-regional faults. These fault domains are associated with mud diapirs. They include shale ridges and massifs shale overhangs as well as vertical mud diapirs that form mud volcanoes. Sedimentologically, this pattern of faulting exists where the rate of sediment supply and deposition are more or less equal to the subsidence and accommodation space.

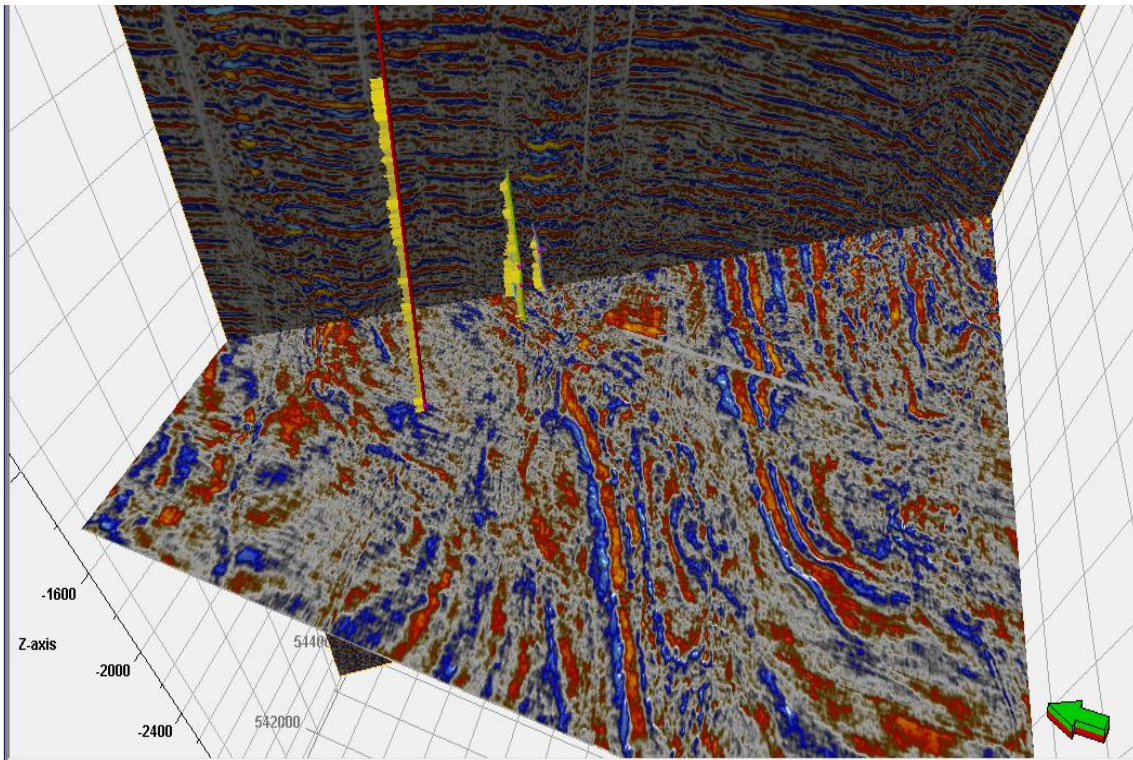


Fig. 4.10: Structural Configuration of the Rence Field

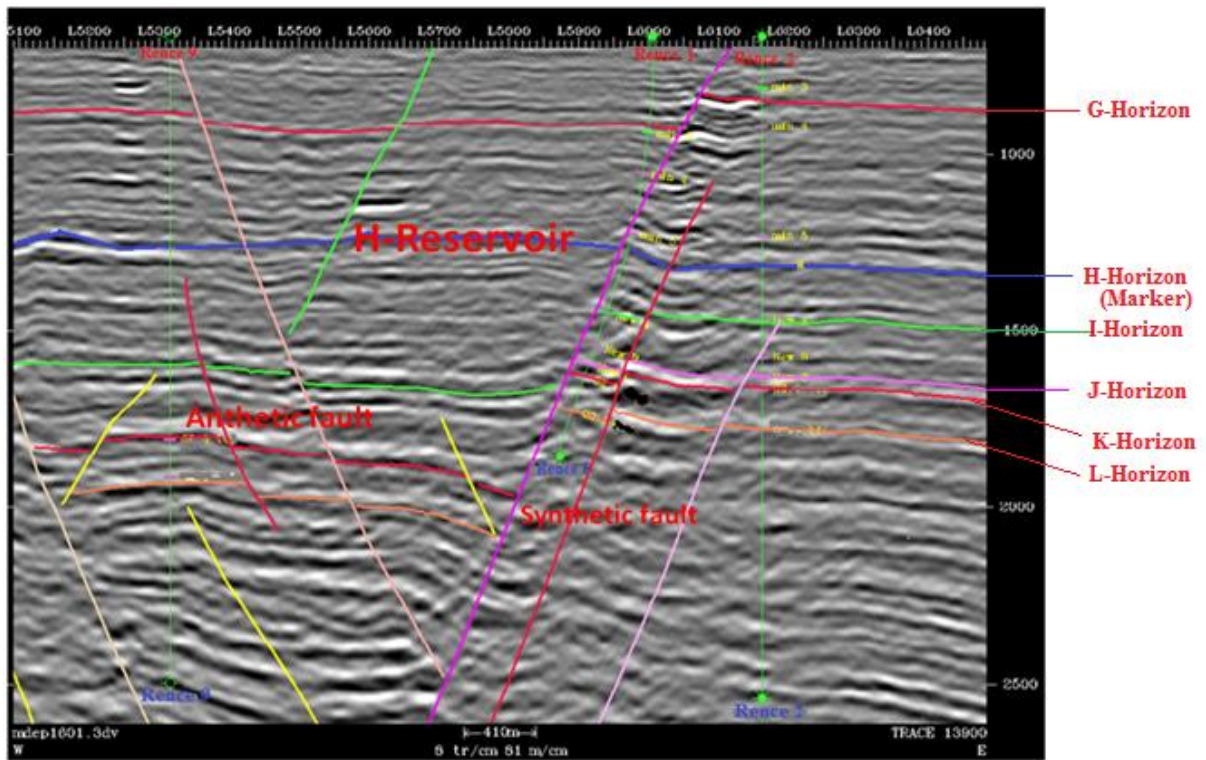


Fig.4.11: Seismic interpreted section on trace 13900 of Rence field

Regular spacing and simplicity of the structures are within the structural styles that characterize the Northern depobelt of the Niger Delta.

In the Niger Delta deltaic system however, this type of faulting are mainly found within the delta front environment, where the deposition of channel lobes cause the Akata Formation to buckle up. It is also evidently seen in the aggradational stacking pattern associated with the gamma ray logs from wells within the Rence Field. The regional faults form both the northern and southern boundaries of the field while the major fault at the centre of the field separated the field into two blocks (Fig. 4.11).

4.2.2 Horizon Interpretation

The seismic event (pick) corresponding to the top of the reservoir was identified using the well tie as a guide to recognizing the event. The H top horizon was mapped across the study area using a 10 x 10 m grid of in-lines and cross-lines (Fig. 4.11). The horizon shows continuity of reflection with relatively uniform amplitude and frequency. Areas that require more detailed examination were mapped using smaller grids. The benefit of using a composite line section at the start of the horizon tracking is to guide the later inline and crossline tracking in areas where well controls are absent. When the composite line tracking is completed, regular in-lines and cross-lines were tracked with an increment of 10m.

Loop-tying the horizons in the in-line and cross-line directions helped in reducing mis-ties that could under/over-estimate the unit's areal extent. After the manual horizon picking was concluded, the horizons were auto-picked. The auto-pick

operation allowed the software to track events along bedding planes across the entire seismic volume, using the hand-picked horizons as constraint.

4.2.3 Time Map Generation

The interpreted horizon grids were converted to time structural maps using convergent gridded algorithm in Petrel. The map generated in time for the top of the interval is shown in Fig. 4.12. The time-structure maps show the geometry of the basin and changes in topographic relief through time.

4.2.4 Time to Depth Conversion

The first step to converting a time structural surface is by defining the velocity model. The estimation of realistic velocity model parameters involves a delicate balance of well and surface data. Interval velocity is the closest equivalent in the raw data of the instantaneous velocity used in the velocity modeling process. It was therefore useful to create and view this data before building the velocity model (Fig. 4.13). A curvilinear equation (equation 4.4) was generated from the velocity modeling using regression analysis.

$$y=0.0001x^2 + 1.1346x + 46.6442 \quad (4.4)$$

Where, y is the measured depth which is the dependent variable

x is the two way travel time which is the independent variable

Interval velocity was used to create the velocity model within the H-Reservoir level.

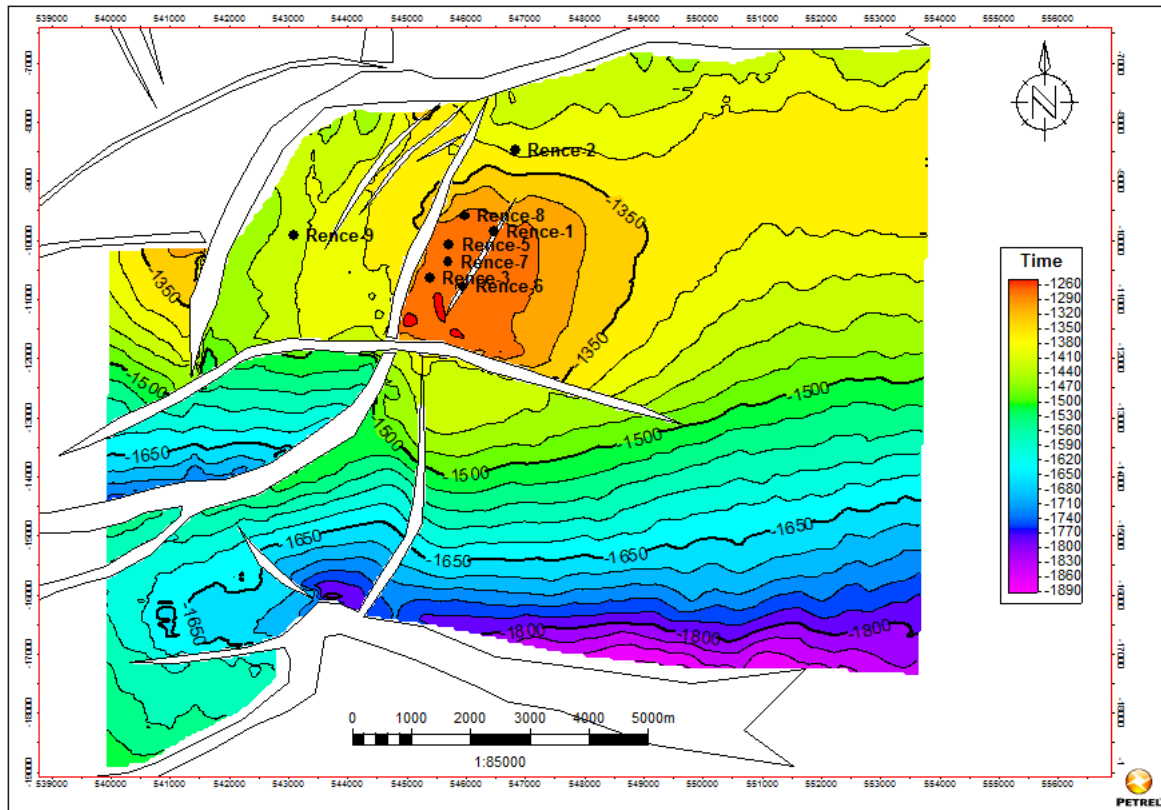


Fig.4.12: Time-structure map of H top reservoir horizon (Contour interval is 30 ms)

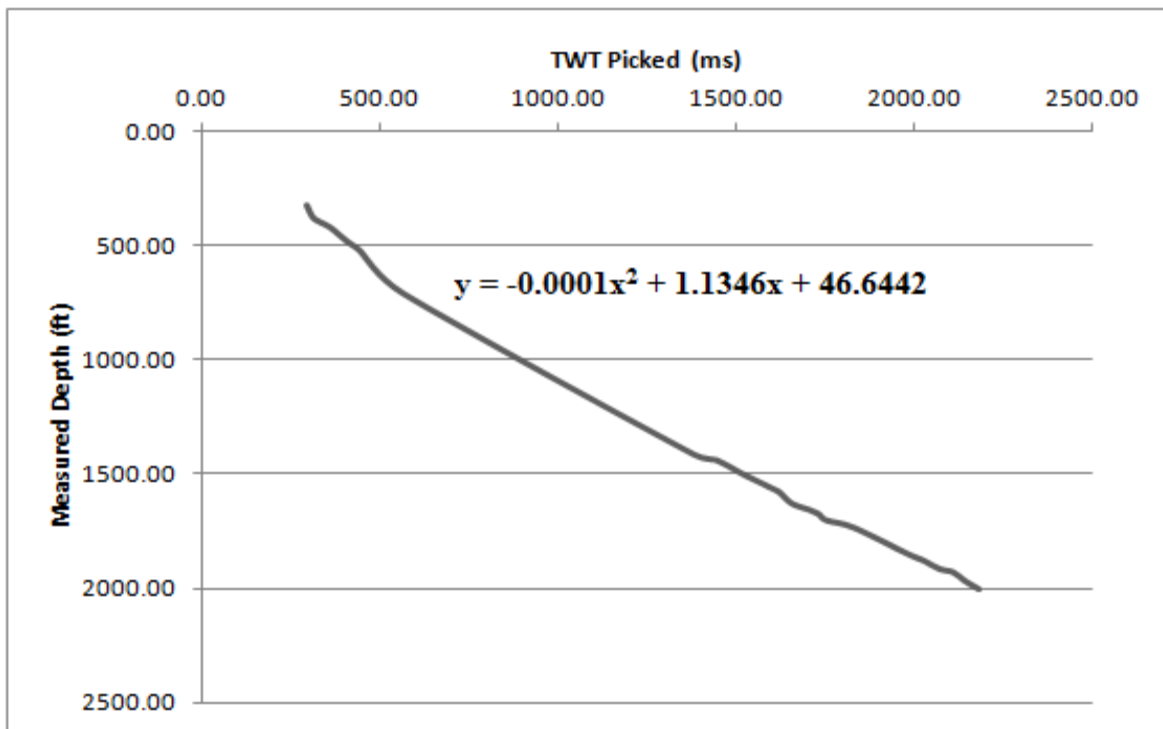


Fig.4.13: Rence Field velocity curve.

The values were estimated using the time depth relationship (TDR) through the zone for each well and a single velocity constant value was used. Petrel[®] employs a minimum depth error method to estimate this value. Corrections were done using the well tops correlated across the wells. Using the create model algorithm, it was possible to convert time objects; including structural maps, 3D seismic volume, 3D geologic model and seismic attributes to depth (Fig. 4.14).

4.2.5 Result of Reservoir Petrophysics

The Table 4.1 below shows the results of the average petrophysical properties of the hydrocarbon bearing sands encountered in Rence wells. The results obtained from the estimation works were calibrated using the available log and core data from the wells. After the petrophysical attributes were estimated, the hydrocarbon reserve for the H-horizon mapped was estimated. The petrophysical results include net to gross which ranges from 0.84 to 0.93 with an average of 0.90 while the volume of shale ranges from 0.21 to 0.36 with an average of 0.28. Also, the porosity of the identified reservoir ranges from 0.17 to 0.37 with an average of 0.28 whereas the water saturation ranges from 0.14 to 0.36 with an average of 0.24.

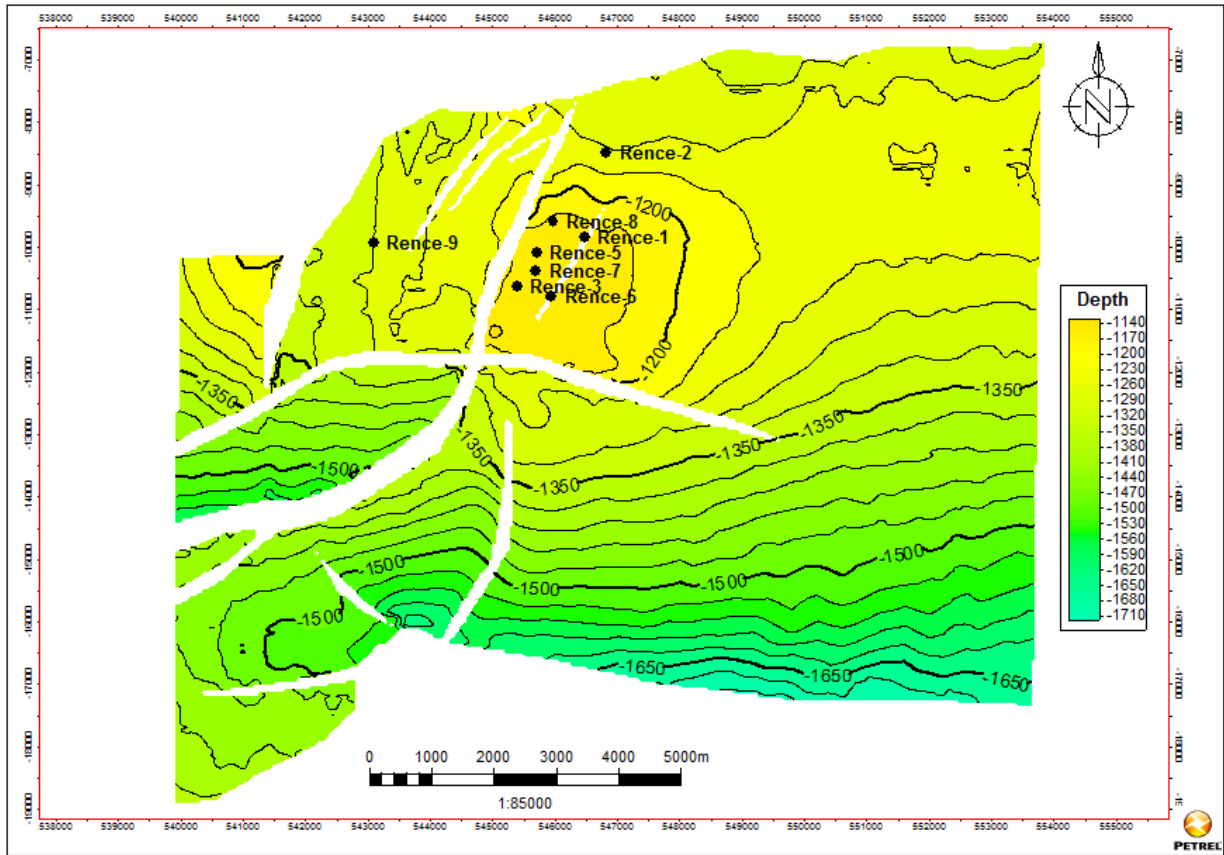


Fig. 4.14: Depth-structural map of H top reservoir horizon (Contour interval is 30 m)

Table 4.1: Summary of Petrophysical Properties in the study area for H-Reservoir

Well Identifier	Sand	Top (ft) TVD	Top of Sand (ft)	Bottom of Sand (ft)	Bottom (m)	Gross (ft)	Net (ft)	NTG	Volume of Shale	Porosity	Water Saturation
Rence 1	H	1276.63	1285.63	1483.75	1492.75	207.12	187.12	0.90	0.26	0.28	0.32
Rence 2	H	1329.57	1355.48	1486.36	1512.30	156.82	141.82	0.90	0.21	0.17	0.25
Rence 3	H	1265.70	1581.24	1307.19	1648.61	67.37	62.37	0.93	0.19	0.31	0.33
Rence 5	H	1264.55	1324.45	1419.17	1519.06	194.61	174.61	0.90	0.32	0.33	0.14
Rence 6	H	1289.72	1561.42	1484.43	1854.88	293.46	268.46	0.91	0.27	0.37	0.18
Rence 7	H	1269.07	1355.56	1436.42	1540.16	184.60	164.60	0.89	0.29	0.23	0.36
Rence 8	H	1280.50	1543.83	1280.50	1790.85	247.02	217.02	0.88	0.33	0.34	0.14
Rence 9	H	1375.31	1401.22	1536.38	1562.29	161.07	136.07	0.84	0.36	0.23	0.18

4.2.6 Result of Volume Estimation

The volume estimation of hydrocarbon in H-reservoir was estimated using the calculated petrophysical parameters (Table 4.6) and data derived from the depth structural map (Fig. 14). Thus, the values extracted are:

- Area of oil closure (A) = 6088.677 acre
- Net pay thickness (h)= 169.0088ft
- NTG=0.89375
- VSH= 0.27875
- Porosity (ϕ)= 0.2825
- Water saturation (S_w)= 0.2375
- Hydrocarbon saturation (S_h)= 0.7625
- Formation volume factor for oil (B_{oil})= 10.14958

Hence, the estimated original oil in place (OOIP) is 47.2 million barrels and estimated stock tank original oil in place (STOOIP) is 479.4 million barrels.

4.2.7 Result of Oil-Water Contact

Fig.4. 15 shows clearly the oil/water contact which is represented by the blue lines. Oil bearing sands can be evidently discriminated by the acoustic impedance. High porosity sands are always characterized by the lowest AI values (Figs. 4.15 and 4.16). Acoustic differences between Oil Sand clusters are caused by Porosity changes. Wet lithologies show a common acoustic range. All the Water bearing lithologies

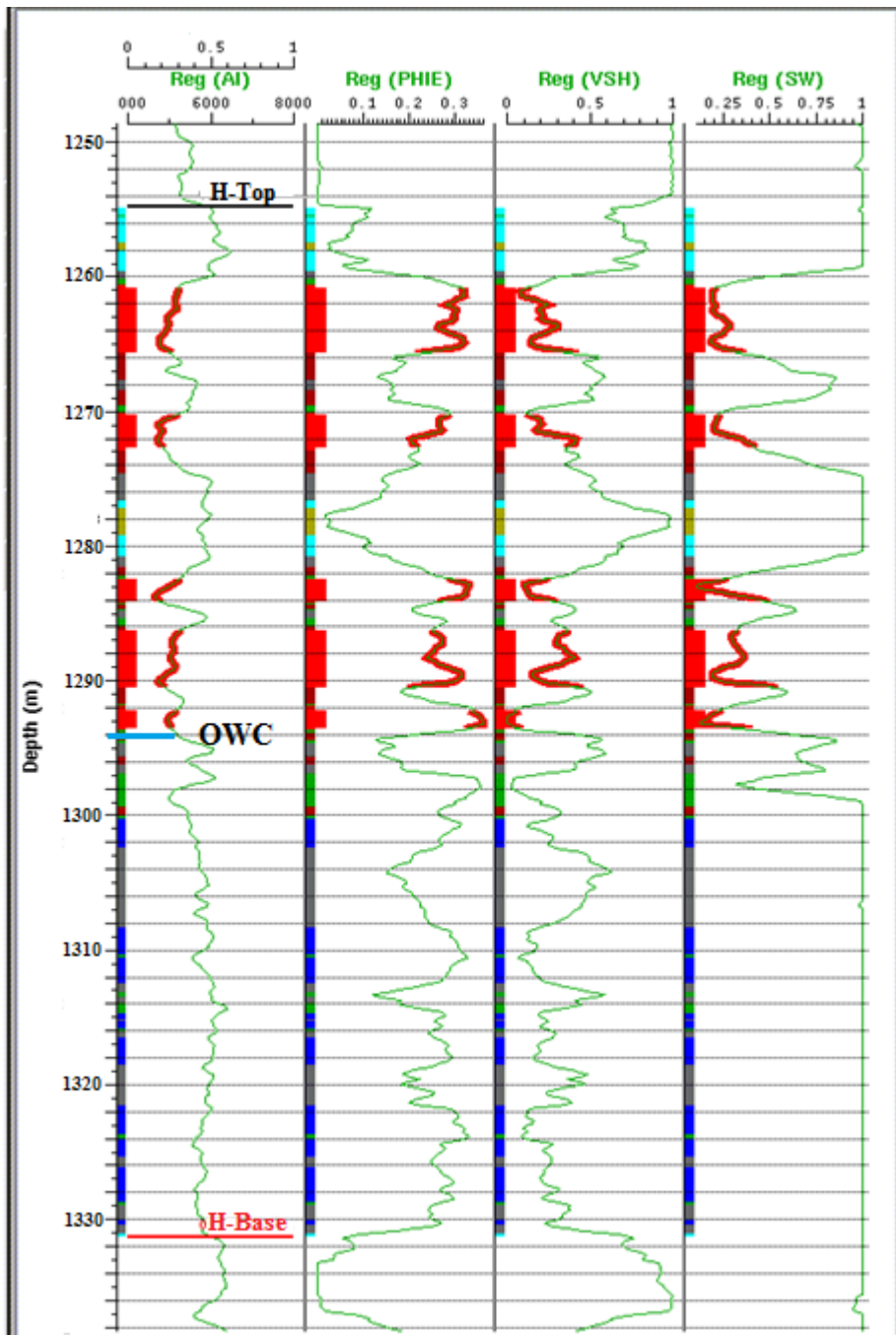


Fig.4.15: Multi-graph showing the oil/water contact in the study area

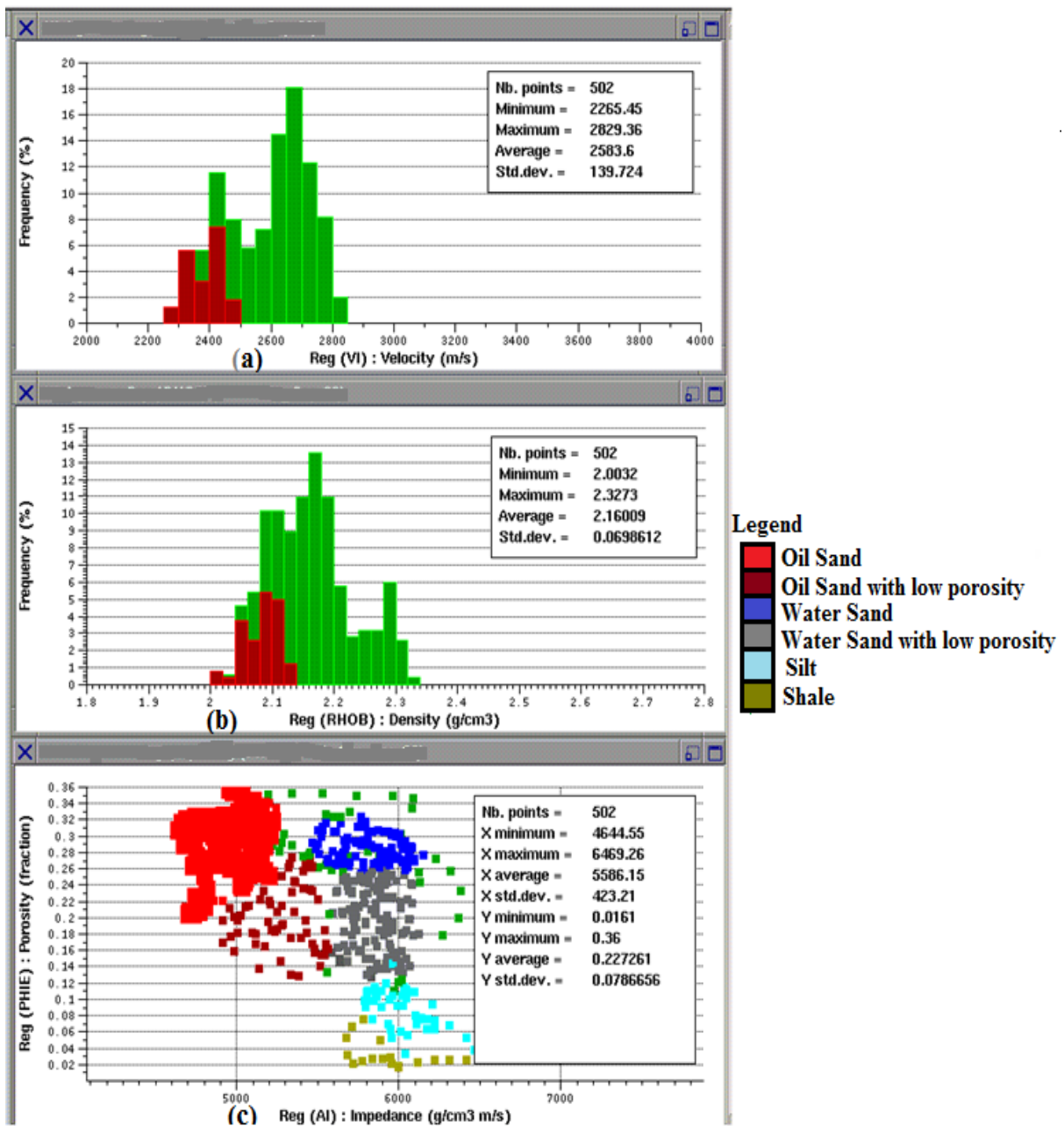


Fig.4.16: Petro-Acoustic Analysis showing Oil/Water sand: (a) Histogram of velocity and frequency (b) Histogram of Density and Frequency (c) Crossplot of AI and porosity.

described in this H-reservoir are characterized by a common Acoustic Impedance range (AI overlap).

The oil zone have values ranging from 1258m (4063ft) to 1294m (4180ft) at H-reservoir and the oil/water contact is delineated at the depth of 1294m (4180ft).

Fig.4.16 shows that oil sand have lower acoustic impedance ranging from 4600 to 5450 $\text{g/cm}^3 \cdot \text{m/s}$ with the highest porosity of 0.36. But, water sand has higher acoustic impedance ranging from 5500 to 6150 $\text{g/cm}^3 \cdot \text{m/s}$ with the lowest porosity of 0.12.

4.3 RESULT OF SEISMIC ATTRIBUTES

4.3.1 Result of Single Attributes

Eight seismic attributes were particularly used in this study. They include average energy, RMS amplitude, instantaneous frequency, reflection acoustic impedance, iso-frequency, dominant frequency, signal envelope/ reflection strength and coherence attributes. These seismic attributes were generated across the study area and are shown in Figs. 4.17, 4.18a-d and 4.19a-e. The maps displaying the distribution of the different facies show depositional morphologies similar to the aerial photography of modern depositional systems. Application of single seismic attributes on a geoprobe from interpreted 3D seismic data (Figs. 4.18b-d and 4.19a-e) has very low impact in the visualization of channel features. Meanwhile, the generation of an amplitude map (Fig. 4.17) reveals area where there is bright spot which is a good hydrocarbon indicator.

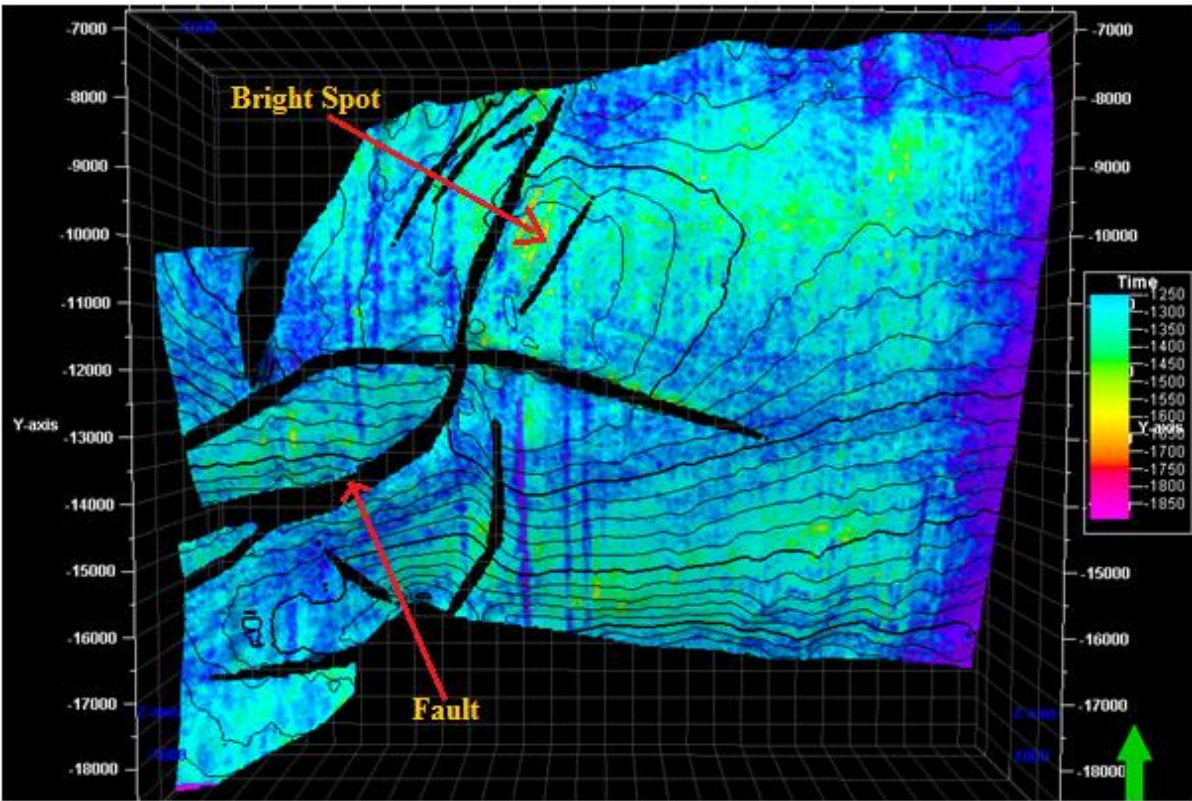


Fig. 4.17: Amplitude map generation for H-Horizon.

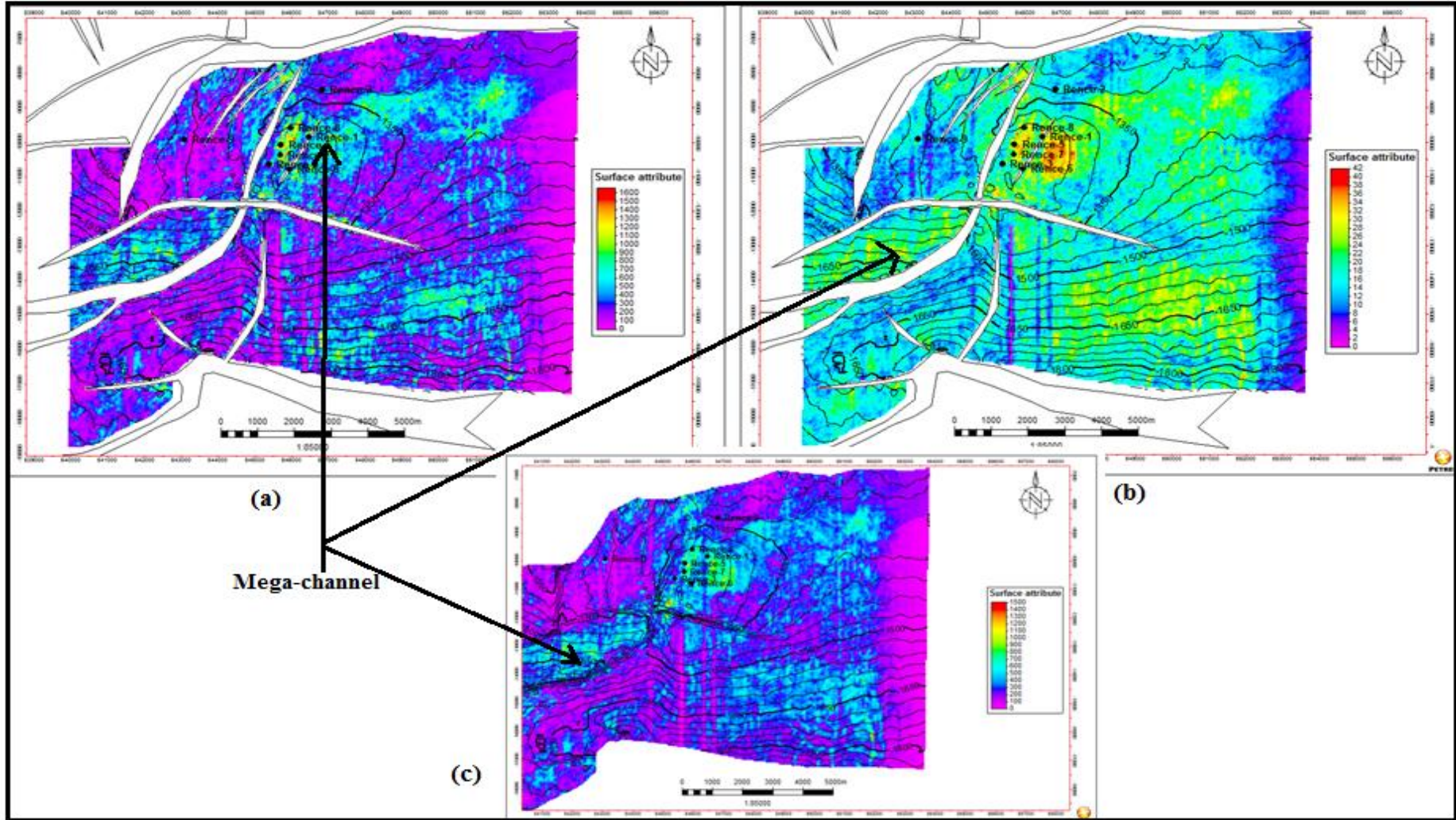


Fig. 4.18: Individual seismic attribute showing mega channel: (a) Signal Envelope attribute, (b) Instantaneous phase attribute and (c) Average Energy attribute.

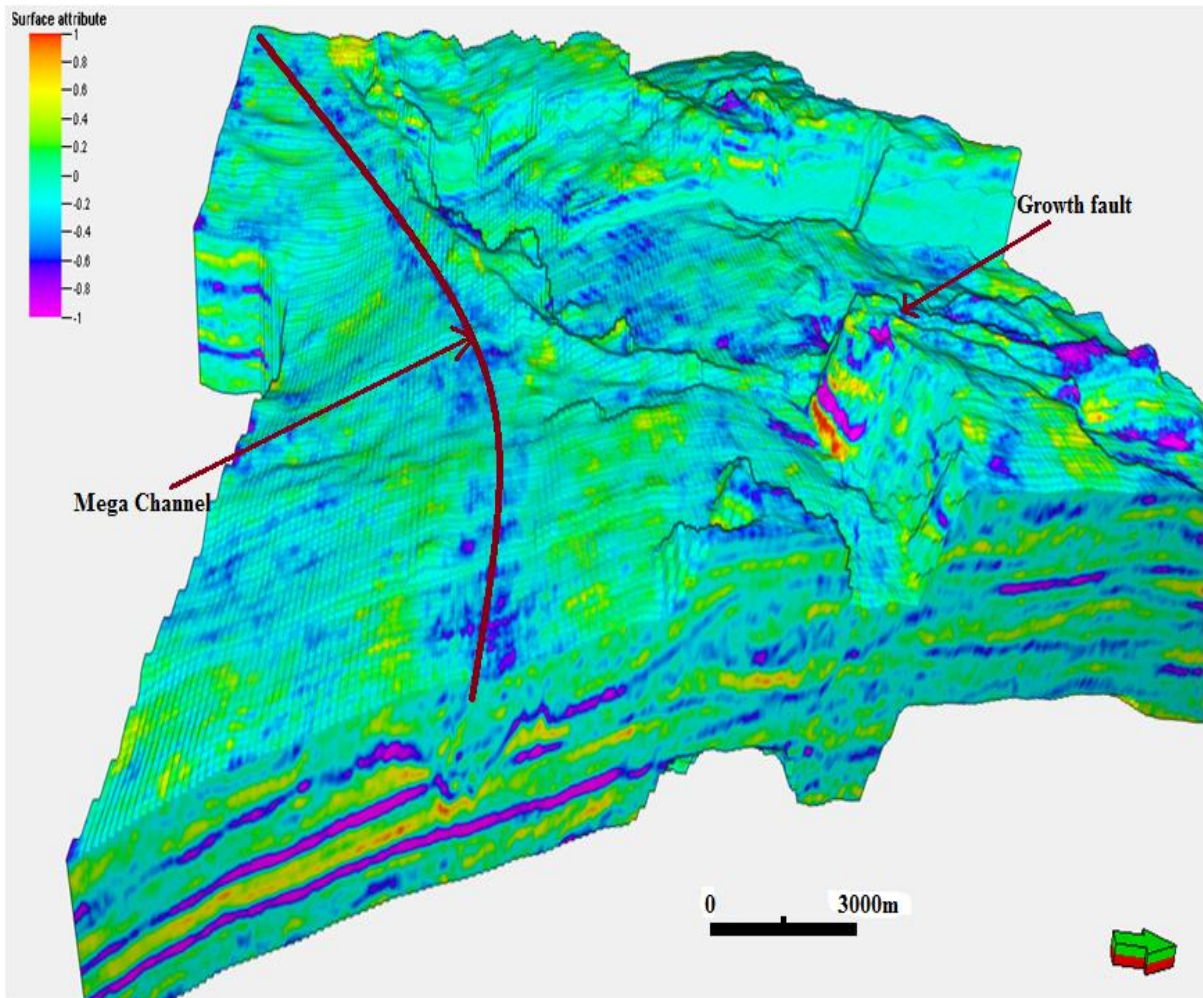


Fig. 4.19a: Morphological modelling of geoprobe through coherency attributes showing mega channel.

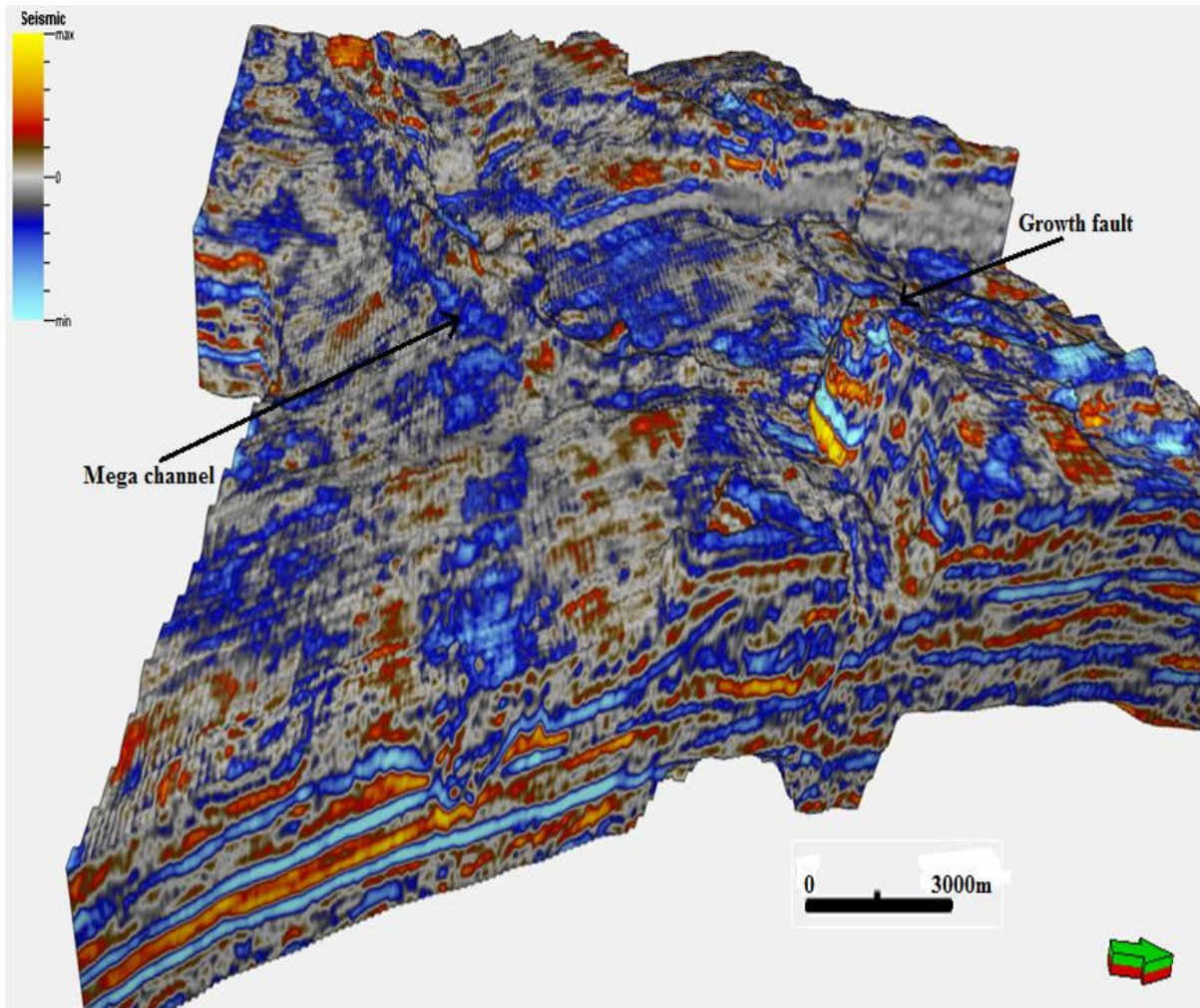


Fig. 4.19b: Morphological modelling of geoprobe through instantaneous frequency attributes showing mega channel.

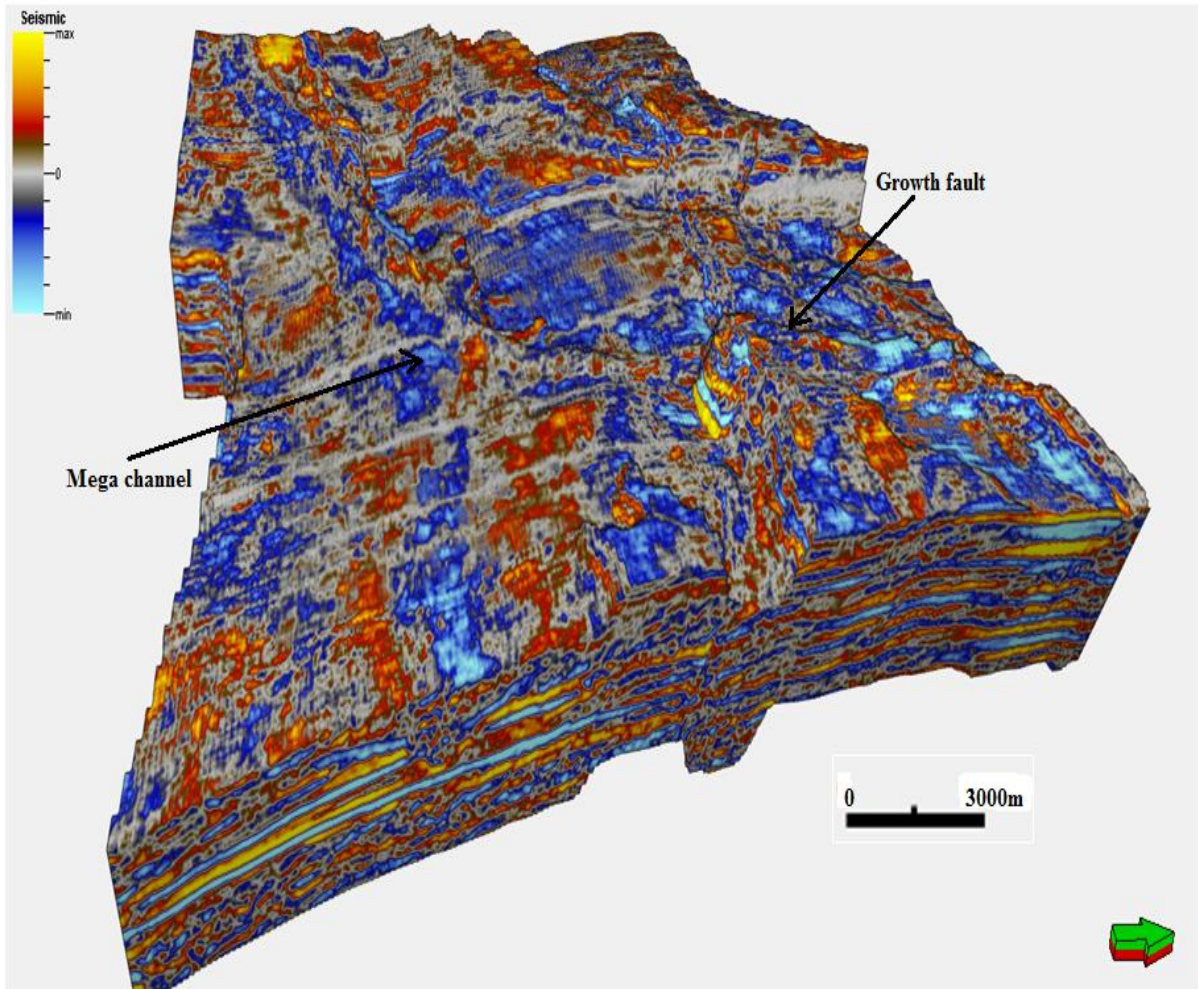


Fig. 4.19c: Morphological modelling of geoprobe through reflection acoustic impedance attributes showing mega channel.

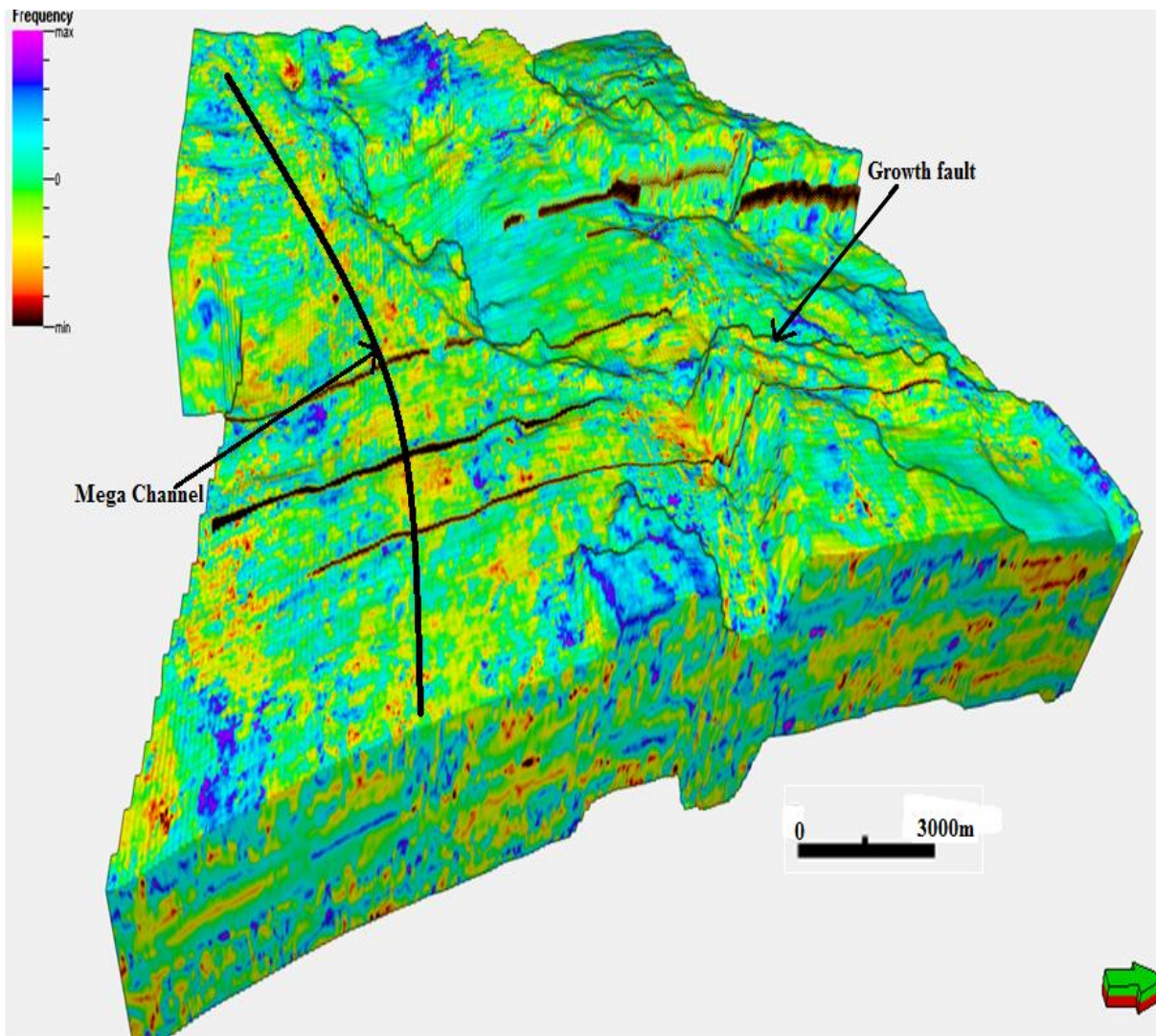


Fig. 4.19d: Morphological modelling of geoprobe through iso-frequency attributes showing mega channel.

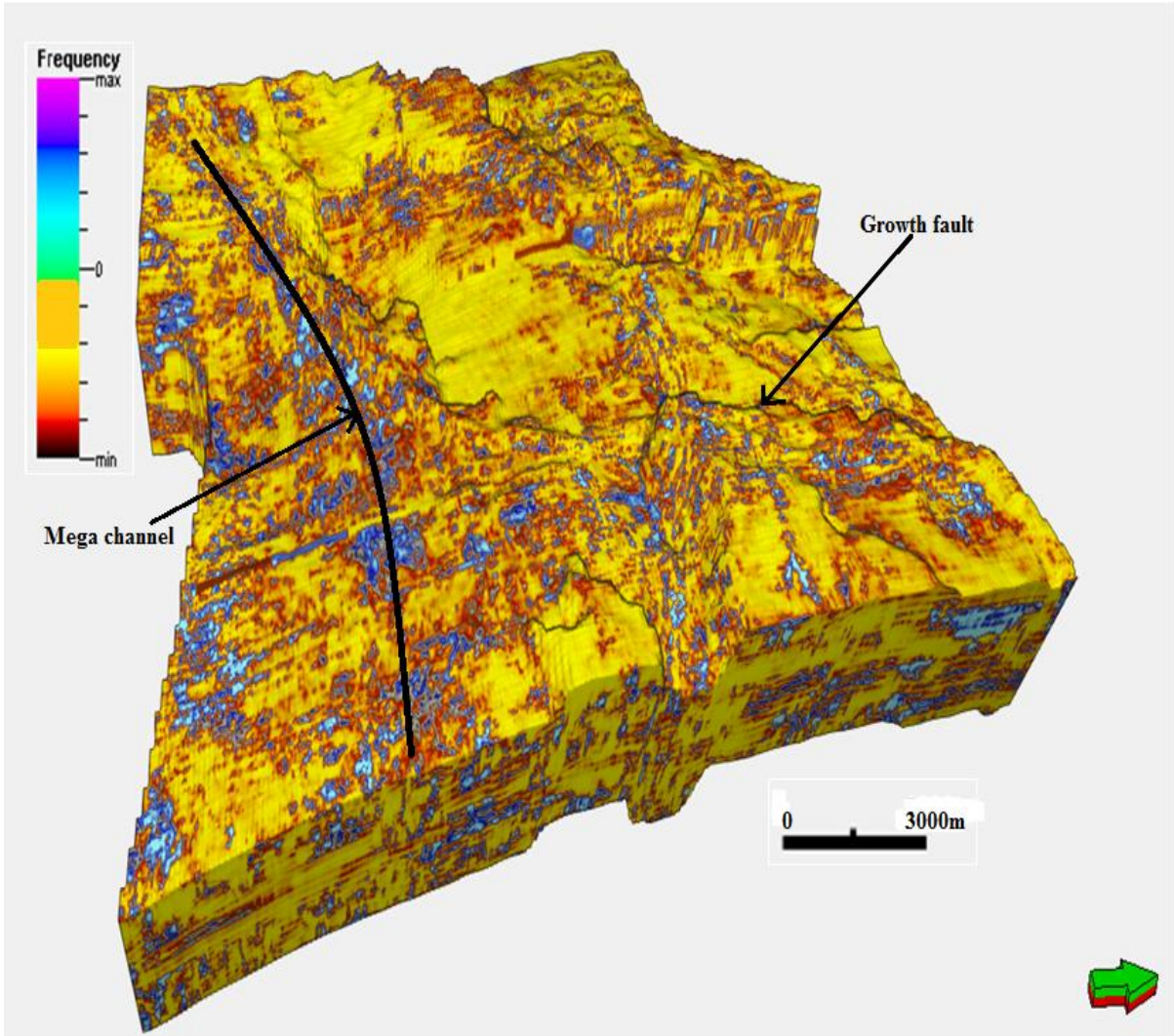


Fig. 4.19e: Morphological modelling of geoprobe through dominant frequency attributes showing mega channel.

4.3.2 Result of Co-blending Attributes

Co-blending of seismic attributes has proven of particular use in this region. The results of the Co-blending of various seismic attributes are shown in Fig. 4.20a-d. The results of the co-blending of seismic attributes reveal the enhancement of visualizing channel geometry, whereas the surrounding areas are essentially unchanged.

One mega-channel feature is clearly seen in the middle of the attribute maps produced which runs in east-west direction. This channel exhibits differential compactions, and the edge of the channel is well defined by co-blending attributes used in this study.

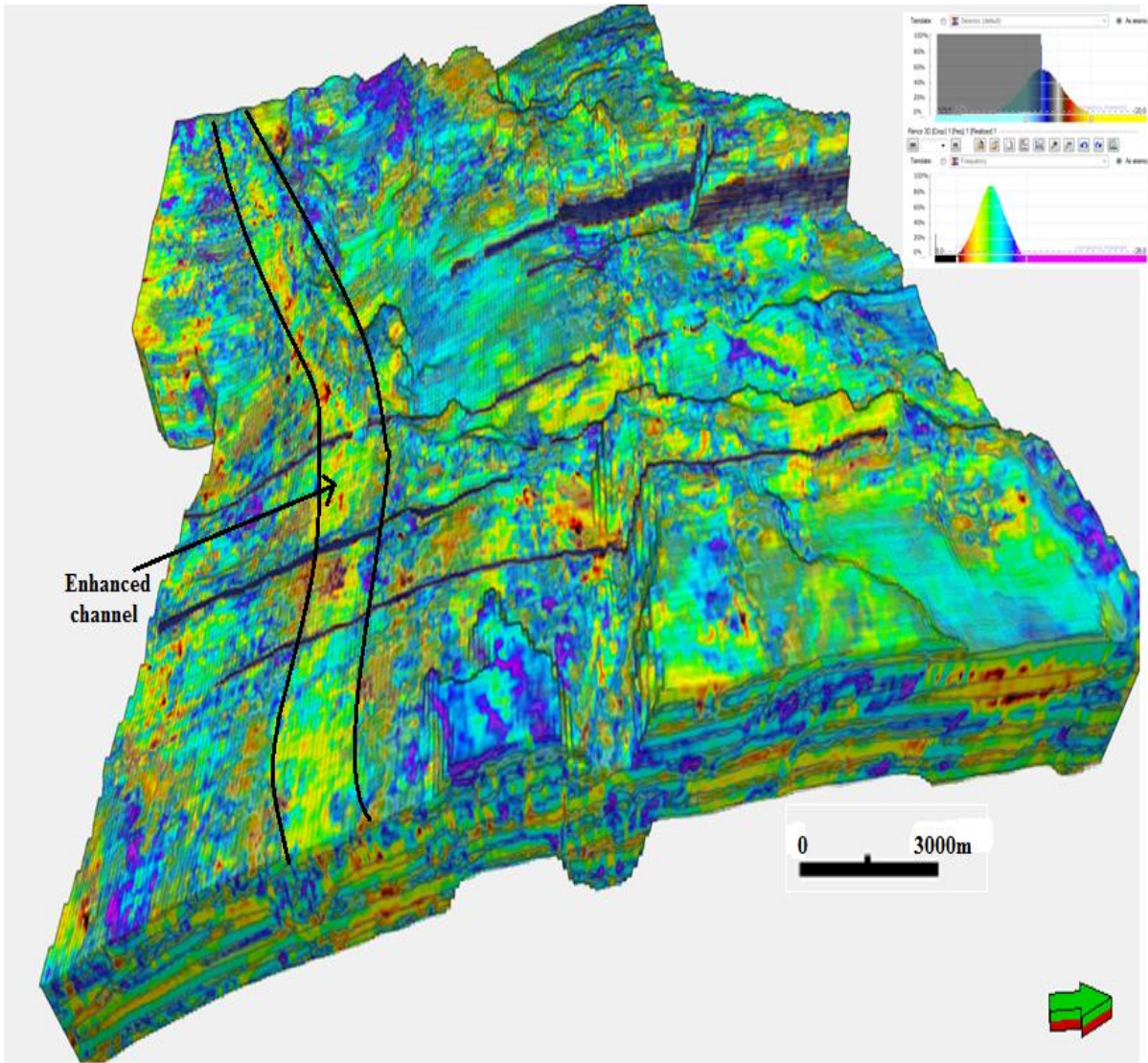


Fig. 4.20a: Co-blending of signal envelope and dominant frequency attributes.

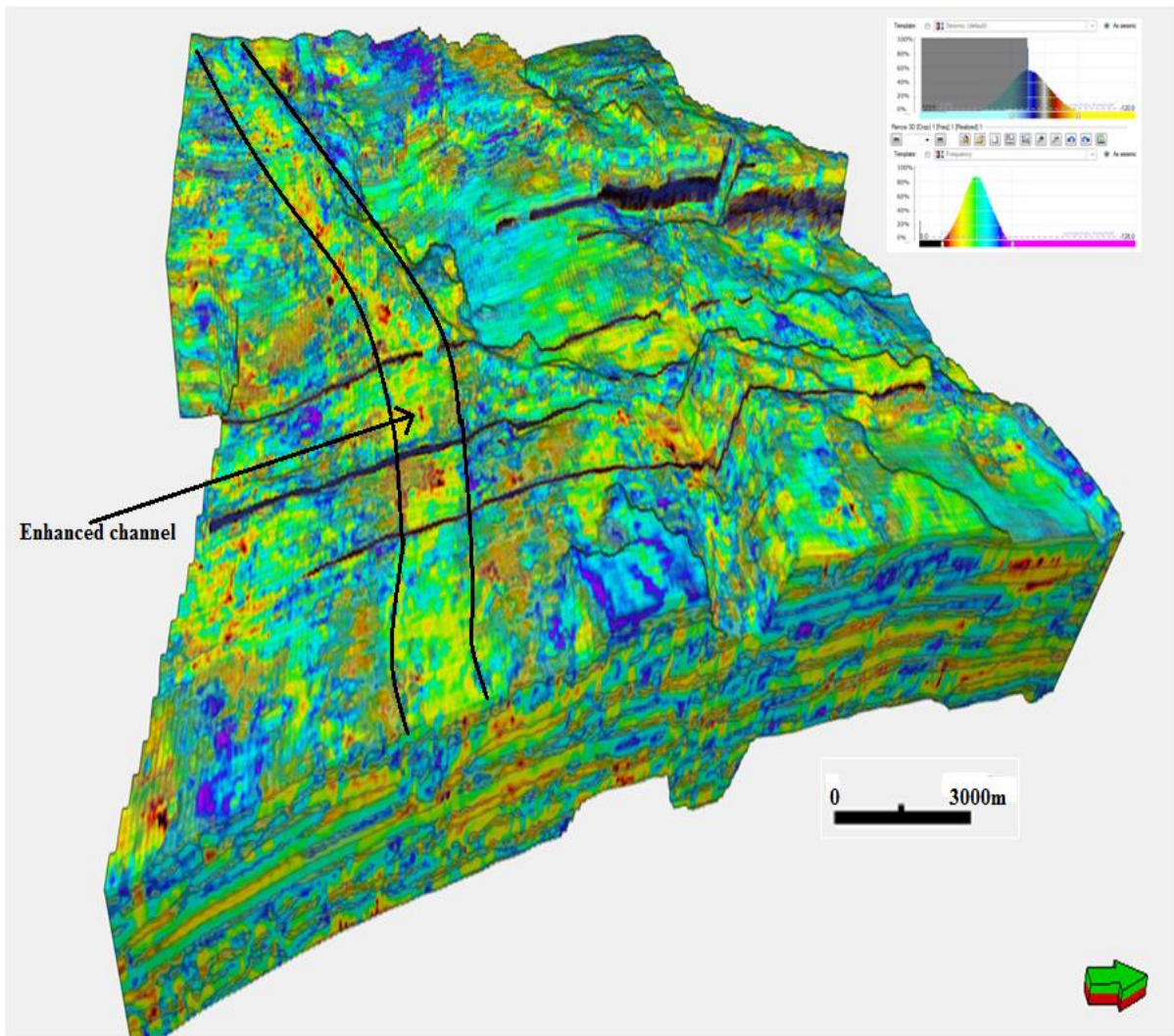


Fig. 4.20b: Co-blending of reflection acoustic impedance and RMS amplitude attributes.

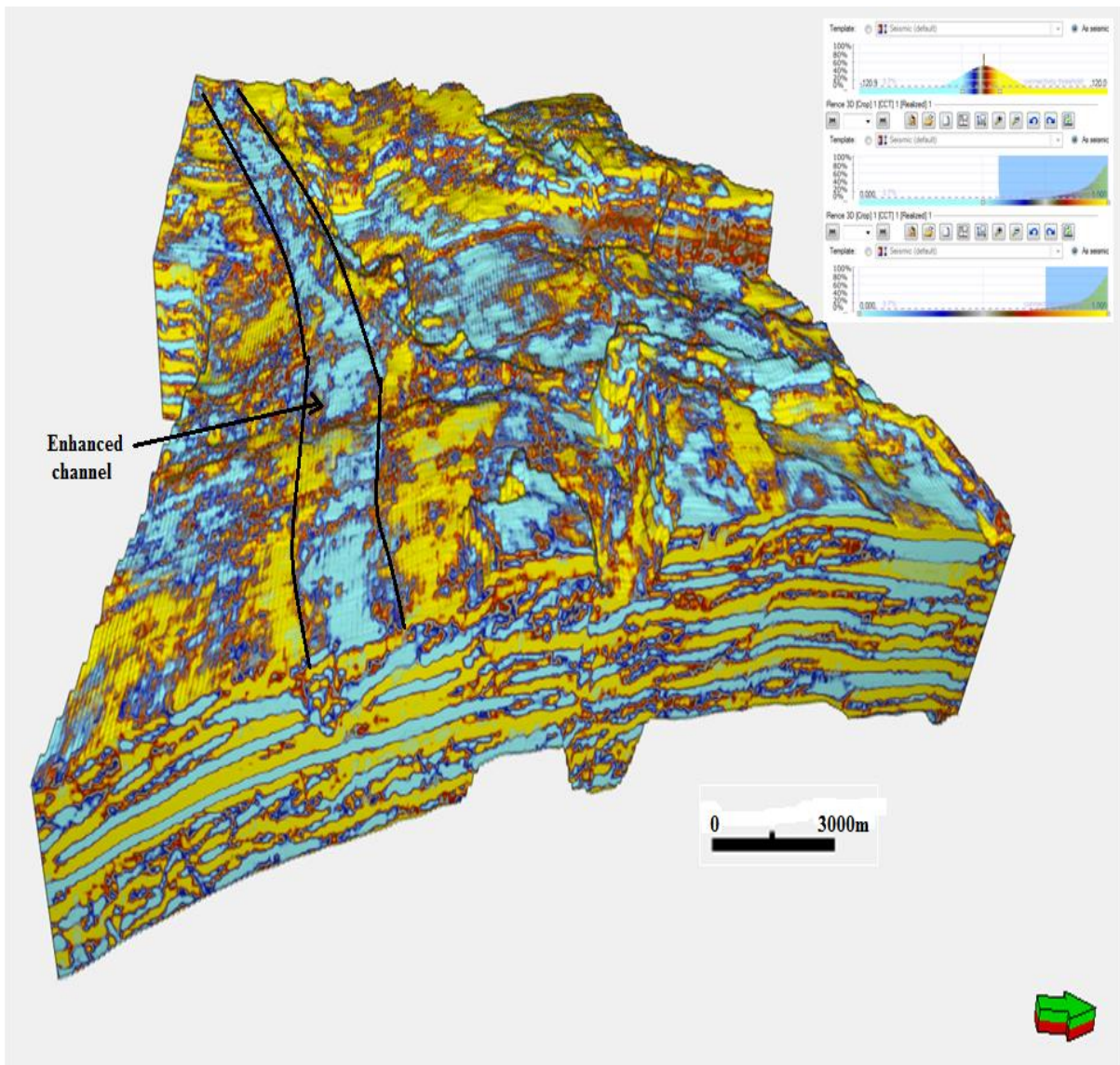


Fig. 4.20c: Co-blending of reflection acoustic impedance, instantaneous frequency and average energy attributes.

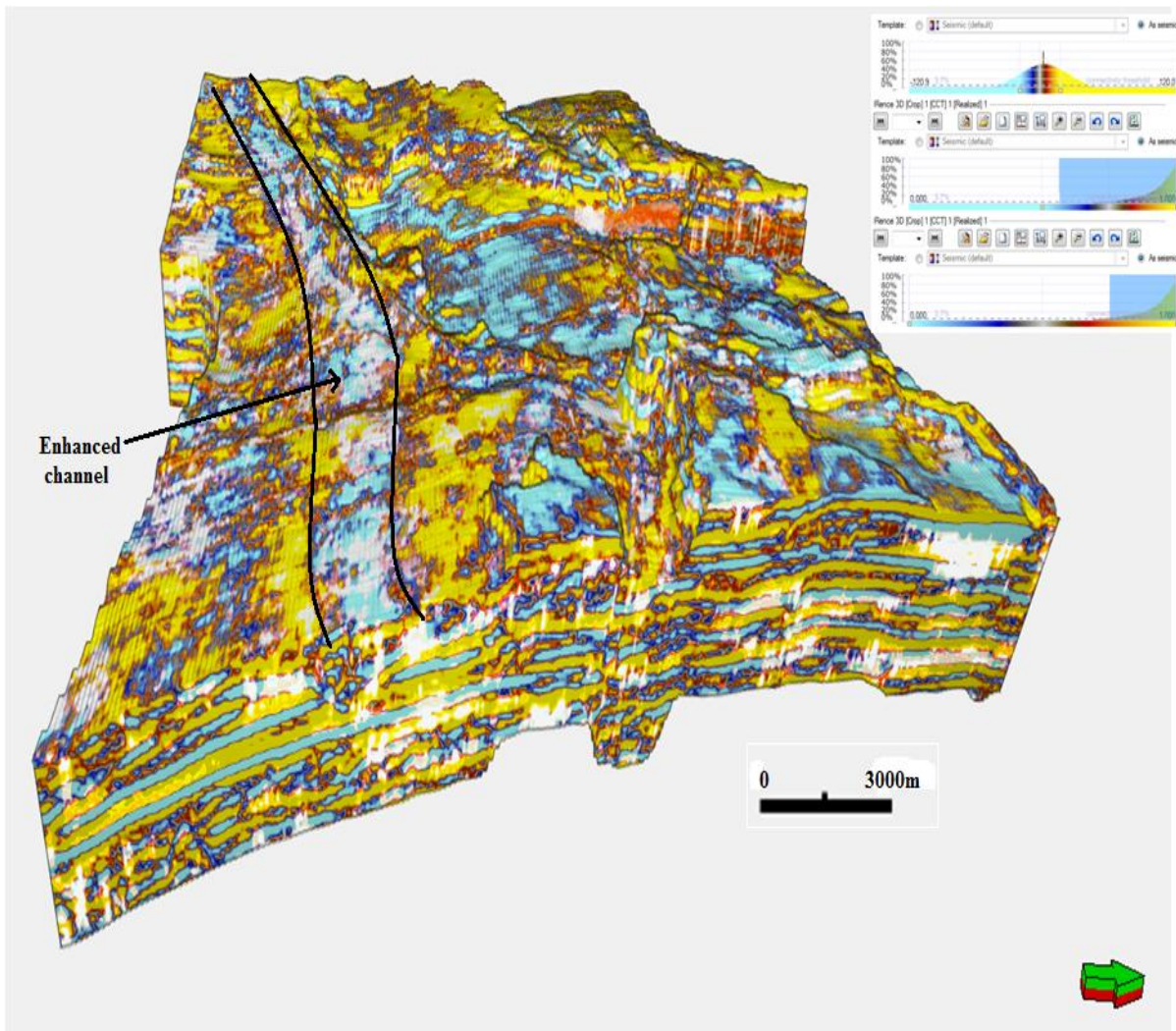


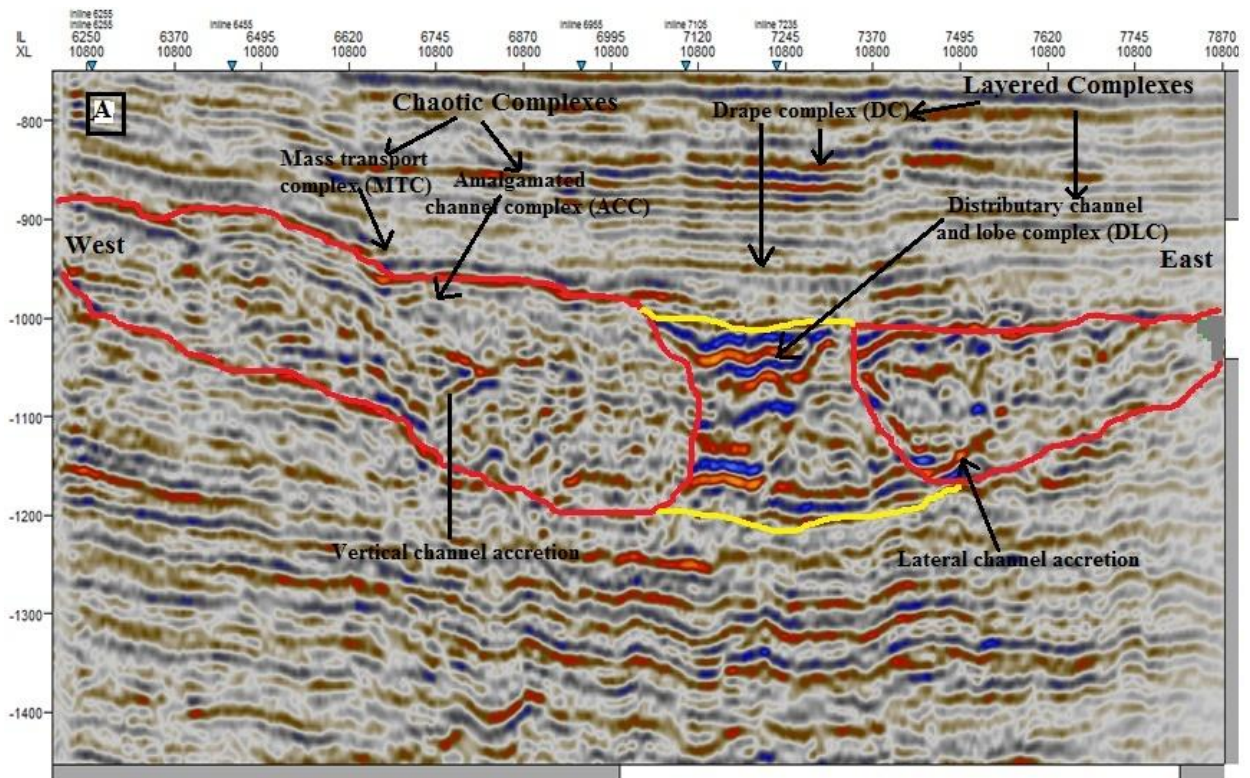
Fig. 4.20d: Co-blending of reflection acoustic impedance, iso-frequency and coherency attributes.

4.4 SEISMIC FACIES AND STRATIGRAPHIC ANALYSIS

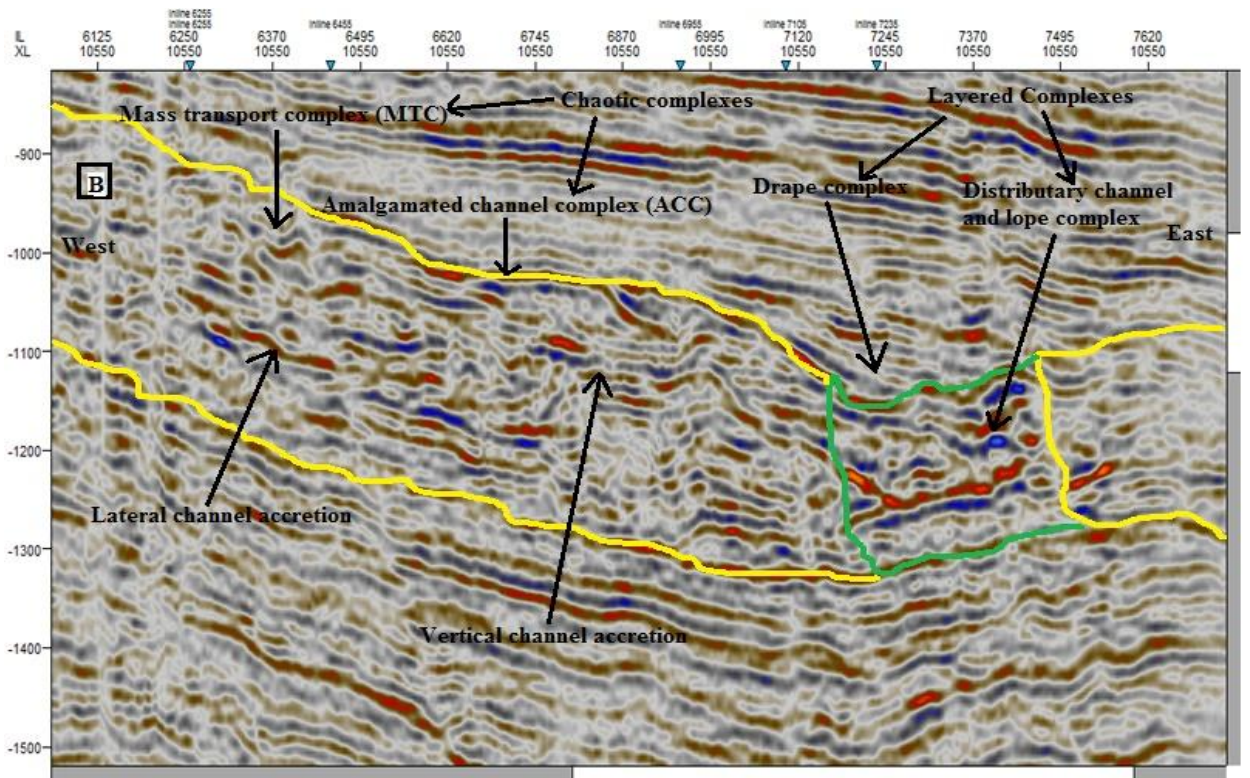
The result of the seismic facies and stratigraphic analysis reveals that the study area can be distinguished into two categories of seismic facies namely layered complexes, and chaotic complexes (Fig. 4.21a-b). These two categories can be further subdivided into four distinct seismic facies (see Fig. 4.21 and Table 4.2): (1) mass transport complexes (MTC), (2) distributary channel and lobe complexes (DCLC), (3) amalgamated or accretionary channel complexes (ACCs), and (4) drape complexes (DCs).

4.4.1 Mass Transport Complexes

The mass transport complexes in the study area are mostly reflection-free and consist of chaotic and transparent, low-amplitude, poor continuity seismic reflections. They correspond to the 'B1' facies of Prather *et al.* (1998) and consist of a variable lithology of mud-rich complexes of slumps, slides and debris-flow deposits. At depth, the MTCs represent the highest volume of sediment, but their thickness is reduced drastically up section. The MTCs are very erosive. They eroded part or all of the underlying drapes, part of the underlying distributary lobe and channel complexes, and part of the amalgamated channel complexes (Fig. 4.20a-b). As a result, the lower boundaries of MTCs in this area are truncation surfaces. They form the base of depositional units and bound each depositional cycle.



(a)



(b)

Fig. 4.21: Seismic section showing seismic facies recognized in the study area: (a) crosslines (10800) (b) crosslines (10550).

Table 4.2: Characteristics of different facies within the Rence field

Seismic Facies	Seismic Configuration	Interpreted Depositional System
Mass Transport Complexes (MTC)	Mainly reflection-free and consisting of chaotic and transparent, low-amplitude, poor continuity seismic reflections	Consists of a variable lithology of mud-rich complexes of slumps, slides and debris-flow deposits. Due to the associated seismic character, it could be suggested that ACCs consist of coarser-grained sands than DLCs, which are usually deposited further basinward.
Amalgamated Channel Complexes (ACC)	They are distinguished based on characteristic chaotic, discontinuous, high-impedance seismic reflections.	
Distributary Channel and Lobe Complexes (DLC)	DLCs are made up of layered, continuous, high-impedance seismic reflections.	Coarse-grained sands
Drape Complexes (DC)	They are characterized by high or low impedance, laterally continuous seismic reflections that can be traced for a long distance. DCs are very mappable seismic reflections	Mostly of clay-rich shales or marl (foraminifera-rich calcareous clay)

4.4.2 Distributary Channel and Lobe Complexes (DLCs)

DLCs are made up of layered, continuous, high-impedance seismic reflections. Well logs and core data have proved DLCs to be the most sand-prone facies in other basins (Prather *et al.*, 1998). This conclusion is also plausible for the study area, due to the high-impedance, layered nature and continuity of seismic reflections associated with this facies. DLCs correspond to the 'Cbh' facies of Prather *et al.*, (1998), and are mostly restricted to topographic depressions in the study area (Fig. 4.21).

4.4.3 Amalgamated or Accretionary Channel Complexes (ACCs)

Amalgamated or accretionary channel deposits are seismic facies recognized in the study area. Amalgamated channel or accretionary channel complexes are distinguished based on characteristic chaotic, discontinuous, high-impedance seismic reflections. Although MTCs also have chaotic, discontinuous seismic reflections, the high impedance reflectors are absent within MTCs. The ACCs occur in two forms in the study area: (1) lateral accretionary channel complexes developed as a result of channels constantly shifting positions, and (2) vertically stacked channel deposits formed due to stacking of rejuvenated channels over older channel deposits. ACC fills are often mounded in external geometry (Fig. 4.21a-b), and represent the 'Bh' facies of Prather *et al.*, (1998). Due to the associated seismic character, it could be suggested that ACCs consist of coarser-grained sands than DLCs, which are usually deposited further basin ward.

4.4.4 Drape Complexes (DCs)

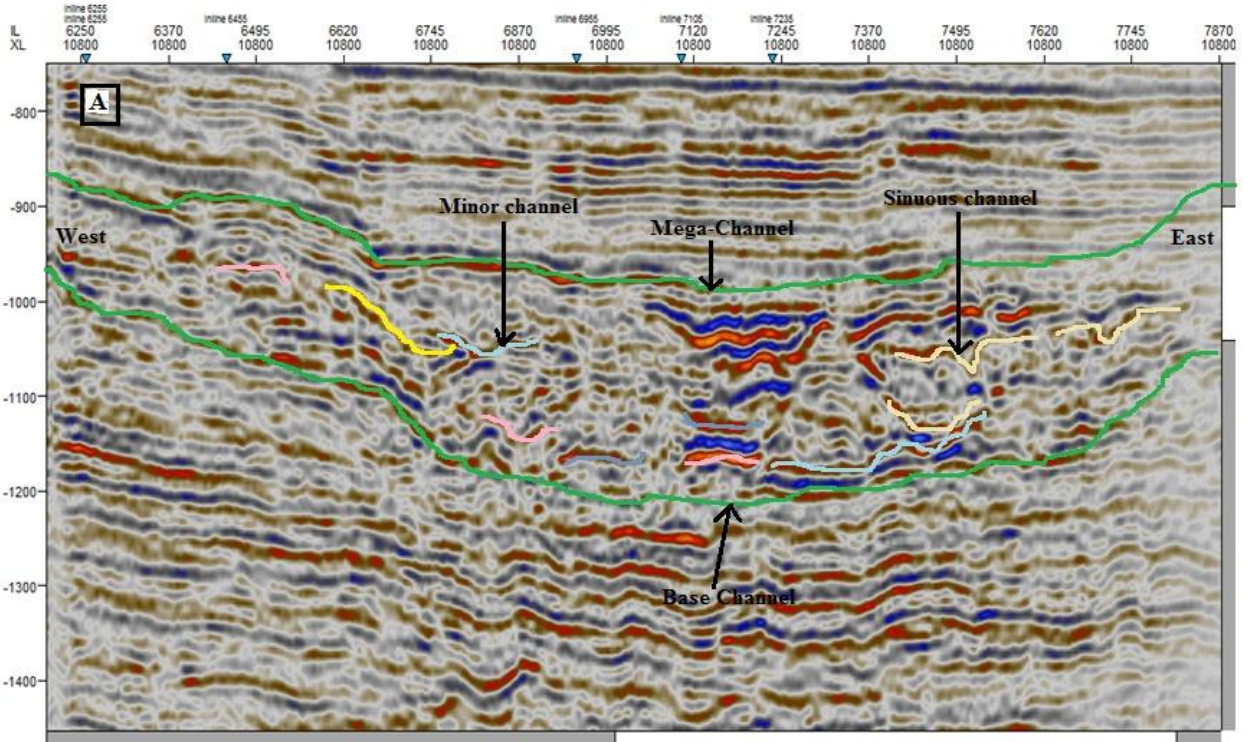
Drape complexes are characterized by high or low impedance, laterally continuous seismic reflections that can be traced for a long distance. DCs mostly consist of clay-

rich shales or marl (foraminifera-rich calcareous clay). DCs are very mappable seismic reflections, some of which are interpreted as horizons due to their lateral continuity (Fig. 4.20a-b). DC is the equivalent of the D/E facies of Prather *et al.*, (1998).

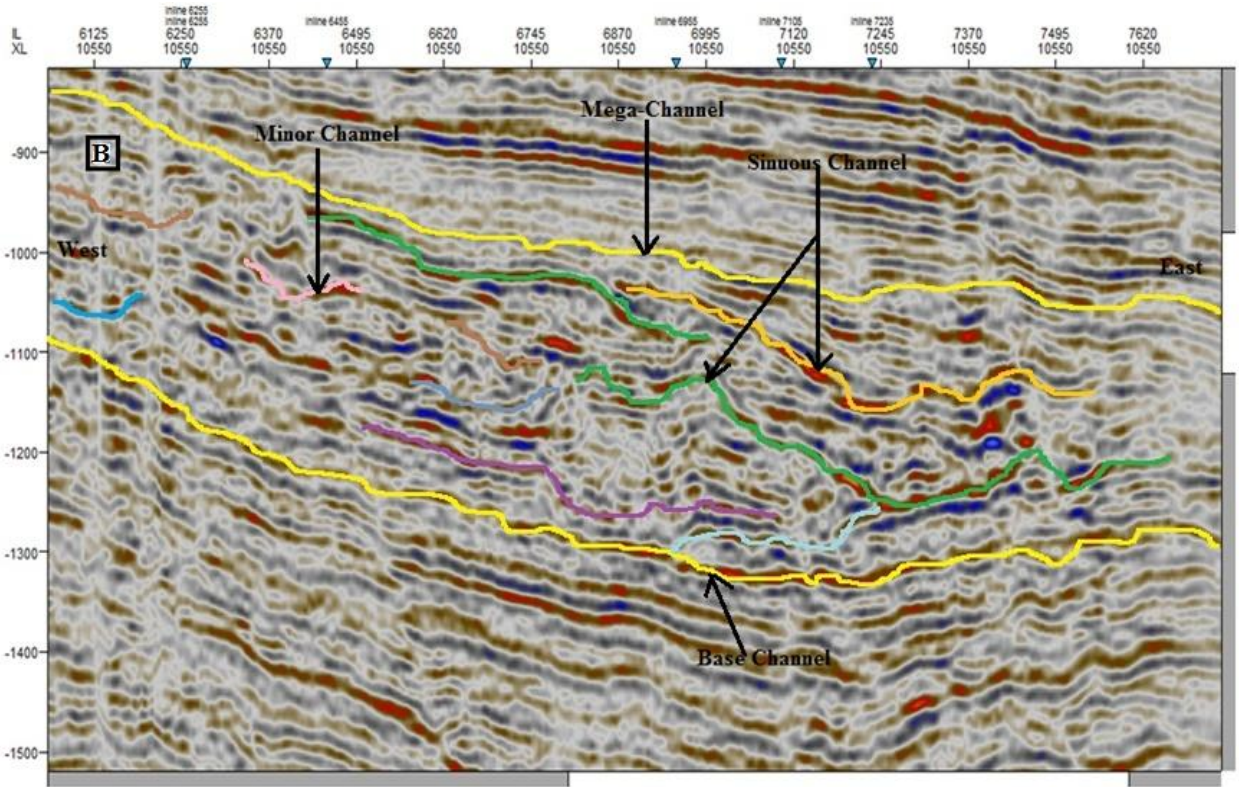
4.5 CHANNEL SYSTEM AND DEPOSITIONAL ELEMENTS DISTRIBUTION

Using the available data set and the results of seismic attributes application, one mega-channel and many minor channels are easily distinguishable within the study section (Figs. 4.22a-b and 4.17-4.21). From the interpretation of the seismic attributes maps generated, it was noted that channel pattern and morphology are consistent for up to 40 ms.

The morphology of the channels varies, and so do the architectural elements associated with the channels. Mega channel was actively filled (that is, channels were filled with sediments and abandoned as a result of the filling), whereas minor channels were passively filled (meaning sediments gradually filled the channel while fluid still flowed in it). This section provides descriptions of the channels (Fig. 4.22a-b). Using an average velocity of 2260 m/s within the study area, the channel geometries of the Rence field were estimated (Table 4.3). The channel runs from the east-west beyond the study area. Seismic character of the meander loop/overbank deposits indicates a very sandy channel fill (Fig. 4.23).



(a)



(b)

Fig. 4.22: Line of section showing Channel morphology and architecture

Table 4.3: Estimated channel geometries within the Rence field

S/N	Channel Parameters	Obtained Value
1	Sinuosity	1.3
2	Length	22,500m
3	Distance	17,500m
4	Average Depth	170m
5	Amplitude	1670m
6	Wavelength	7640m

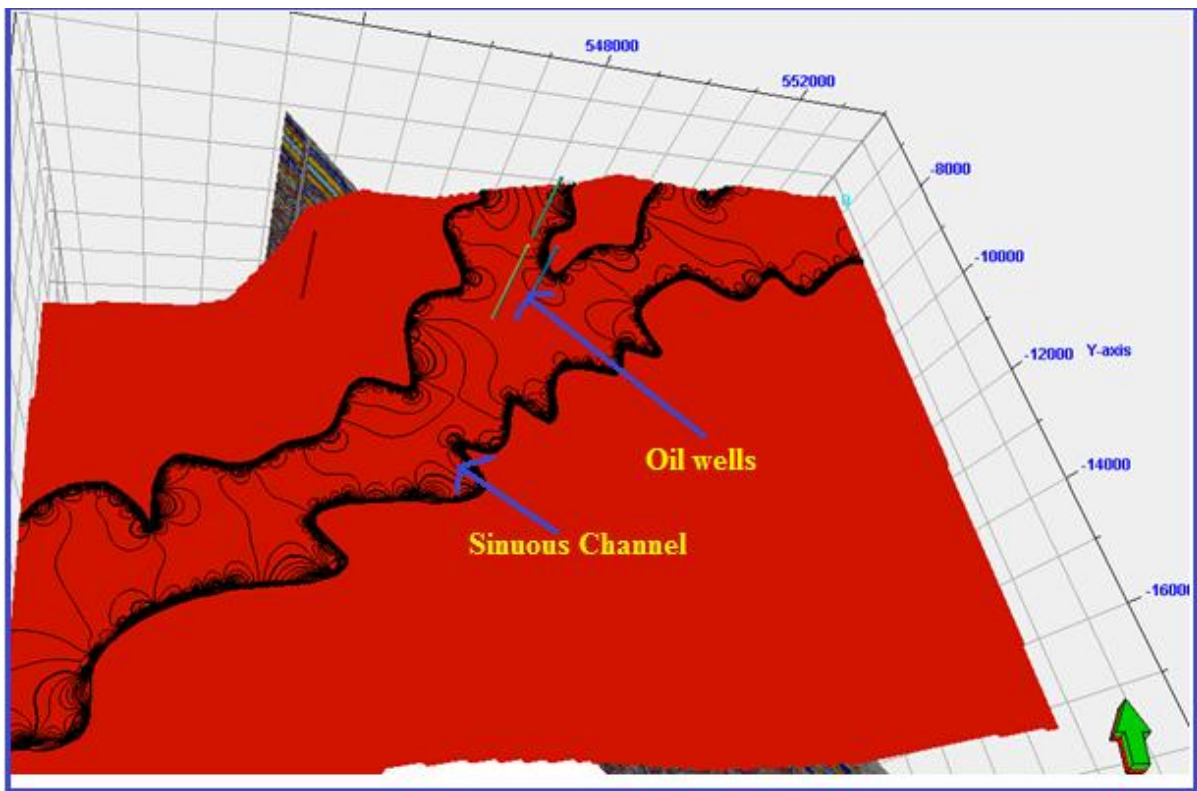


Fig. 4.23: Visible channel resulting from co-blending of reflection acoustic impedance, coherency and instantaneous frequency

4.6 DISCUSSIONS

In this study we are concerned with shallow marine water channels, i.e. those that occur on the continental shelf of some parts of Niger Delta, Nigeria. Channel sinuosity is measured as the ratio between the channel axis length and the overall down-channel distance for a given section of channel. A sinuosity of 1 therefore represents a straight section of channel, with increasing values representing increasing sinuosity. For the purposes of this study, a truly sinuous channel is defined as one that displays a minimum average sinuosity of 1.3. This is comparable to the result obtained by Clark *et al.*, (1992) and Clark and Pickering (1996). It should be noted that maximum sinuosities of relatively straight channels may locally exceed 1.3, and also that some sinuous channels display peak sinuosities well in excess of this value. Different causes of sinuosity in channels are discussed by Mayall *et al.*, (2006). Hence the channel sinuosity of 1.3 was obtained in the study area.

Lithologic units were identified on the logs and correlated across the wells. The stratigraphic cross-sections produced show a general lateral continuity of the lithologic units across the field. Seismic-to-well ties revealed that, high amplitude reflection events correspond to sand units, whereas, low amplitude reflection events correspond to shale units. Closures considered as good hydrocarbon prospects were identified and delineated. Stratigraphic plays such as pinch-outs, unconformities, sand lenses and channels are also suspected. The integration of seismic data with well logs proved to be a useful tool in structural and stratigraphic mapping and in predicting lateral and vertical variations in the lithologic units.

Consequently, the result of petrophysical analysis on the well data showed high reservoir qualities. The averages for the analyzed parameters are 90% NTG, 28% porosity, 27% volume of shale, and 24% water saturation; these values by the ranges of regional petrophysical averages indicate that the reservoir materials are of pay quality. The stratigraphic correlation of the H level in wells across the field was integrated with the horizon and fault interpreted on seismic to develop the reservoir models (Fig. 4.24).

4.6.1 Filling History, Sediment Response and Timing of Structural Growth

Two basic facies assemblages have been interpreted in the study area: (1) partially confined facies assemblages, and (2) by-pass facies assemblages (Fig. 4.25). The occurrence of either of the assemblages in the study area depends largely on structural movement rather than seismic facies association or sediment type. However, some seismic facies are more common in partially confined facies assemblages than in by-pass facies assemblages, and vice versa.

Partially confined facies assemblages in the study area consist largely of the lower mass transport deposits (MTC) that spilled into the basin after a more proximal basin was filled to spill point. Other facies included in partially confined facies assemblages are distributary channel and lobe complexes (DLC), amalgamated or accretionary channel complexes (ACC), remnants of eroded drape complexes (DC), and the lower part of the overlying MTCs. Generally, a change from partially confined to bypass facies recorded loss of accommodation space and progradation over captured point and barrier bars after the basin was filled to equilibrium level. Hence, area with by-pass facies assemblage should be avoided during oil well drilling.

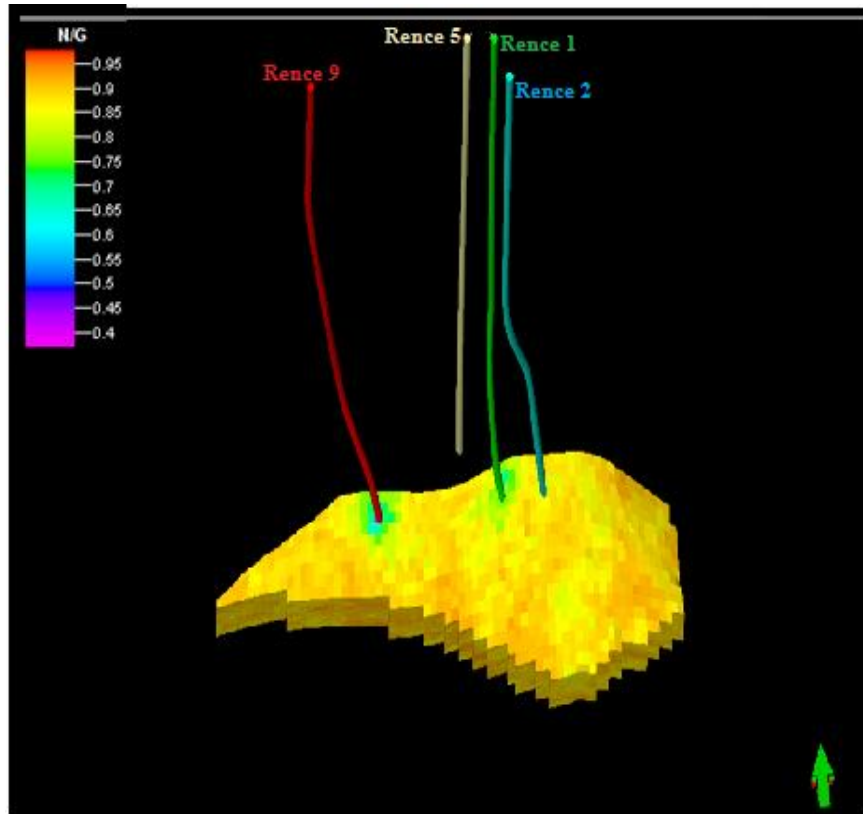


Fig. 4.24a: 3D Reservoir modelling of net to gross (NTG) within the study area

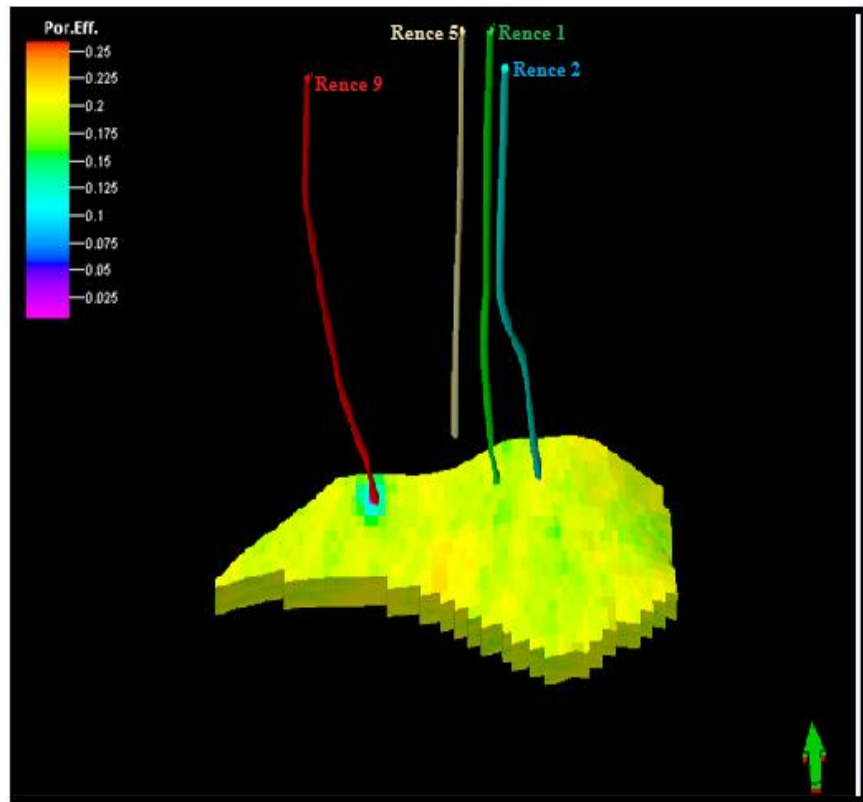


Fig. 4.24a: 3D Reservoir modelling of porosity within the study area

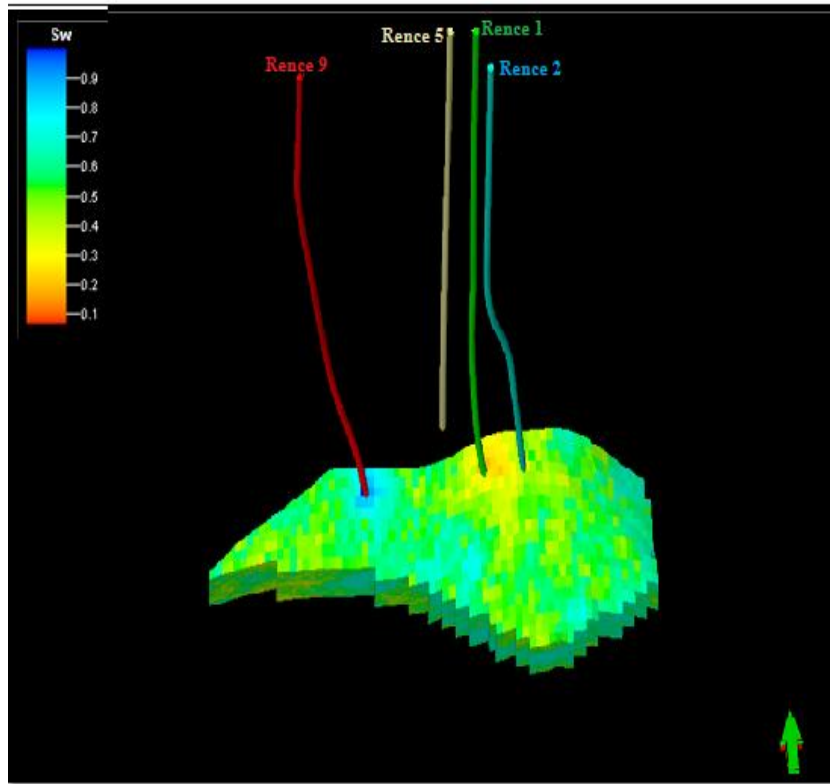


Fig. 4.24c: 3D Reservoir modelling of water saturation within the study area

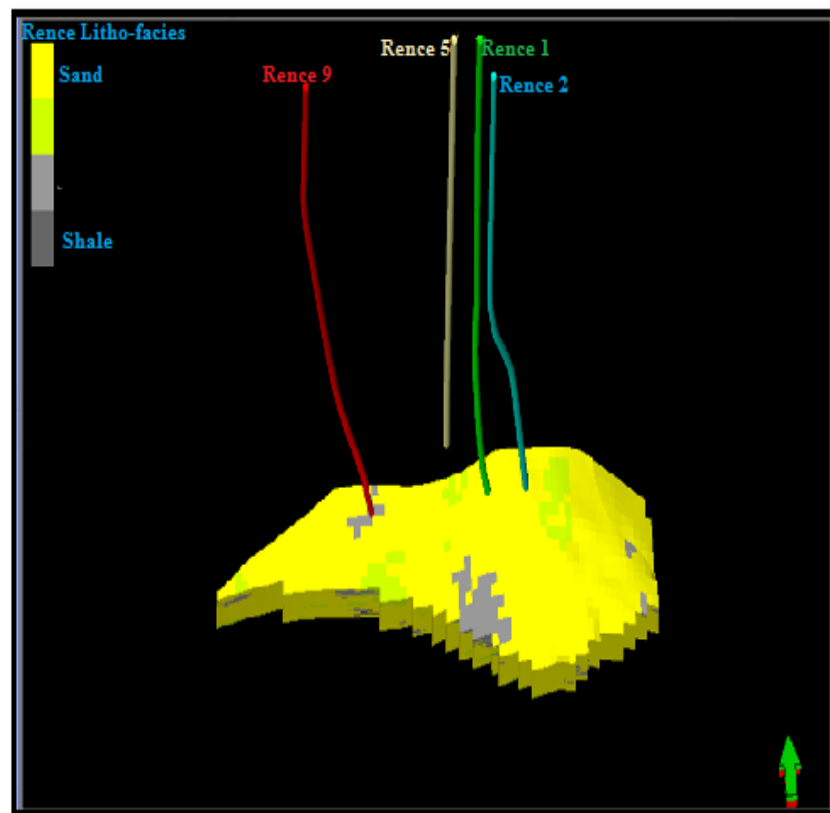


Fig. 4.24d: 3D Reservoir modelling of lithofacies within the study area

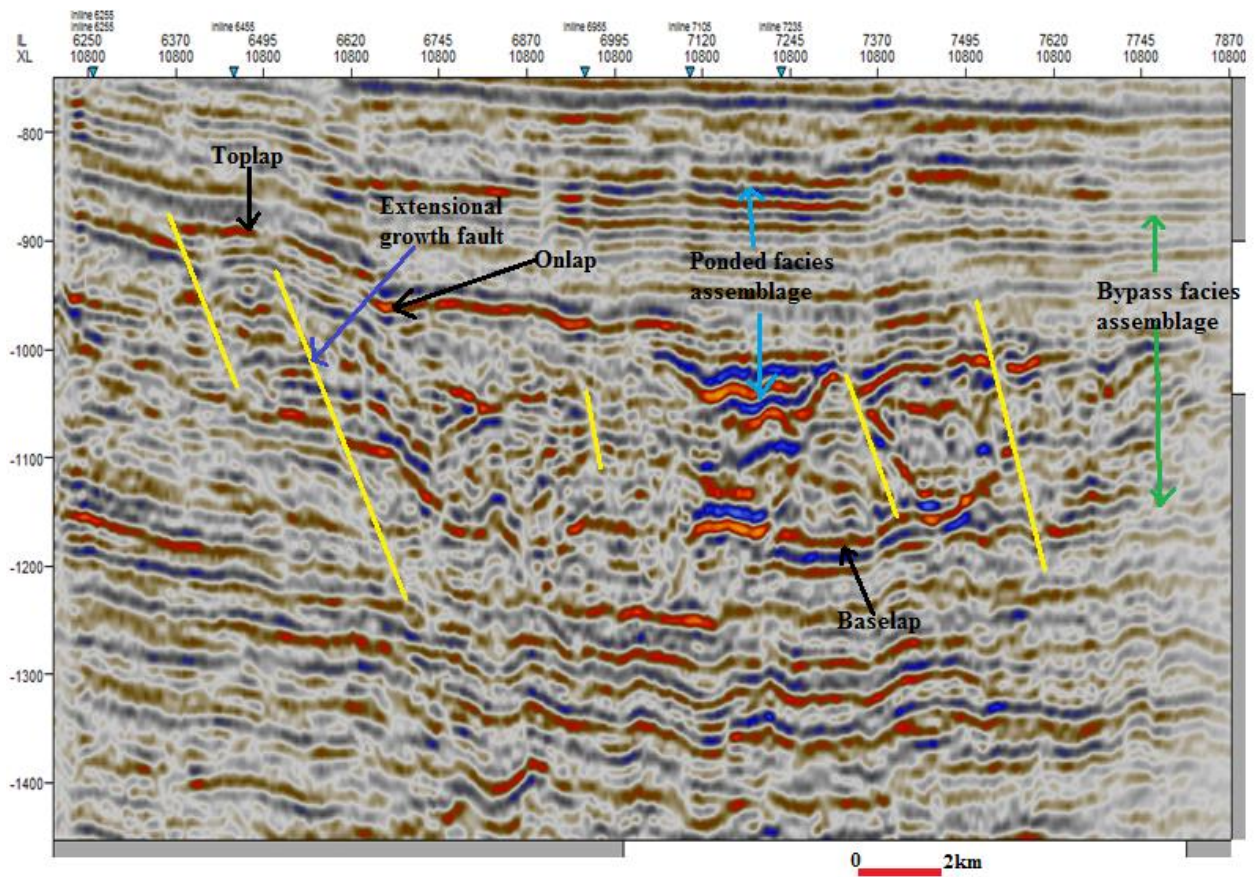


Fig.4.25: Line of section showing stratal termination, fault pattern and facies assemblage within the study area.

Hence, strata termination patterns methods were used to interpret the filling history, timing, and the sediment response to structural growth in the study area. This method is discussed in more detail below.

4.6.2 Stratal Termination Patterns

Stratal termination patterns were interpreted to give an overall idea of the depositional mechanisms and sedimentation processes prevalent in time and space in the study area. Strata termination patterns observed in the study area are: (1) onlap, (2) downlap, (3) toplap, (4) erosional truncation, and (5) internal convergence (Figs. 4.25 and 4.26). It was observed that baselapping facies are mostly restricted to partially confined facies assemblages within the study area. Internal convergence is associated with both partially confined facies assemblages and bypass facies assemblages, whereas toplap is mainly associated with the transition between partially confined facies assemblages and bypass facies assemblages.

4.6.3 Depositional Model

Co-blending of seismic attributes has been of significant use in the study area (Figs. 4.27 and 4.28). The maps displaying the distribution of the different facies show depositional morphologies similar to the sub-aqueous channel depositional environment. Channel geometries and morphology as well as flood plains can be inferred from the detailed images, and the sediment nature and its properties can be predicted based on the depositional model (Adepelumi *et al.* 2011).

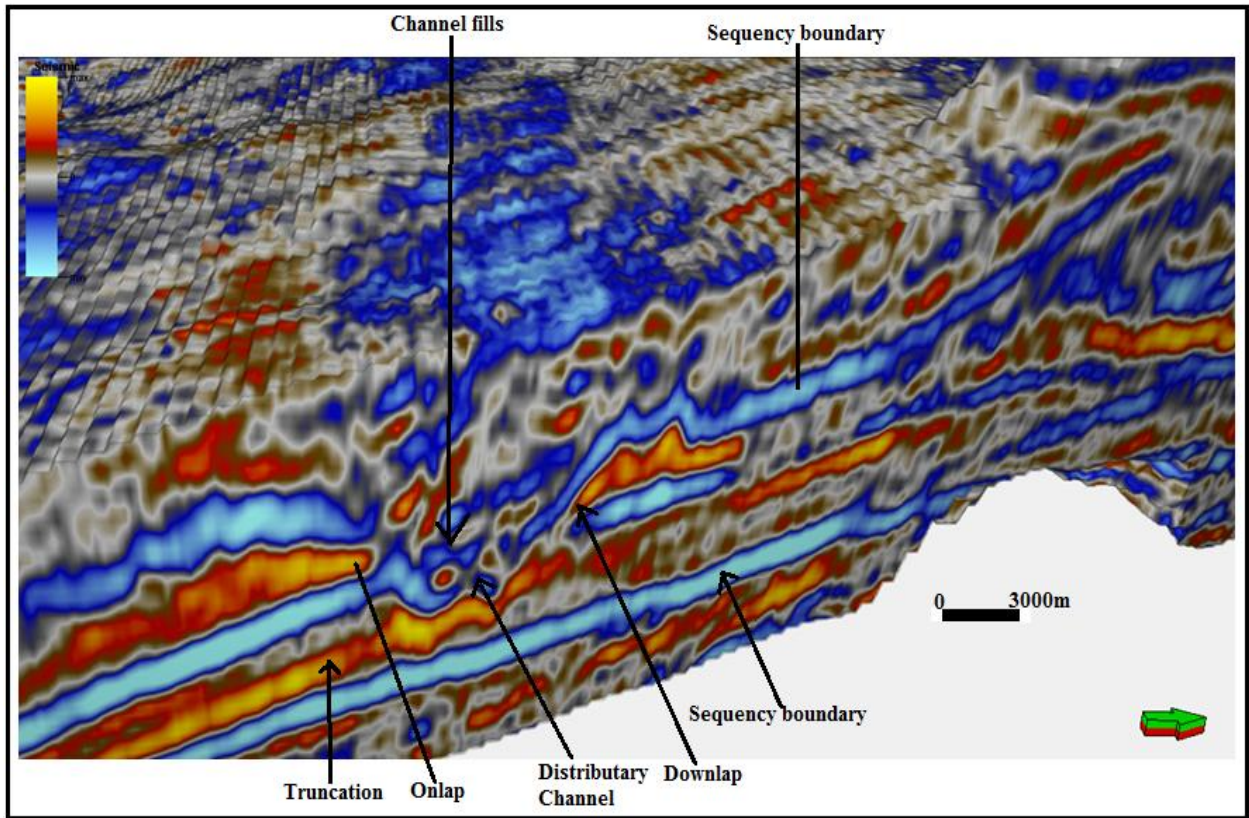


Fig. 4.26: Distinct stratal patterns within the study area

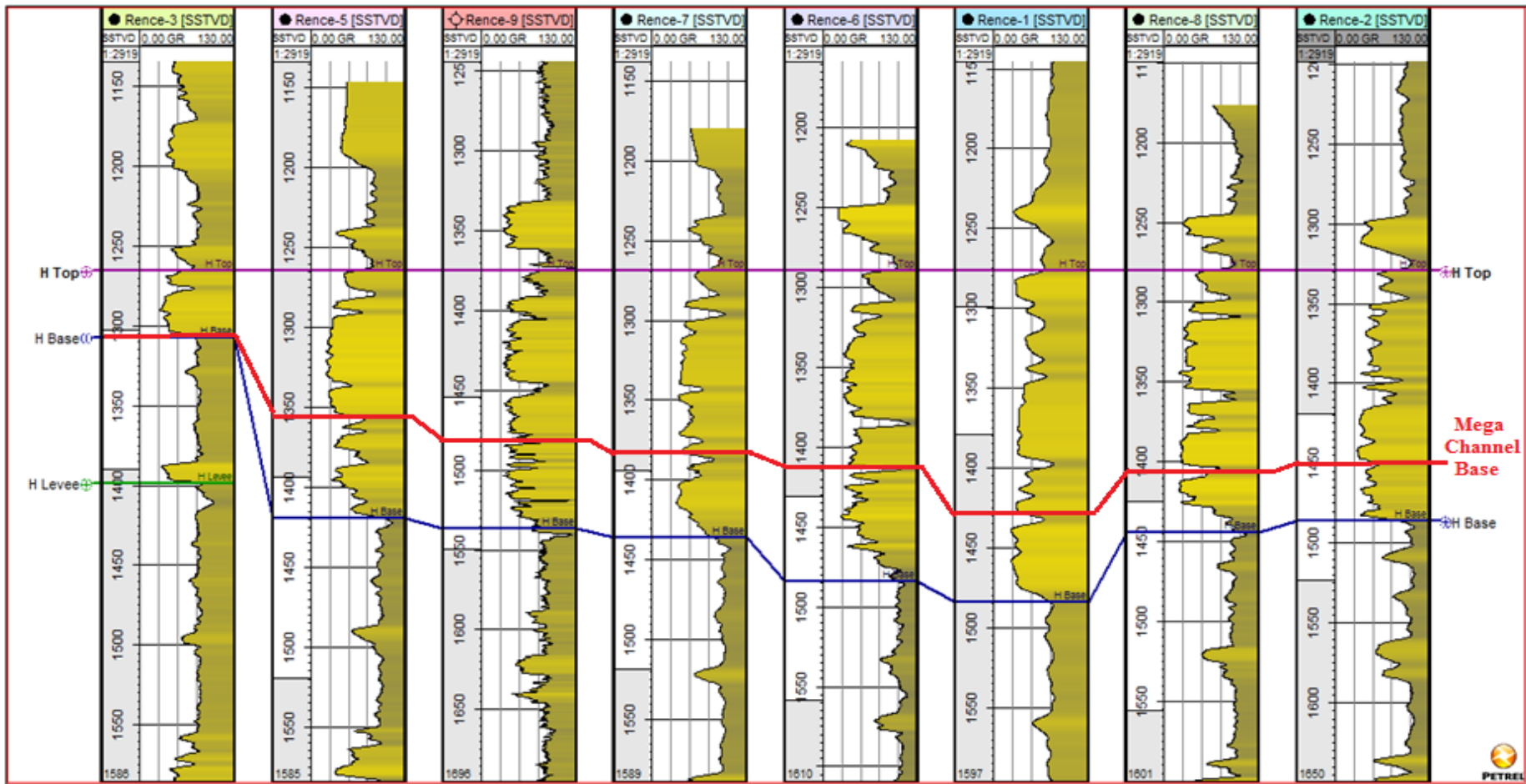


Fig. 4.27: Multi-well stratigraphic cross-section (Datum: H Reservoir top) showing mega channel within the Rence Field

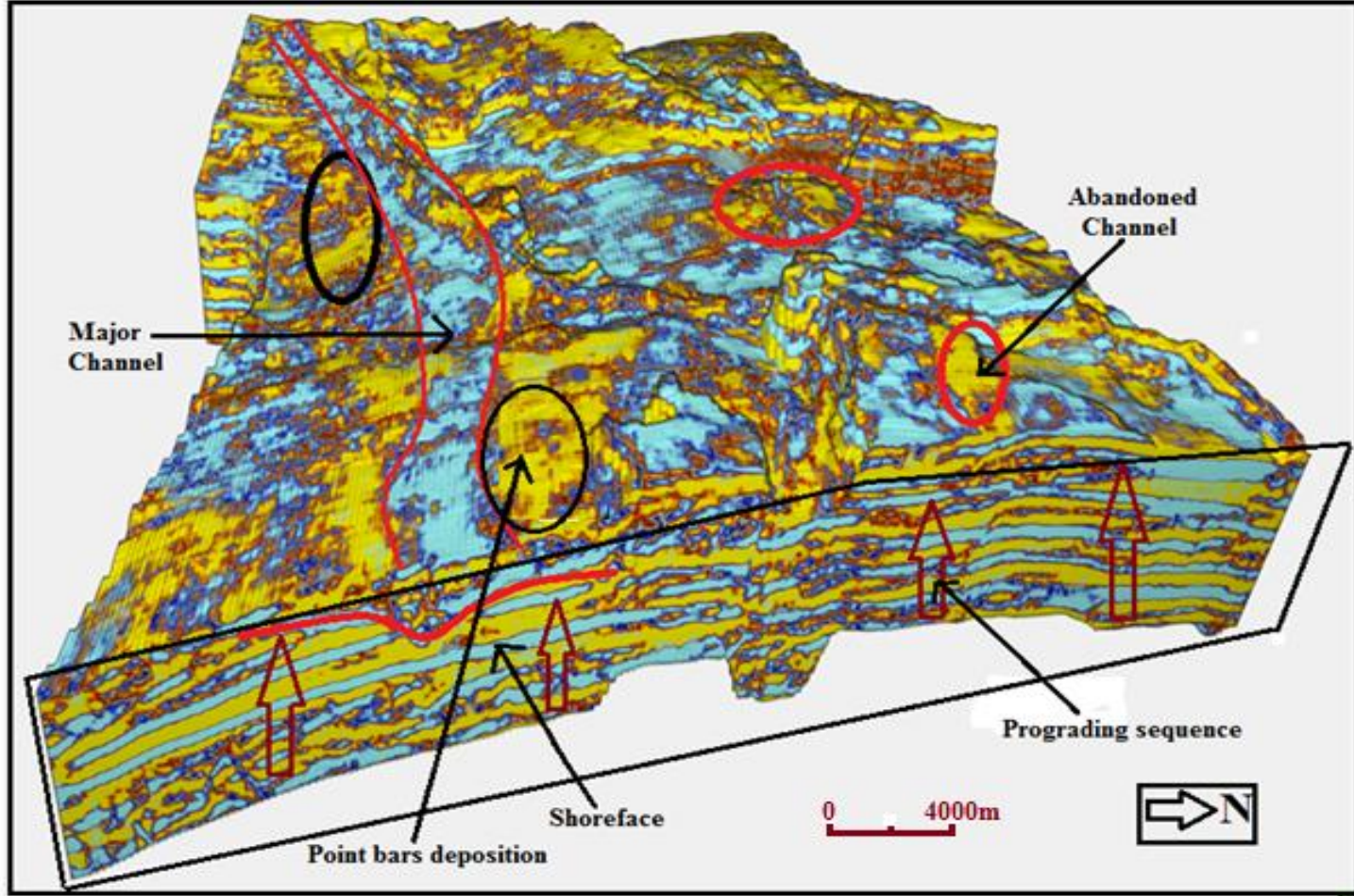


Fig. 4.28: Characterization of the depositional features within the study area

Where a well penetrates the fluvial sequence (Fig. 4.27), detailed interpretation of the petrophysical properties within the borehole and the core data give added calibration points that significantly increase the reliability of the facies maps.

Using sub-aqueous channel models, the channels were interpreted as being sand-filled and the sand point bar sequences were interpreted at the flanks of the channels. Fig. 4.28 shows the sand filled point bar lithology, barrier bars and the prominent channel (indicated by red line) using co-blending of reflection acoustic impedance, instantaneous frequency and average energy attributes. The red arrow shows a good shoreface which is prograding upwards (coarsening upward).

Stratal termination patterns on seismic sections, reservoir facies distributions shown by various seismic attribute maps and reservoir modeling provided information to construct a depositional and stratigraphic evolution model for the Rence Field, offshore Niger delta, Nigeria (Fig. 4.29). In this model, the environment of depositions and stratigraphic structure are shown clearly. They include point bars deposition, abandoned channels, barrier bars, flood plain and the channel structure. The model indicates that finer materials are deposited at the bottom while the coarser materials are deposited at the top, thus the model shows coarsening upward sequence of deposition.

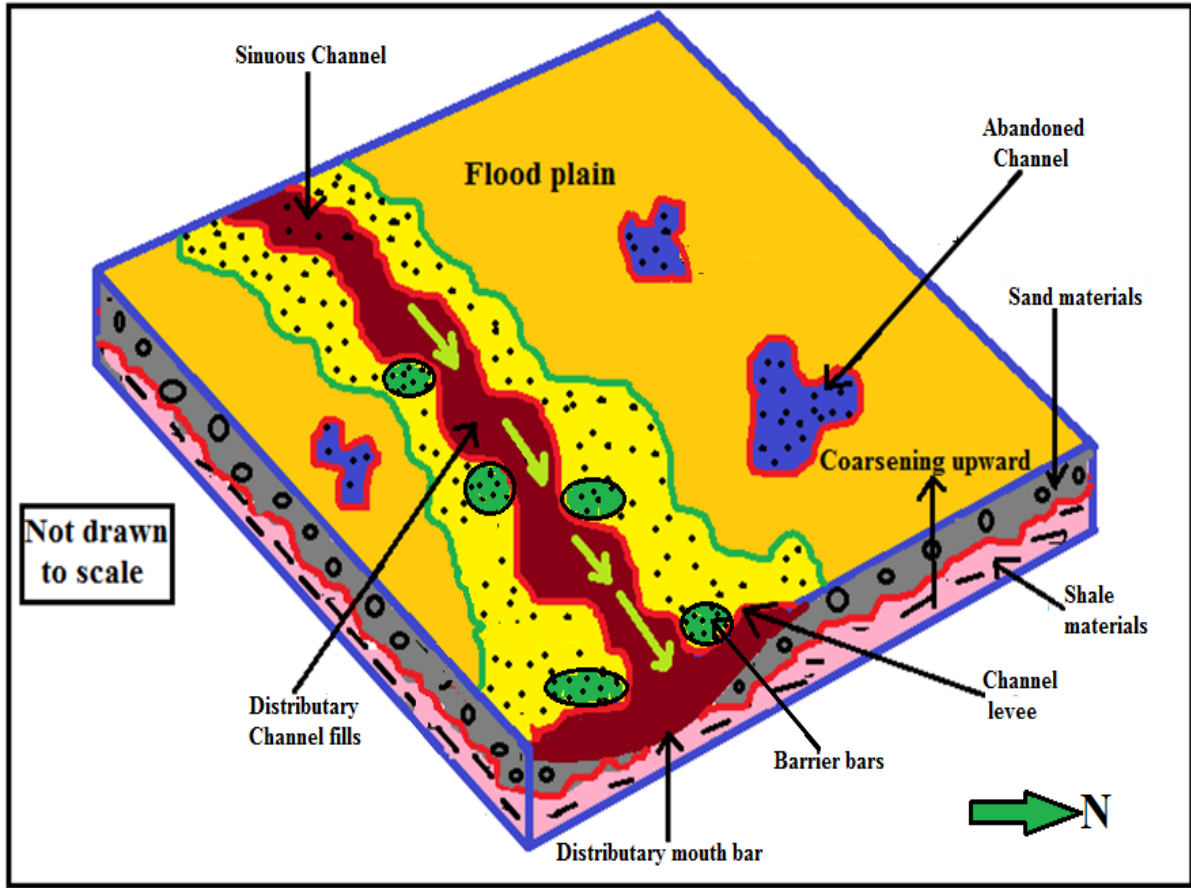


Fig.4.29: Idealized diagram of depositional model within the study area

4.6.4 Validation – Taking Seismic Time Slice on the attribute Map

A time slice at 1703ms is taken on the best attribute map generated from co-blending of reflection acoustic impedance, iso-frequency and coherency attributes in order to validate the efficiency of the method used. The new map produced (Fig. 4.30) indicates that all the existing wells in the study area are targeting the mega-channel hence confirming that both structural and stratigraphic traps are necessary for hydrocarbon accumulation.

More so, the result of well correlation showed that delineated H-reservoir surfaces were not laterally continuous. These truncations were inferred to be caused by syndepositional faults in the field. These faults also constitute the major traps for hydrocarbon accumulation.

The Rence structure generally is a well identified culmination controlled to the North by a major down-to-the-basin growth fault and to the west by a prominent fault (Fig. 4.11). The azimuth of the identified faults coincides with that of the growth fault which enhances trapping mechanism for the hydrocarbons (Ologe *et al.*, 2013). Also migration of oil from the Cretaceous section (Akata Shale) into the reservoirs in the Agbada would require an intricate faults/fracture network like in the study area.

Gamma Ray Log values and signatures (fining and coarsening upward signatures) and the co-blended results helped in determining lithofacies and depositional environments of the different rock units in the Rence field (Fig. 4.31). The blocky log pattern within the

interpreted mega-channel confirms that incised valley fills are common in the study area based on Allen and Posamentier, (1993) criteria. Also, the serrated nature of the Gamma Ray Log signature is indicative of tide/wave activity (Emery and Myers, 1996). Bell shaped log patterns on Gamma Ray Logs indicating increasing clay contents up section or fining upward trends or an upward increase in gamma ray value is a typical feature of fluvial channel deposits.

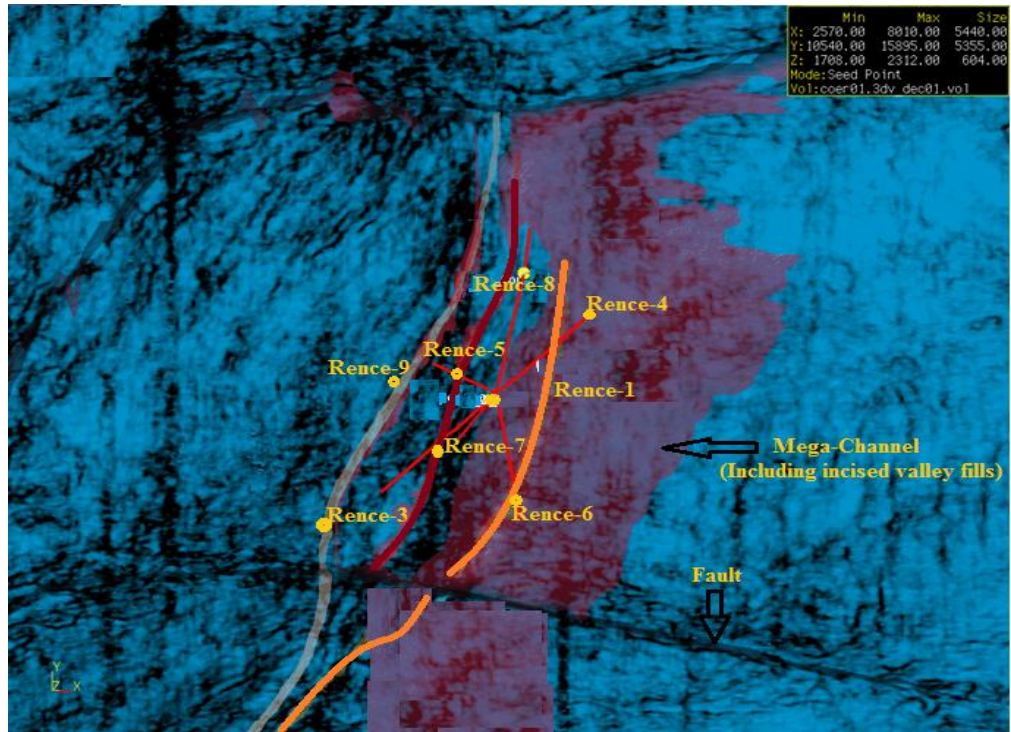


Fig. 4.30:- Co-blended Seismic Time Slice showing mega-channel and fault

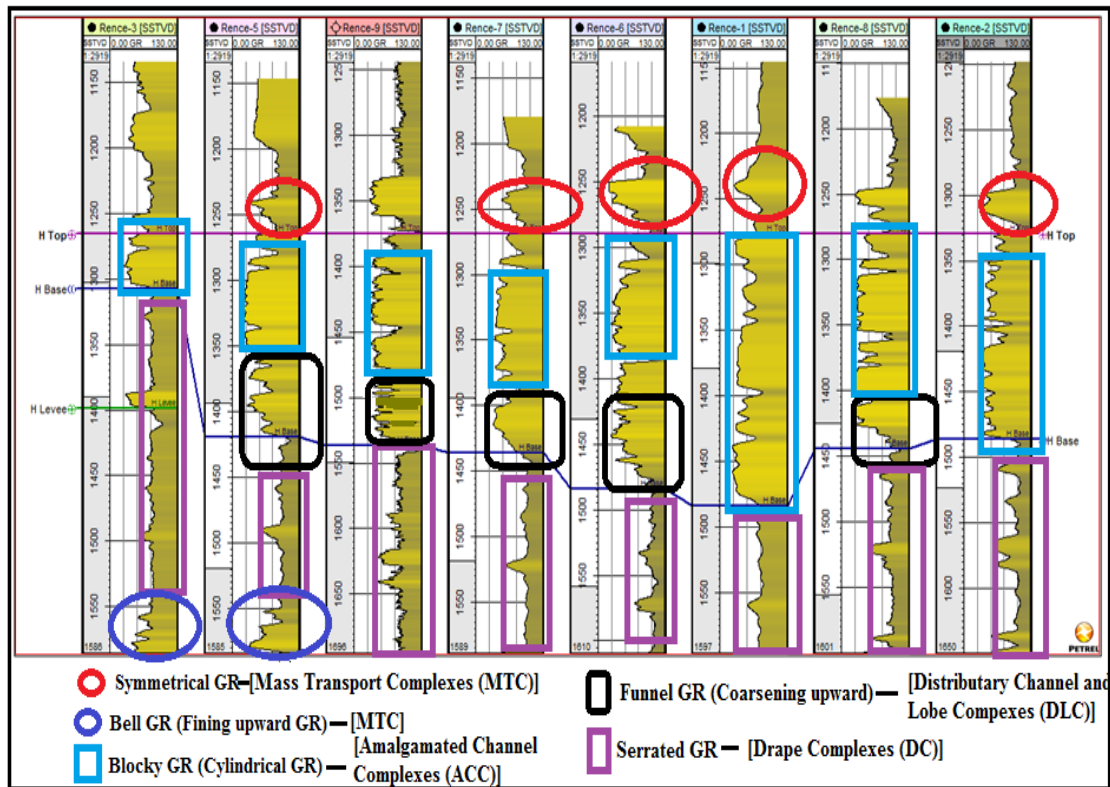


Fig. 4.31: Integration of Gamma Ray log patterns and seismic facies of the area

4.6.4 Hydrocarbon Exploration and Production Significance of Study

The structural features like the extensional growth faults and normal faults determined the distribution and architecture of reservoir facies in this shallow marine part of the Niger Delta, Nigeria. There are channels and few sheet reservoir elements identified in the study area (Figs. 4.17- 4.21, 4.30, 4.31 and 4.32).

4.6.4.1 Channel Elements

The channel elements found within the study area are: (1) meander loop cut-off and over-bank deposits, (2) lateral accretionary channel deposits and (3) vertical accretionary channel deposits (Fig. 4.31).

1. Meander loop cut-off and over-bank deposits

Based on seismic character and log sequence, these deposits are interpreted to consist of relatively coarser-grained sediments. These deposits are found within the meander loop cut-off that was eventually filled with sand-sized sediments, and the overbank of channels (Figure 4.31a). In a sandy depositional environment such as the study area, this facies can form important reservoir targets.

2. Lateral accretionary channel deposits

These deposits formed as a result of channels frequently changing their positions due to high sediment volume. These sediments were deposited within the channel axes before they were abandoned for areas of lower elevation. These channel deposits are laterally amalgamated (Fig. 4.31b) and could form major reservoir targets in a sandy system such

as the study area. Using both thickness and lateral extent, lateral accretion deposits are the second largest of channel reservoir deposits.

3. Vertical accretionary channel deposits

This is similar to lateral accretionary channel deposits but it consists of amalgamated channel deposits. The difference, however, is that vertical accretionary channel deposits are made up of individual channels vertically stacked on top of each other (Fig. 4.31c). Using thickness and lateral extent, the vertically stacked channel deposits are volumetrically the largest of all channel deposits. When formed in a very sandy system like the study area, such deposits can form major reservoir.

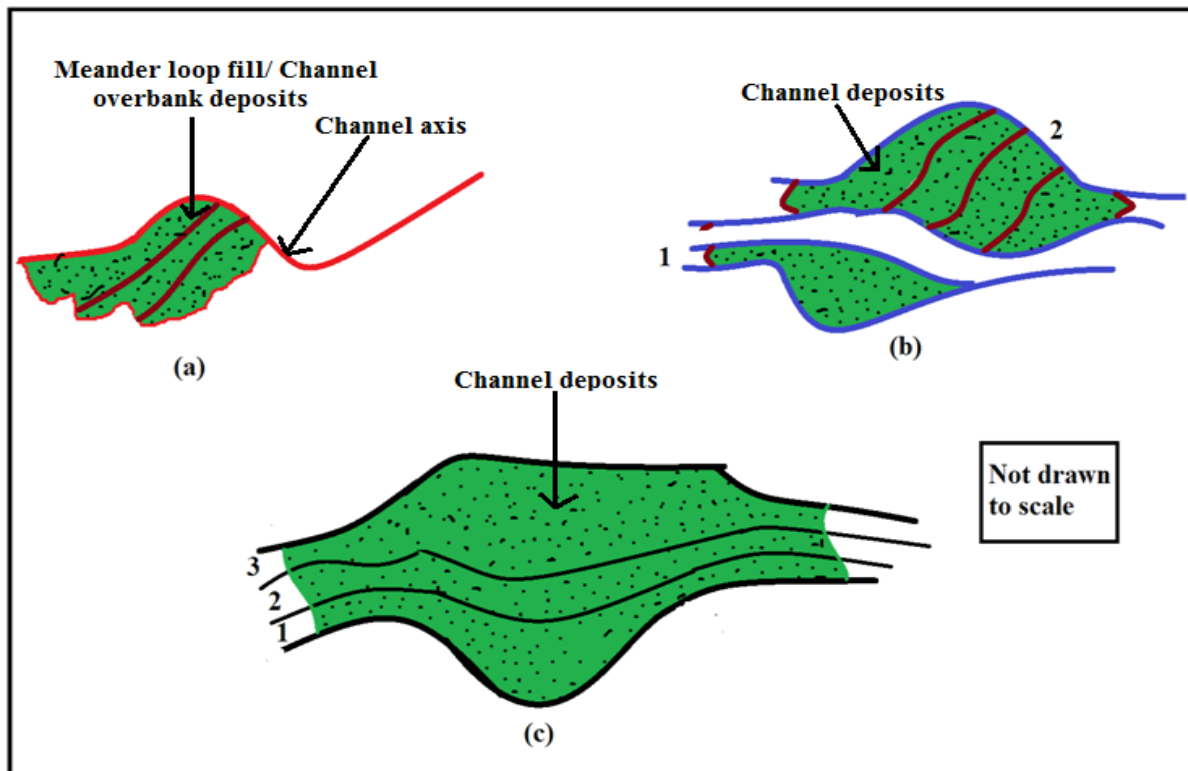


Fig. 4.32: Channel reservoir elements within the study area (a) meander loop cut-off and over-bank deposits, (b) Lateral accretion deposits, (c) Vertical accretion deposits.

4.6.4.2 Hydrocarbon Implication of H-Reservoir Amplitude Thickness Map

The amplitude thickness map computed on H-horizon using acoustic impedance threshold equal to 5000 units is very conservative and useful in showing the main thickened areas (Fig. 4.33). The maximum thickness can be found in the southern part of the study area which pave way for high hydrocarbon accumulation than the north-eastern area is characterized by very low thickness values.

The petroleum in the study area is produced from sandstones and unconsolidated sands mainly in the Agbada Formation of Pliocene in age (Tuttle *et al.*, 1999). Then, the reservoirs identified across the study area occurred within the Pliocene age. They are often stacked and range in thickness from 15 m to 45 m thick (Evamy *et al.*, 1978). The thicker reservoirs across the nine wells likely represent composite bodies of stacked channels within the study area. The targeted reservoir in the wells (Fig. 4.5), which are stacked channel sands has been confirmed by the attribute maps generated (Fig. 4.20). Based on reservoir quality and geometry in the Rence Field, the most important reservoir types are the point bars of distributary channels and barrier bars intermittently cut by sand-filled channels which host the hydrocarbon accumulation in the area.

Certainly, the hydrocarbons generated in the Akata Formation definitely migrated up dip through growth faults that were identified in the study area in order to accumulate in shallow reservoirs of the Agbada Formation within the study area (Rence field).

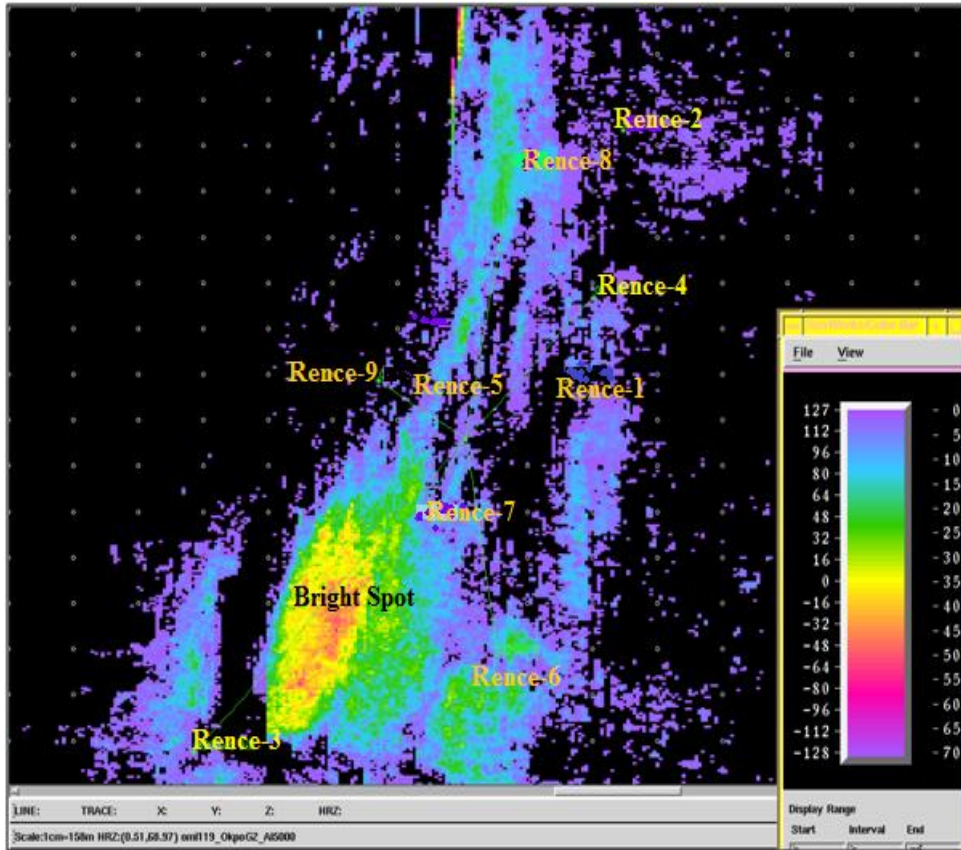


Fig. 4.33: Amplitude thickness map of H-Reservoir

The Akata Shale is present in large volumes beneath the Agbada Formation and is volumetrically sufficient to generate enough oil for a world-class oil province such as the Niger Delta (Stacher, 1995).

By the application of co-blending techniques, mapping channels and depositional features becomes possible such that it is easier to delineate the depositional environment and interpret prospective hydrocarbon potential areas such as channel levees, barrier bars, point bars, distributary channel fills, and vertical accretionary channel deposits within the study area. Also by mapping the channel geometries such as sinuosity, length, depth, amplitude, wavelength and special relation of meandering channels from the attribute maps generated, it can be concluded that the channel fills within the Rence field are sand prone which is a major target for hydrocarbon accumulation and it is supported by Liu and Marfurt (2006) and Naseer, T.M., et al. (2014).

CHAPTER FIVE

SUMMARY, CONCLUSION AND RECOMMENDATION

5.1 CONTRIBUTION TO KNOWLEDGE

The major contributions to knowledge in this research work are:

- In the past, hydrocarbon exploration had centred on the traditional prospecting for structural traps alone. Presently, prospects are more often defined by stratigraphic traps such as channels, incised valley fills, barrier bars and pinch-out. The particular interpretational advantage emphasized in this study is the additional value obtained by co-blending of seismic attributes. The multi-attributes seismic characterization had displayed superior images of the channels because co-blending improves imaging of geological structures and strongly defines the depositional environment. The enhanced channel image of co-blended attributes compensates for poor visualization of the channel by single attributes only.
- As far as Niger Delta Basin is concerned, only three distinct seismic facies have been identified namely mass transport complexes (MTC), distributary channel/lobe complexes (DLC) and drape complexes. However, the present study has revealed the extra (fourth) distinct seismic facies named amalgamated or accretionary channel complexes (ACC). This newly identified seismic facies is plausible because sand-rich deposits can form major reservoir target.
- The study also identified bypassed seismic facies assemblages which are invariably overpressured zones. These areas are to be avoided during search of hydrocarbon.

- The study area is situated within the continental shelf and normally channels are not supposed to be found on the continental shelf. However, the present study has been able to identified channel structure within the continental shelf based on their chaotic pattern, sinusoidal feature and channel geometry. This is an evidence of major rare processes like storm, tsunami, tidal waves and others.
- In the study, a sub-aqueous channel environment have been deduced from the sinusoidal channel geometry, fining upwards log curves, and other seismic stratigraphic relationships such as incised valley fills, barrier bars and channels.
- Importance of tectonics is also suggested by the mega-channel and incised valley-fill (IVF) running east to west (E-W), which conforms to the EW-trending graben and growth fault in Niger Delta.
- The findings of this work will be applicable to nearby active areas in the region as well as other areas that exhibit similar challenges such as the Gulf of Mexico Basin.

5.2 SUMMARY

This research work is summarized as follows:

- The integration of seismic data with well logs is plausible in structural and stratigraphic mapping and in predicting lateral and vertical variations in the lithologic units. Lithologic units were identified on the logs and correlated across the wells in the Rence field.

- Seismic-to-well ties revealed that, high amplitude reflection events correspond to sand units, whereas, low amplitude reflection events correspond to shale units. Closures considered as good hydrocarbon prospects were identified and delineated.
- The Rence structure generally is a well identified culmination controlled to the North by a major down-to-the-basin growth fault and to the west by a prominent fault (Fig. 4.11). The azimuth of the identified faults coincides with that of the growth fault which enhances trapping mechanism for the hydrocarbons.
- Stratigraphic and seismic facies analysis for this shallow marine basin revealed that the study area can be distinguished into two categories of seismic facies namely layered complexes and chaotic complexes.
- Seismic facies analysis reveals that the distributary channel and lobe complexes (DLC) are banked against a normal fault. Higher reflectivity at this location may be a function of higher sand content and hydrocarbon presence due to sealing fault properties.
- Co-blending of seismic attributes through time slice maps showed that the morphology of the continental shelf channels changed through time and space. At depth, the channels are more sinuous, whereas the shallower channels have relatively lower sinuosity.
- Seismic attributes maps revealed that there were shifting in the locations of barrier bars, caused mainly by the growth fault in the study area. Recognition of at

least three reservoir elements with distinct architectural characteristics in the study area can be used as analog to study deeper prospective levels.

- A depositional model generated for this continental shelf basin shows the environment of depositions and the stratigraphic structure. Using meandering sub-aqueous model, the channels can be interpreted as being sand-filled and the sand point bar sequences as being on the channel inner bends.

5.3 CONCLUSIONS

This study reached the following conclusions:

- The result of well to seismic ties revealed that, high amplitude reflection events (bluish colour) correspond to sand units, whereas, low amplitude reflection events (yellowish colour) correspond to shale units.
- Seismic structural interpretation of Rence Field reveals that the study area has four (4) major regional faults and twelve (12) minor faults. Seven (7) of the faults are antithetic and dips landwards to the continent while the rest are synthetic faults dipping basin ward.
- Both time and depth maps for the top of the H-reservoir within the Rence field were generated and the time-structure map shows the geometry of the basin and changes in topographic relief through time.
- The H Reservoir of Rence Feild within shallow marine environment is petrophysically characterized with average properties of 90% NTG, 28% porosity,

27% volume of shale, and 24% water saturation; these values by the ranges of regional petrophysical averages indicate that the reservoir materials are of pay quality.

- Estimation of the volumetric parameters was possible within the H-reservoir. They include oil original in place (OOIP) of 47.2 million barrels with stock tank oil original in place (STOOIP) to be 474.4 million barrel.
- The oil/water contact is delineated at the depth of 1294m (4180ft) in the H-reservoir. Oil bearing sands have lower acoustic impedance values ranging from 4600 to 5450 $\text{g/cm}^3 \cdot \text{m/s}$ with the highest porosity value of 0.36. But, water sands has higher acoustic impedance values ranging from 5500 to 6150 $\text{g/cm}^3 \cdot \text{m/s}$ with the lowest porosity value of 0.12.
- Application of the eight (8) seismic attributes on a time slice from the interpreted 3D seismic data of the Rence field really enhanced the visibility of channels. Thus, the seismic continuity of channels is improved while surrounding areas are essentially unchanged.
- Co-blending of seismic attributes shows the observed sinusoidal shape patterns of the channel morphology within the Rence field. One mega-channel feature is clearly seen in the middle of the time slices. This channel exhibits differential compactions, and the edge of the channel is well defined by co-blending attributes used in this study.

- The channel geometries within the study area are 1.3 for sinuosity; 22500m for length; 17500m for distance; average depth of channel is about 170 m; amplitude is about 1670 m, and wavelength is as high as 7640 m. The channel runs from the NW beyond the study area to the SE.
- The result of the seismic facies and stratigraphic analysis reveal that the study area is distinguished into two categories of seismic facies namely layered complexes and chaotic complexes.
- Channels in the study area vary in both morphology and associated depositional elements. Channel sinuosity was found to generally reduce with decreasing age of occurrence. Knowledge of channel architectural variation will give an idea of the type of deposit to anticipate within each shelf channel.
- Three different types of reservoir elements were identified in the study area. Three reservoir elements associated with the channel axis are: (1) meander loop fill and overbank deposits, (2) lateral accretionary channel deposits, and (3) vertical accretionary channel deposits. Each of these varies greatly from the other in its architectural characteristics. Knowledge of these variations as well as identification of the different elements is paramount to a successful exploration and development plan.
- The depositional model generated for the study area, and for any similar shallow marine basins shows a good shoreface which is prograding upwards and the channels can be interpreted as being sand-filled and the sand point bar sequences as being on the channel inner bends.

5.4 RECOMMENDATIONS

- Multi-seismic attributes application in mapping structural and stratigraphic traps within in deep marine environment of Niger Delta, Nigeria.
- Application of seismic attributes for delineation of channel geometries and analysis of various aspects in terms of lithological and structural perspectives of Agbada Formation, Niger Delta, Nigeria.
- Seismic discontinuity for faults and stratigraphic features using coherence cube.
- Interpretational applications of spectral decomposition in reservoir characterization and channel identification.
- Curvature attributes and their application to 3-D interpreted horizons.

REFERENCES

- Adeogba, A.A., McHargue, T.R. and Graham, S.A.; 2005. Transient fan architecture and depositional controls from near-surface 3-D seismic data, Niger Delta continental slope: AAPG Bulletin, vol.89, pp. 627-643.
- Adepelumi, A. A., Alao, O. A., and Kutemi, T. F.; 2011. Reservoir characterization and evaluation of depositional trend of the Gombe sandstone, southern Chad basin Nigeria. Journal of Petroleum and Gas Engineering Vol. 2, no. 6, pp. 118-131.
- Ainsworth, R.B., Sanlung, M., and Duivenvoorden, S.T.C.; 1999. Correlation techniques, perforation strategies, and recovery factors: An integrated 3-D reservoir modeling study, Sirikit Field, Thailand. American Association of Petroleum Geologists, Bulletin, vol. 83, no. 5, p.1535–1551.
- Aizebeokhai, A.P., and Olayinka, I.; 2011. Academic Journals Structural and stratigraphic mapping of Emi field, offshore Niger Delta. Journal of Geology and Mining Research, vol. 3, no. 2, pp. 25-38.
- Allen, G. P. and Posamentier, H. W. (1993). Sequence Stratigraphy and Facies Model of an Incised Valley Fill: The Gironde Estuary, France. Journal of Sedimentary Petrology, vol. 63, no. 3, 1993, pp. 378-391.
- Amadi A. N., Olasehinde P. I., Yisa J., Okosun E. A., Nwankwoala H. O., and Alkali Y. B.; 2012. Geostatistical Assessment of Groundwater Quality from Coastal Aquifers of Eastern Niger Delta, Nigeria. Geosciences, vol. 2, no. 3, pp. 51-59.
- Anakwuba, E. K., Ajaegwu, N. E., Akpunonu, E. O., Obiadi, I. I. and Onyido, C. P.; 2008. 3-D Seismic Interpretation and Overpressure Prediction of Diok Field, Niger Delta. Proceedings from the 2008 NAPE Conference, pp. 6-10.
- Anakwuba, E. K., Ajaegwu, N. E., Akpunonu, E. O. and Obiadi, I. I.; 2010. High-Resolution Miocene Sequence Stratigraphy of Diok Field, Eastern Niger Delta. Journal of Mining and Geology, vol. 46, no. 2, pp. 163-171.
- Anakwuba, E. K., Onwuemesi, A. G., Anike, O. L., Onyekwelu, C. U., Chinwuko, A. I. Akachikelu, N. C., Obiadi, I. I., and Yakubu, H. M. (2013). Application

- of geostatistical seismic inversion in reservoir characterization of Igloo Field, Niger Delta, Nigeria. Paper presented at the First Near Surface Geophysics Asia Pacific Conference (NSGAPC). Beijing, China, p. 454-458.
- Anakwuba, E.K., Onyekwelu, C.U., and Chinwuko, A.I.; 2015. Integrated Workflow Approach to Static Modeling of Igloo R3 Reservoir, Onshore Niger Delta, Nigeria. *Interpretation* Vol. 3, no. 3, pp. sz1-sz14.
- Asquith, G., and Krygowski, D.; 2004. Basic Well Log Analysis: AAPG Methods in Exploration Series, pp. 6- 16.
- Archie, G.E.; 1942. The electrical resistivity log as an aid in determining some reservoir characteristics. *Trans. Am. Inst. Min. Metal. & Petr. Eng.*, vol. 146, pp.54-62.
- Armentrout, J. M., S. J. Malecek, P. Braithwaite, and C. R. Beeman,1991, Seismic facies of slope basin turbidite reservoirs, East Breaks 160-161 field: Pliocene–Pleistocene, northwestern Gulf of Mexico, *in* P. Weimer and M. H. Link, eds., *Seismic facies and sedimentary processes of submarine fans and turbidite systems*: New York, Springer-Verlag, 223–239pp.
- Avbovbo, A. A.; 1978. Tertiary lithostratigraphy of Niger Delta. AAPG, vol. 62, pp. 295-300.
- Badalini, G., Kneller, B., and Winker, C. D.; 2000. Architecture and processes in the late Pleistocene Brazos-Trinity turbidite system, Gulf of Mexico continental slope, *in* Weimer, P., Slatt, R. M., Coleman, J., Rosen, N. C., Nelson, H., Bouma, A. H., Styzen, M. J., and Lawrence, D. T. (Eds.), *Deep-Water Reservoirs of the World: Gulf Coast Society of Economic Paleontologists and Mineralogists Foundation, 20th Annual Research Conference*, pp. 16-34.
- Bahorich, M. and Farmer, S.; 1995. 3D Seismic Discontinuity for Faults and Stratigraphic Features: The Coherence Cube. *The Leading Edge*, vol. 14, pp.1053-1058.
- Barnes, A.E.; 1992. Instantaneous spectral bandwidth and dominant frequency with applications to seismic reflection data. *Geophysics*, vol. 58, no. 3, pp. 419-428.

- Barnes, A., Cole, M., Michaels, T., Norlund, P., and Sembroski, C. (2011). Making seismic data come alive. *First Break*, vol. 29, pp. 33-38.
- Beaubouef, R. T., and Friedmann, S. J.; 2000. High-resolution seismic/sequence stratigraphic framework for the evolution of Pleistocene intra slope basins, Western Gulf of Mexico: depositional models and reservoir analogs, in Weimer, P., Slatt, R. M., Coleman, J., Rosen, N. C., Nelson, H., Bouma, A. H., Styzen, M. J., and Lawrence, D. T., (Eds.), *Deep-Water Reservoirs of the World: Gulf Coast Society of Economic Paleontologists and Mineralogists Foundation, 20th Annual Research Conference*, pp. 40-60.
- Beka, F.T., and Oti, M.N.; 1995. The distal offshore Niger delta: frontier prospects of a mature petroleum province, *in* Oti, M.N., and Postma, G., (Eds.), *Geology of Deltas: Rotterdam, A.A. Balkema*, pp. 237-241.
- Bezdek, J.C., Tsao, E.C.K. and Pal, N.R.; 1992. Fuzzy Kohonen clustering networks: *IEEE International Conference on Fuzzy Systems*, pp.1035–1043.
- Bouma, A. H., and J. M. Coleman, 1986, Intraslope basin deposits and potential relation to the continental shelf, northern Gulf of Mexico: *Gulf Coast Association of Geological Societies Transactions*, vol. 36, pp. 419–427.
- Brown, A.R.; 1996. Seismic attributes and their classification: *The Leading Edge*, vol. 15, no.10, pp. 1090-1092.
- Brown, A.R.; 2001. Understanding seismic attributes: *Geophysics*, vol. 66, no. 1, pp. 47-48.
- Brown, A. R.; 2013. What Is Seismic Interpretation?. *AAPG Explorer*, vol. 5, no. 6, pp. 14-19.
- Bubb, J. N., and Hatledid, W. G.; 1977. Seismic recognition of carbonate builds ups in seismic stratigraphy, *in* Payton, C. E. (ed.), *Applications to hydrocarbon exploration: AAPG Memoir*, vol. 26, pp. 185–204.
- Burke, K.; 1972. Longshore drift, submarine canyons and submarine fans in development of Niger Delta. *AAPG Bulletin*, vol. 56, no.4, pp. 1975-1983.

- Cant, D.J.; 1992. Subsurface Facies Analysis. In: Walker, R.G. and James N.P. (Eds.), *Facies Models: Response to Sea Level Change*. Geological Association of Canada, pp. 405- 409.
- Chopra, S. and Marfurt, K. J., 2006. Seismic Attribute Mapping of Structure and Stratigraphy. *Canadian Society of Exploration Geophysicists (CSEG) Recorder, Special Edition*, pp. 110-121.
- Chopra, S.; 2008. Emerging and future trends in seismic attributes. *The Leading Edge*, vol. 27, no. 3, pp. 298-318.
- Chopra, S. and Marfurt, K. J.; 2011. Blended Data Renders Visual Value. *AAPG Explorer, Geophysical Corner*, vol. 3, no. 10, pp. 38-40.
- Chopra, S. and Michelena, R. J.; 2011. Introduction to this special section: Reservoir Characterization. *The Leading Edge*, vol. 30, no.1, pp. 35-37.
- Chopra, S. and Marfurt, K. J.; 2012. Seismic attribute expression of differential compaction; *SEG Las Vegas 2012 Annual Meeting*, pp.1-5
- Clark, J.D., Kenyon, N.H., and Pickering, K.T.; 1992. Quantitative analysis of the geometry of submarine channels: implications for the classification of submarine fans. *Geology*, vol. 20, no. 3, pp. 633–636.
- Clark, J.D., and Pickering, K.T.; 1996. Architectural elements and growth patterns of submarine channels: applications to hydrocarbon exploration. *AAPG Bulletin*, vol. 80, no. 6, pp. 194–221.
- Cohen, L. (1995). *Time Frequency Analysis: Theory and Applications: Prentice-Hall Signal Processing Series*, New York, 320p.
- Damuth, J. E.; 1994. Neogene gravity tectonics and depositional processes on the deep Niger delta continental margin. *Marine and Petroleum Geology*, vol. 11, no. 3, pp. 320-346.
- Dan G. V. and Robert R.; 1996. Stewart 3-D seismic attributes. *CREWES Research Report*, vol. 8, no. 45, pp. 1-30.
- Dean, L.; 2007. Reservoir Engineering for Geologists. *Canadian Society for Petroleum Geologist (CSPG) Reservoir Magazine*, vol. 34, no. 11, pp. 20-23.

- Doust, H.J., and Omatsola, O.; 1990. Niger Delta In: Edwards, J.D. and Santoyiossi, P.A.(Ed.). Divergent and Passive Margin Basin. AAPG Memoir, no. 48, pp. 201-238.
- Ekweozor, C.M. and Okoye, N.V.; 1980. Petroleum source-bed evaluation of Tertiary Niger Delta: AAPG Bulletin, vol. 64, no. 4, 1251-1259.
- Etris, N. and Stewart, B.; 2003. Net-togross ratio. Canadian Society for Petroleum Geologist (CSPG) Reservoir Magazine, vol. 30, no. 4, pp. 24-25.
- Emery, D., and Myers, K. (1996). Sequence Stratigraphy. Black-well Science Ltd., Oxford, London, 423pp.
- Evarmy, B.D., Haremboure, J., Kamerling, P., Knaap, W.A., Molloy, F.A., and Rowlands, P.H.; 1978. Hydrocarbon Habitat of Tertiary Niger delta, AAPG Bulletin, vol. 62, no. 4, pp. 1-39.
- Feeley, M.H., Buffler, R.T., and Bryant, W.R.; 1985. Depositional units and growth of the Mississippi Fan, *in* Bouma, A. H., Normark, W.R. and Barnes, N.E. (Eds.), Submarine fans and related turbidite systems, New York, Springer- Verlag, pp. 253-257.
- Ferguson, C.J., Avu, A., Schofield, N. and Patton, G.S. (2010) Seismic analysis workflow for reservoir characterization in the vicinity of salt. First Break, vol. 28, no. 10, pp. 107–113.
- Galloway, W. E.; 1975. Process framework for describing the morphologic and stratigraphic evolution of deltaic depositional systems, *in* Broussard, M. L., (Ed.), Deltas, Models for Exploration. Houston Geological Society, pp. 87-98.
- Haack, R.C., Sundararaman, P., and Dahl, J.; 1997. Niger delta petroleum system: Presented at the 1997 AAPG/ABGP Hedberg Research symposium, Rio de Janeiro, Brazil, extended abstracts.
- Hampson, D., Schuelke, J.S., and Quirein, J.A.; 1999. Use of multiattribute transforms to predict log properties from seismic data. Geophysics, vol. 66, no. 4, pp. 220-231.

Hospers, J.; 1965. Gravity field and structure of the Niger delta, Nigeria, West Africa. GSA Bulletin, vol. 74, no.1, pp. 1-12.

[Http://www.glossary.oilfield.slb.com](http://www.glossary.oilfield.slb.com)

Khripounoff, A., Vangriesheim, A., Babonneau, N., Crassous, P., Dennielou, B., Savoye, B.; 2003. Direct observation of intense turbidity current activity in the Zaire submarine valley at 4000m water depth. Marine Geology, vol. 194, no.1, pp. 151–158.

Klein, P., Richard, L. and James, H.; 2008. 3D curvature attributes: a new approach for seismic interpretation. First break, vol. 26, no.1, pp. 105-112.

Klett, T.R.; Ahlbrandt, T.S.; Schmoker, J.W.; and Dolton, J.L.; 1997. Ranking of the world's oil and gas provinces by known petroleum volumes. US Geological Survey Open-file Report, pp.97- 463.

Knox, G. J., and Omatsola, E. M.; 1989. Development of the Cenozoic Niger delta in terms of the “Escalator Regression” model and impact on hydrocarbon distribution. Proceedings of the KNGMG Symposium “Coastal Lowlands, Geology and Geotechnology,” Dordrecht, Kluwer, pp. 181-202.

Kulke, H.; 1995. Nigeria, *in* Kulke, H. (Ed.), Regional petroleum geology of the world Part II: Africa, America, Australia and Antarctica. Berlin, Gebruder Borntraeger, pp.143-172.

Larionov, V.; 1969. Borehole Radiometry. Moscow, U.S.S.R.: Nedra Printing, 227p.

Lehner, P., and De Ruitter, P.A.C.; 1977. Structural history of Atlantic Margin of Africa. AAPG Bulletin, vol. 61, no. 2, pp. 961-981.

Li, M., Li, Z., Jiang, Q., and Cao, T.; 2013. Reservoir Quality, Hydrocarbon Mobility and Implications for Lacustrine Shale Oil Productivity in the Paleogene Sequence, Bohai Bay Basin. Oral presentation presented at American Association of Petroleum Geologists (AAPG) Annual Convention and Exhibition, Pittsburgh, Pennsylvania, USA, pp. 1-34.

- Liu, J.L., and J. S. Watkins, 1992, Seismic facies and depositional processes on the lower continental slope in the Mississippi Canyon area, Gulf of Mexico (abs.): AAPG Bulletin, vol. 76, no. 9, pp. 1462.
- Liu, J.L. and Marfurt, K.; 2007. Multi-Color Display of Spectral Attributes. The Leading Edge, vol. 26, pp. 268-271.
- Marfurt, K. J., Sharp, J. A., Scheet, R. M., Ward, J., Cain, G., and Harper, M. G.; 1998. Suppression of the acquisition footprint for seismic attribute analysis. Geophysics, vol. 63, no. 4, pp. 1024–1035.
- Mayall, M., Jones, E., and Casey, M.; 2006. Turbidite channel reservoirs—key elements in facies prediction and effective development. Marine and Petroleum Geology, vol. 23, no. 3, pp. 821–841.
- Mehdi E. and De-Hua, H.; 2011. 3D Petrophysical modeling using complex seismic attributes and limited well log data; Paper presented at the Annual Meeting of SEG, San Antonio, pp.1887- 1891.
- Mitchum, R.M. Jr., Sangree, J.B., Vail, P.R., and Wornardt, W.W.; 1991. Sequence stratigraphy in the late Cenozoic expanded sections, Gulf of Mexico: *in* Armentrout, J. M., and Perkins, B.F.(Eds.), Sequence stratigraphy as an exploration tool, concepts and practices in the Gulf Coast: Gulf Coast Section, SEPM Foundation, Eleventh Annual Research Conference, pp. 237-256.
- Naseer, T.M., Asim, Shazia, Ahmad, M.N., Hussain, S.F., and Qureshi, S.N.; 2014. Application of seismic attributes for delineation of channel geometries and analysis of various aspects in terms of lithological and structural perspectives of Lower Goru Formation, Pakistan. International Journal of Geosciences, vol. 5, pp. 1490-1502.
- Obah, B., Livinus, A., and Ezugwu, C. M.; 2012. Simplified Models for Forecasting Oil Production: Niger Delta Oil Rim Reservoirs Case. Petroleum Technology Development Journal, vol. 2; no. 2, pp. 1-12.
- Obaje, N.G., Wehner, H., Scheeder, G., Abubakar, M.B., Jauro, A.; 2004. Hydrocarbon Prospectivity of Nigeria’s inland basins: From the viewpoint of organic

- geochemistry and organic petrology. AAPG Bulletin, vol. 88, no. 3, pp. 325-353.
- Okodudu, S.; 2007. Niger Delta in the Era of Globalization. MSS Printing, Port-Harcourt, Nig., 137p.
- Omoboriowo, A.O., Chiadikobi, K.C. and Chiaghanam, O.I.; 2012. Depositional Environment and Petrophysical Characteristics of “LEPA” Reservoir, Amma Field, Eastern Niger Delta, Nigeria. Int. J. Pure and Appl. Sci. Technol., vol. 10, no. 2, pp. 38-61.
- Oyanyan, R. O., Soronnadi-Ononiwu, C. G. and Omoboriowo, A. O.; 2012. Depositional environments of sam-bis oil field reservoir sands, Niger Delta, Nigeria. Advances in Applied Science Research, vol. 3, no. 3, pp. 1624-1638.
- Partyka, G., Gridley, J. and Lopez, J.; 1999. Interpretational Applications of Spectral Decomposition in Reservoir Characterization. The Leading Edge, vol. 18, pp. 353-360.
- Peter, O., and Peter, A., 2013. Formation Evaluation and Its Implication on Hydrocarbon Production in Imoye Field, Niger Delta. Journal of Environment and Earth Science, vol. 3, no.1, pp. 98-109.
- Peyton, L., Bottjer, R. and Partyka, G.; 1998. Interpretation of Incised Valleys Using New 3-D Seismic Techniques: A Case History Using Spectral Decomposition and Coherency. The Leading Edge, vol. 17, pp. 1294-1298.
- Pilcher, R.S. and Blumstein, R.D. (2007). Brine volume and salt dissolution rates in Orca basin, northeast Gulf of Mexico. AAPG Bulletin, vol. 91, pp. 823–833.
- Pirmez C., Beaubouef, R. T., Friedmann, S. J., and Mohrig, D. C.; 2000. Equilibrium profile and base level in submarine channels: examples from Late Pleistocene systems and implications for the architecture of deep-water reservoirs: *in* Weimer, P., Slatt, R. M., Coleman, J., Rosen, N. C., Nelson, H., Bouma, A. H., Styzen, M. J., and Lawrence, D. T., (Eds.), Deep-Water Reservoirs of the World. Gulf Coast Society of the Society of Economic Paleontologists and Mineralogists Foundation, 20th Annual Research Conference, pp. 782-805.

- Pokhriyal, S. K.; 2011. A new seismic attribute aids to map the embedded geological features from low bandwidth seismic data: The 2nd South Asian Geoscience Conference and Exhibition, pp. 1-6.
- Posamentier, H. W., and R. D. Erskine, 1991. Seismic expression and recognition criteria of ancient submarine fans, *in* P. Weimer and M. H. Link, eds., *Seismic facies and sedimentary processes of submarine fans and turbidite systems*: New York, Springer-Verlag, p. 197–222.
- Posamentier, H. W., and Kolla, V.; 2003. Seismic geomorphology and stratigraphy of depositional elements in deep-water settings. *Journal of Sedimentary Research*, vol. 73, no. 3, pp. 367-388.
- Prather, B. E., J. R. Booth, G. S. Steffens, and P. A. Craig, 1995. Classification and stratigraphic succession of seismic facies in intraslope basins, deep-water Gulf of Mexico, U.S.A. (abs.): AAPG Annual Meeting Program with Abstracts, pp. 77A.
- Prather, B. E., Booth, J. R., Steffens, G. S., and Craig, P. A.; 1998. Classification, lithologic calibration, and stratigraphic succession of seismic facies of intraslope basins, deep-water Gulf of Mexico. *AAPG Bulletin*, vol. 82, no. 1, pp. 701-728.
- Pokhriyal, .S. K.; 2011. A new seismic attribute aids to map the embedded geological features from low bandwidth seismic data: The 2nd South Asian Geoscience Conference and Exhibition, pp. 1-6.
- Rider , M.H.; 1996. *Well Geological Interpretation of Well Logs*. Interprint Ltd., London, England, 398p.
- Reijers, T.J.A., Petters, S.W., and Nwajide, C.S.; 1997. The Niger Delta Basin, *in* Selley, R.C. (Ed.), *African Basins--Sedimentary Basin of the World 3*: Amsterdam, Elsevier Science, pp. 151-172.
- Rijks, E. J. H., and Jauffred, J. E. E. M.; 1991. Attribute extraction: An important application in any 3-D interpretation study. *The Leading Edge*, vol. 10, no. 9, pp. 11–19.

- Sangree, J.B., Waylett, D.C., Amery, G.B., Fennessy, W.J., and Frazier, D.E.; 1978. Recognition of continental-slope seismic facies, offshore Texas-Louisiana, *in* A. H. Bouma, G.T. Moore, and J.M. Coleman, (Eds)., *Beyond the shelf break*. AAPG Short Course 2, pp. 1-54.
- Schultz, P. S., Ronen, S., Hattori, M., Corbett, C., and Mantran, P.; 1994. Seismic guided estimation of log properties, parts 1, 2, and 3. *The Leading Edge*, vol. 13, no. 1, pp. 305–310.
- Schlumberger. (1968). *Log Interpretation /charts*:. Schlumberger Well Services, Inc. Houston, 10-30pp.
- Schlumberger, 1974. *Log Interpretation Charts*. Schlumberger Educational Services, New York, US, 83p.
- Sheriff, R.E.; 1973. *Encyclopedic Dictionary of Exploration Geophysics*. SEG, Tulsa, OK, 266p .
- Sheriff, R.E. 1992. *Reservoir Geophysics: Investigations in Geophysics Series*. SEG, vol. 7, pp. 45-52.
- Sheriff, R.E. and Geldart, L.P.; 1995. *Exploration Seismology*. Cambridge University Press, New York, USA, 592 p.
- Short, K.C. and Stauble, A.J.; 1967. *Outline of Geology of Niger Delta*. AAPG Bulletin, vol. 51, no. 1, pp. 761 – 779.
- Sigismondi, M. E. and Soldo, J. C.; 2003. Curvature attributes and seismic interpretation: Case studies from Argentina basins. *The Leading Edge*, vol. 22, no. 11, pp. 1122-1126.
- Siddiqui, N.A., EL-Ghali, M.A., Abd Rahman, A., Mijinyawa, A., and Ben-Awuah, J.; 2013. Depositional Environment of Shallow-Marine Sandstones from Outcrop Gamma-Ray Logs, Belait Formation, Meragang Beach, Brunei Darussalam. *Research Journal of Environmental and Earth Sciences*, vol. 5, no. 6, pp. 305-324.

- Siguaw, S.G., Estes-Jackson, J.E., Ingraham, S.E., Shewmake, D.W.; 2001. An integrated 3-D reservoir characterization at Riverton Dome Field, Wyoming. *The Leading Edge*, vol. 20, no. 11, pp. 1226-1238.
- Smith, T. and Starcey, D.; 2011. Seismic Attribute analysis can benefit from unsupervised neural network. *Geology and Geophysics Offshore*, vol. 40, no. 2, pp. 1-4.
- Stacher, .P.; 1995. The Niger delta hydrocarbon habitat. *NAPE Bull.*, vol. 9, no. 1, pp. 67-75.
- Subrahmanyam, D.; 2008. Seismic Attributes- A Review. Paper presented at 7th International Conference and Exposition on Petroleum Geophysics, pp.398-404.
- Taner, M.T.; 2001. Seismic attributes. *CSEG Recorder*, vol. 26, no. 7, pp. 48-56.
- Taner, M. T., Schuelke, J. S. Doherty, R. O. and Baysal, E.; 1994. Seismic attributes revisited: 64th Annual International Meeting of SEG, Expanded Abstracts, pp.1104–1106.
- Taner, M.T., Koehler, F., and Sheriff, R.E.; 1979. Complex seismic trace analysis. *Geophysics*, vol. 44, no. 6, pp. 1041-1063.
- Timur, A.; 1968. An investigation of permeability, porosity, and residual water saturation relationship for sandstone reservoirs. *The Log Analyst*, vol. 9, no. 4, pp. 8-13.
- Tinker, S.W.; 1996. Building the 3-D jigsaw puzzle: Application of sequence stratigraphy to 3-D reservoir characterization, Permian Basin. *AAPG Bulletin*, 80: 460-482.
- Tuttle, M. L. W., Charpentier, R. R., and Brownfield, M. E.; 1999. The Niger delta petroleum system: Niger delta province, Nigeria, Cameroon, and Equatorial Guinea, Africa: USGS Open-file report, pp. 50-99.

- Urazimanova, A., Patterson, E., Deng, J., Althoff, C., Yalcin, B., and Totten, M.; 2013. Iterative Depositional Model Interpretations Using Seismic Attributes. School of Geology and Geophysics, University of Oklahoma, Ok, 131p.
- Vail, P.R., and Wornardt, W.; 1991. An integrated approach to exploration and development in the 90s: Well-log seismic sequence stratigraphy analysis. Transactions of the Gulf Coast Association of Geological Societies, vol. 41, pp. 630-650.
- Wagner, J.B., Kofron, B.M., Morin, R.W., Ford, D.W., and Marthur, V.R. 1992. An applied sequence stratigraphic approach to basin analysis. AAPG Annual Meeting Program, 136p.
- Weber, K.J.; 1971. Sedimentological aspects of oil fields in the Niger Delta. Geologie en Mijnbouw, vol. 50, pp. 559–576.
- Weber, K. J. and Daukoru, E.; 1975. Petroleum Geology of the Niger Delta. Paper presented at 9th World Petroleum Congress, Tokyo, Japan, pp.1-14.
- Whiteman, A. J.; 1982. Nigeria: Its petroleum geology, resources and potential. Graham and Trotman Publishers, London, England, vol. 2, 241p.
- Wynn, R. B., Cronin, B. T., and Peakall, J.; 2002. Sinuous deep-water channels: Genesis, geometry and architecture. Marine and Petroleum Geology, vol. 24, no. 1, pp. 341–387.
- Xiao, H., and Suppe, J.; 1992. Origin of rollover. AAPG Bulletin, vol. 76, no. 3, pp. 509-229.
- Yenugu, M. R., Marfurt, K. J., Wickstrom, C. and Matson, S.; 2011. Seismic Attribute Mapping for Identification of Cypress Sands, Illinois Basin, Indiana, USA; Search and Discovery Article (#40808), Adapted from oral presentation at AAPG Annual Convention and Exhibition, Houston, Texas, USA, pp. 10-13.

Appendix I: Result of Well Correlation Table for the Wells in the study area

Well identifier	Surface	X	Y	Z	MD	TWT auto
Rence-1	A Top	546474.3	-9845.39	-562.89	571.89	718.56
Rence-1	A Base	546474.3	-9845.39	-582.89	591.89	726.56
Rence-1	C Top	546474.3	-9845.39	-620.37	629.37	764.95
Rence-1	C Base	546474.3	-9845.39	-742.11	751.11	855.32
Rence-1	D Top	546474.3	-9845.39	-863.25	872.25	972.3
Rence-1	D Base	546474.3	-9845.39	-901.34	910.34	1003.3
Rence-1	E Top	546474.3	-9845.39	-962.89	971.89	1050.27
Rence-1	E Base	546474.3	-9845.39	-1077.77	1086.77	1139.81
Rence-1	F Top	546474.3	-9845.39	-1124.32	1133.32	1184.08
Rence-1	F Base	546474.3	-9845.39	-1140.62	1149.62	1193.92
Rence-1	G Top	546474.3	-9845.39	-1221.56	1230.56	1243.71
Rence-1	G Base	546474.3	-9845.39	-1254.85	1263.85	1265.67
Rence-1	H Top	546474.3	-9845.39	-1276.63	1285.63	1281.52
Rence-1	H Base	546474.3	-9845.39	-1483.75	1492.75	1492.92
Rence-1	I Top	546474.3	-9845.39	-1551.89	1560.89	1545.14
Rence-1	I Base	546474.3	-9845.39	-1573.08	1582.08	1560.98
Rence-1	J Top	546474.3	-9845.39	-1618.87	1627.87	1612.12
Rence-1	J Base	546474.3	-9845.39	-1664.61	1673.61	1648.27
Rence-1	K Top	546474.3	-9845.39	-1681.29	1690.29	1657.55
Rence-1	K Base	546474.3	-9845.39	-1702.49	1711.49	1673.02
Rence-1	L Top	546474.3	-9845.39	-1714.79	1723.79	1686.53
Rence-1	L Base	546474.3	-9845.39	-1894.46	1903.46	1811.46
Rence-1	M Top	546474.3	-9845.39	-1922.33	1931.33	1833.38
Rence-1	M Base	546474.3	-9845.39	-2121.27	2130.27	1973.18
Rence-1	N Top	546474.3	-9845.39	-2143.14	2152.14	1994.46
Rence-1	N Base	546474.3	-9845.39	-2292.33	2301.33	2103.24
Rence-1	O Top	546474.3	-9845.39	-2311.13	2320.13	2116.95
Rence-1	O Base	546474.3	-9845.39	-2366.19	2375.19	2157.1
Rence-1	P Top	546474.3	-9845.39	-2421.18	2430.18	2197.2
Rence-1	P Base	546474.3	-9845.39	-2490.29	2499.29	2247.59
Rence-1	Q Top	546474.3	-9845.39	-2511.55	2520.55	2263.09
Rence-1	Q Base	546474.3	-9845.39	-2548.32	2557.32	2289.9
Rence-1	R Top	546474.3	-9845.39	-2694.87	2703.87	2396.77
Rence-1	R Base	546474.3	-9845.39	-2716.08	2725.08	2412.23
Rence-1	S Top	546474.3	-9845.39	-2745.73	2754.73	2433.85
Rence-2	A Top	546827.2	-8479.02	-485.93	511.84	643.49
Rence-2	A Base	546827.2	-8479.02	-507.26	533.17	673.74
Rence-2	B Top	546827.2	-8479.02	-537.5	563.41	708.65
Rence-2	B Base	546827.2	-8479.02	-558.75	584.66	716.9

Rence-2	C Top	546827.2	-8479.02	-595.18	621.09	731.49
Rence-2	C Base	546827.2	-8479.02	-750.52	776.43	860.91
Rence-2	D Top	546827.2	-8479.02	-854.24	880.15	964.47
Rence-2	D Base	546827.2	-8479.02	-897.9	923.81	1001.53
Rence-2	E Top	546827.2	-8479.02	-958.35	984.26	1045.98
Rence-2	E Base	546827.2	-8479.02	-1071.97	1097.88	1137.88
Rence-2	F Top	546827.2	-8479.02	-1119.88	1145.79	1181.39
Rence-2	G Top	546827.2	-8479.02	-1293.2	1319.11	1293.57
Rence-2	G Base	546827.2	-8479.02	-1322.9	1348.81	1369.06
Rence-2	H Top	546827.2	-8479.02	-1329.57	1355.48	1385.9
Rence-2	H Base	546827.2	-8479.02	-1486.39	1512.3	1495.11
Rence-2	I Top	546827.2	-8479.02	-1555.2	1581.11	1547.67
Rence-2	I Base	546827.2	-8479.02	-1586.49	1612.4	1570.97
Rence-2	J Top	546827.2	-8479.02	-1631.1	1657.01	1629.64
Rence-2	J Base	546827.2	-8479.02	-1681.29	1707.2	1657.55
Rence-2	K Top	546827.2	-8479.02	-1688.03	1713.94	1662.47
Rence-2	K Base	546827.2	-8479.02	-1706.93	1732.84	1676.27
Rence-2	L Top	546827.2	-8479.02	-1727.02	1752.93	1702.51
Rence-2	L Base	546827.2	-8479.02	-1906.46	1932.37	1821.8
Rence-2	M Top	546827.2	-8479.02	-1934.28	1960.19	1842.1
Rence-2	M Base	546827.2	-8479.02	-2133.22	2159.13	1987.22
Rence-2	N Top	546827.2	-8479.02	-2156.89	2182.8	2004.48
Rence-3	A Top	545833.7	-10168.1	-546.76	580.01	712.25
Rence-3	A Base	545830.2	-10171.3	-570.19	603.91	721.48
Rence-3	B Top	545823.1	-10178.2	-610.82	645.74	752.62
Rence-3	B Base	545820	-10181.3	-625.51	661.07	769.99
Rence-3	C Top	545812.9	-10189.2	-658.94	696.16	801.33
Rence-3	C Base	545767	-10237	-819.96	870.67	935.75
Rence-3	D Top	545684.1	-10331.8	-956.37	1056.99	1043.74
Rence-3	D Base	545653.3	-10367.2	-992.33	1116.15	1078.09
Rence-3	E Top	545615	-10408.8	-1033.12	1185.9	1105.92
Rence-3	E Base	545560.1	-10464.8	-1089.78	1282.62	1143.8
Rence-3	F Top	545521.4	-10505.1	-1130.96	1352.04	1188.09
Rence-3	F Base	545444.9	-10584.9	-1210.68	1488.39	1236.87
Rence-3	G Top	545408.5	-10622	-1248.47	1552.67	1261.03
Rence-3	G Base	545396.8	-10634	-1261.12	1573.67	1270.23
Rence-3	H Top	545392.5	-10638.3	-1265.7	1581.24	1273.56
Rence-3	H Base	545355.4	-10676.1	-1307.19	1648.61	1331.51
Rence-3	H Levee	545276.9	-10759.3	-1398.74	1795.08	1431.19
Rence-3	I Top	545198.5	-10841.2	-1488.05	1939.46	1496.38
Rence-3	I Base	545186.1	-10853.8	-1501.84	1961.88	1506.91
Rence-3	J Top	545138.6	-10902.5	-1556.77	2049.31	1548.84
Rence-3	J Base	545077.2	-10965.6	-1626.72	2161.81	1623.37

Rence-3	K Top	545058.6	-10984.5	-1648.52	2196.13	1639.32
Rence-3	K Base	545045.4	-10997.8	-1664.52	2220.78	1648.22
Rence-3	L Top	545035.9	-11007.4	-1676.29	2238.73	1654.77
Rence-3	L Base	544900.5	-11154	-1838.11	2495.98	1762.92
Rence-3	M Top	544860.9	-11200.4	-1889.12	2575.52	1806.86
Rence-3	M Base	544723.5	-11345.9	-2062.23	2840.22	1921.77
Rence-3	N Top	544704.8	-11364.9	-2087.45	2876.93	1933.43
Rence-3	N Base	544609.7	-11461.9	-2208.77	3059.13	2042.31
Rence-3	O Top	544581.5	-11490.4	-2239.36	3109.58	2064.62
Rence-3	O Base	544543.4	-11529.2	-2279.54	3177.14	2093.86
Rence-3	P Top	544499.3	-11575.5	-2328.61	3257.8	2128.78
Rence-3	P Base	544434	-11640.5	-2401.11	3375.05	2179.54
Rence-3	Q Top	544422.4	-11652.3	-2414.46	3396.28	2188.73
Rence-3	Q Base	544402.5	-11671.7	-2436.77	3431.96	2204.18
Rence-3	R Top	544262.1	-11801.1	-2586.08	3674.38	2309.13
Rence-3	R Base	544247.2	-11814.9	-2602	3700.18	2320.29
Rence-4	J Base	546553.6	-9466.09	-1686.2	2086.27	1661.13
Rence-4	K Top	546570.9	-9451.04	-1711.42	2120.37	1682.13
Rence-4	K Base	546583.6	-9440.23	-1729.71	2145.12	1703.62
Rence-4	L Top	546588.4	-9436.14	-1736.64	2154.5	1706.47
Rence-5	F Base	545743.7	-10097.8	-1200.32	1251.71	1230.35
Rence-5	G Top	545727.2	-10088.2	-1238.19	1294.14	1254.17
Rence-5	G Base	545719.1	-10083.6	-1255.33	1313.63	1266.02
Rence-5	H Top	545714.2	-10080.8	-1264.55	1324.45	1272.73
Rence-5	H Base	545611.6	-10022.7	-1419.17	1519.06	1439.38
Rence-5	H Base	545611.6	-10022.7	-1419.17	1519.06	1439.38
Rence-5	I Top	545564.2	-9995.7	-1487.53	1606.52	1495.98
Rence-5	I Base	545553.1	-9989.54	-1502.9	1626.42	1507.72
Rence-5	J Top	545521.2	-9971.07	-1547.63	1684.39	1541.89
Rence-5	J Base	545469.2	-9939.1	-1622.15	1780.73	1616.83
Rence-5	K Top	545455.5	-9930.4	-1641.5	1805.98	1635.42
Rence-5	K Base	545444.9	-9923.57	-1656.43	1825.54	1643.73
Rence-5	L Top	545436.7	-9918.23	-1667.86	1840.57	1650.08
Rence-5	L Base	545340.3	-9857.82	-1806.25	2019.77	1735.47
Rence-6	F Base	545939.5	-10723.5	-1227.85	1473.28	1247.67
Rence-6	G Top	545941.8	-10746.3	-1250.78	1505.7	1262.71
Rence-6	G Base	545944.6	-10775.1	-1279.43	1546.43	1283.56
Rence-6	H Top	545945.7	-10786	-1289.72	1561.42	1291.04
Rence-6	H Base	545987.9	-11001.3	-1484.43	1854.88	1493.48
Rence-6	I Top	545997.1	-11049.6	-1526.69	1919.7	1525.89
Rence-6	I Base	546002.1	-11074.5	-1548.77	1953.36	1542.76
Rence-6	J Top	546005.4	-11090.6	-1563.63	1975.57	1553.95
Rence-6	J Base	546020.9	-11169.1	-1637.01	2084.11	1632.93

Rence-6	K Top	546029.3	-11219.7	-1685.17	2154.47	1660.38
Rence-6	K Base	546030.6	-11229.5	-1694.31	2167.93	1667.05
Rence-6	L Top	546032.5	-11243.7	-1707.45	2187.41	1676.93
Rence-7	F Base	545714.2	-10353.9	-1207.2	1287.08	1234.68
Rence-7	G Top	545705.5	-10365.6	-1238.13	1321.27	1254.14
Rence-7	G Base	545701	-10371.7	-1254.19	1339.04	1265.19
Rence-7	H Top	545696.9	-10377.7	-1269.07	1355.56	1276.02
Rence-7	H Base	545660.6	-10446.5	-1436.42	1540.16	1453.68
Rence-7	I Top	545641.6	-10476.4	-1518.09	1629.22	1519.32
Rence-7	I Base	545636.3	-10483.7	-1539.57	1652.53	1535.73
Rence-7	J Top	545625.1	-10498.4	-1581.94	1698.76	1567.58
Rence-7	J Base	545604.1	-10526.8	-1655.32	1780.21	1643.11
Rence-7	K Top	545594.8	-10540.1	-1686.23	1815.11	1661.15
Rence-7	K Base	545590.9	-10545.4	-1698.8	1829.3	1670.33
Rence-7	L Top	545587.3	-10550.5	-1710.75	1842.77	1681.26
Rence-8	F Base	545945.9	-9696.85	-1195.69	1405.14	1227.44
Rence-8	G Top	545960.5	-9636.2	-1243.73	1483.88	1257.66
Rence-8	G Base	545969.4	-9602.42	-1270.49	1527.9	1277.05
Rence-8	H Top	545972.6	-9590.44	-1280.5	1543.83	1284.33
Rence-8	H Base	546010.8	-9409.39	-1443.93	1790.85	1459.91
Rence-8	I Top	546024.2	-9322.97	-1515.44	1903.83	1517.3
Rence-8	I Base	546028.8	-9295.15	-1539.27	1940.74	1535.5
Rence-8	J Top	546038.2	-9240.84	-1585	2012.37	1569.86
Rence-8	J Base	546055.9	-9149.45	-1661.09	2132.61	1646.32
Rence-8	K Top	546062.6	-9119.04	-1687.45	2173.41	1662.05
Rence-8	K Base	546067.7	-9097.2	-1706.58	2202.88	1676
Rence-8	L Top	546069.4	-9090.19	-1712.74	2212.35	1683.85
Rence-9	A Top	543091.3	-9925.2	-503.95	529.86	669.05
Rence-9	A Base	543091.3	-9925.2	-519.79	545.7	688.81
Rence-9	B Top	543091.3	-9925.2	-559.5	585.41	717.2
Rence-9	B Base	543091.3	-9925.2	-572.18	598.09	722.27
Rence-9	C Top	543091.3	-9925.2	-632.79	658.7	777.11
Rence-9	C Base	543091.3	-9925.2	-772.71	798.62	901.11
Rence-9	D Top	543091.3	-9925.2	-879.42	905.33	986.07
Rence-9	D Base	543091.3	-9925.2	-911.31	937.22	1008.41
Rence-9	E Top	543091.3	-9925.2	-978.88	1004.79	1065.38
Rence-9	E Base	543091.3	-9925.2	-1058.46	1084.37	1120.98
Rence-9	F Top	543091.3	-9925.2	-1141.08	1166.99	1194.2
Rence-9	F Base	543091.3	-9925.2	-1223.27	1249.18	1244.79
Rence-9	G Top	543091.3	-9925.2	-1329.6	1355.51	1385.93
Rence-9	G Base	543091.3	-9925.2	-1364.19	1390.1	1418.15
Rence-9	H Top	543091.3	-9925.2	-1375.31	1401.22	1422.35
Rence-9	H Base	543091.3	-9925.2	-1536.38	1562.29	1533.29

Rence-9	H Levee	543091.3	-9925.2	-1536.38	1562.29	1533.29
Rence-9	I Top	543091.3	-9925.2	-1615.53	1641.44	1607.35
Rence-9	I Base	543091.3	-9925.2	-1647.85	1673.76	1638.96
Rence-9	J Top	543091.3	-9925.2	-1688.03	1713.94	1662.47
Rence-9	J Base	543091.3	-9925.2	-1751.56	1777.47	1712.62
Rence-9	K Top	543091.3	-9925.2	-1784.99	1810.9	1726.4
Rence-9	K Base	543091.3	-9925.2	-1806.2	1832.11	1735.43
Rence-9	L Top	543091.3	-9925.2	-1815.17	1841.08	1743.15
Rence-9	L Base	543091.3	-9925.2	-1960.81	1986.72	1853.04
Rence-9	M Top	543091.3	-9925.2	-1985.96	2011.87	1869.43
Rence-9	M Base	543091.3	-9925.2	-2194.25	2220.16	2031.72
Rence-9	N Top	543091.3	-9925.2	-2219.43	2245.34	2050.08
Rence-9	N Base	543091.3	-9925.2	-2352.7	2378.61	2147.26
Rence-9	O Top	543091.3	-9925.2	-2378.07	2403.98	2165.76
Rence-9	O Base	543091.3	-9925.2	-2425.6	2451.51	2200.42